# Physical volcanology and geochemistry of the lower Gawler Range Volcanics in the southern Gawler Ranges

Thesis submitted in accordance with the requirements of the University of Adelaide for an Honours Degree in Geology

Alastair Ross

November 2015


THE UNIVERSITY of ADELAIDE

# PHYSICAL VOLCANOLOGY AND GEOCHEMISTRY OF THE LOWER GAWLER RANGE VOLCANICS IN THE SOUTHERN GAWLER RANGES

## VOLCANOLOGY OF THE SOUTHERN GAWLER RANGES

## ABSTRACT

The Gawler Range Volcanics are a Silicic Large Igneous Province that has been extensively studied due to the atypical nature of its widespread felsic lava flows. These low viscosity lavas form the upper sequence of the GRV, termed the Upper Gawler Range Volcanics (UGRV). The older sequence or Lower Gawler Range Volcanics (LGRV) are readily distinguished from the UGRV as they appear as numerous discrete volcanic centres, the best exposed of which are at Kokatha and Lake Everard. A much less discussed volcanic area of the LGRV are the Southern Gawler Ranges Area Volcanics (SGRAV), which form a curvilinear belt along the southern margin of the GRV. The SGRAV are dominantly represented by two volcanic units, the Bittali Rhyolite (BR) and Waganny Dacite (WD) which are exposed discontinuously for ~200km E-W. The SGRAV may be divided into a western section of dominantly effusive volcanism, with elevated temperatures and halogen contents comparable to that of the UGRV, and a central-eastern section where explosive volcanism predominates. Petrogenetic modelling suggests that assimilation fractional crystallization (AFC) processes which played a role in the development of the LGRV, were active in the formation of the SGRAV. However, using AFC modelling, the SGRAV can be reconstructed through a dominant fractional crystallization process with late stage crustal assimilation, as opposed to continual crustal assimilation in the other LGRV magma systems.

## KEYWORDS

Lower Gawler Range Volcanics, Bittali Rhyolite, Waganny Dacite, volcanology, geochemistry, SLIP, felsic

**TABLE OF CONTENTS**

Physical volcanology and geochemistry of the lower Gawler Range Volcanics in the southern Gawler Ranges ..... i
Volcanology of the southern Gawler Ranges ..... i
Abstract ..... i
Keywords ..... i
List of Figures and Tables ..... 4
Introduction ..... 7
Regional geology ..... 8
Southern Gawler Ranges Area Volcanics (SGRAV) ..... 11
Background ..... 13
Petrogenetic models ..... 13
Emplacement methods ..... 14
Methods ..... 15
Observations and Results ..... 16
Petrography ..... 16
Stratigraphy and Interpretation ..... 16
Toondulya Bluff ..... 17
..... 19
Narlaby Well ..... 19
..... 20
Waganny Dam ..... 20
Thurlga ..... 22
Buckleboo ..... 23
..... 24
Menninnie Dam ..... 24
Wartaka ..... 26
..... 27
Comparisons ..... 27
Structural data ..... 29
Geochemistry ..... 30
Isotopes ..... 31
Discussion ..... 34
Halogen contents and temperature ..... 35
Relation to the rest of the GRV ..... 39

Petrogenesis ..... 39
..... 42
Source ..... 42
AFC modelling ..... 44
Conclusion ..... 49
Acknowledgments ..... 51
References ..... 51
Appendix A: Gps coords, rock/thin section descriptions. ..... 56
..... 57
..... 58
..... 59
Appendix B: Field observations ..... 63
Toondulya Bluff ..... 63
Narlaby Well ..... 64
Waganny Dam ..... 64
Thurlga ..... 64
Buckleboo ..... 65
Menninnie Dam ..... 66
Wartaka ..... 66
Appendix B: Drill core descriptions ..... 68
Appendix C: Microprobe data ..... 69
Appendix D: Full Methods ..... 75
Core logging and taking samples ..... 75
Methods of field work ..... 75
Rock saw ..... 76
Large jaw crusher ..... 76
Vibrating mill (10G tungsten carbide mill head) ..... 77
Pressed pellets ..... 78
Fused discs ..... 79
Preparing samples for fusion ..... 79
Operation of furnace (Refer to laboratory manual for complete instructions) ..... 79
Preparation cont. ..... 79
Fused disc preparation ..... 80
Nd-Sm and Sr isotope analysis ..... 80
Cleaning vials and teflon bombs ..... 80
Sample preparation ..... 81

Separating Nd, Sm and Sr..... 81
Electron microprobe ..... 82
Appendix E: Geochemical and isotopic data..... 86
..... 86

## LIST OF FIGURES AND TABLES

Figure 1. Regional geological map (2M scale) of the Gawler Range Volcanics located north of the Eyre Peninsula in the central Gawler Craton, South Australia. Sub-circular dashed lines denote each of the 3 other areas in which the LGRV crops out; the Ealbara Rhyolite and Konkaby Basalt at Tarcoola (in the north-western corner of the map), Chitanilga Volcanic Complex at Kokatha, and the Glyde Hill Volcanic Complex at Lake Everard. The Bittali Rhyolite and Waganny Dacite crop out along the southern margin of the Gawler Ranges (coloured in pink) at 7 main localities. As labelled on the map they are referred to in this paper by the following locality names (from west to east); Toondulya Bluff, Narlaby Well, Waganny Dam, Thurlga, Buckleboo, Menninnie Dam and Wartaka. Note the contrasting outcrop distribution between rocks of the LGRV; the linear-like Southern Gawler Ranges Area Volcanics in the south and the volcanic centres in the north-west. Inset map from Allen et al. 2003. ..... 9
Figure 2. An outline of the stratigraphy of the Upper Gawler Range Volcanics and prominent volcanic complexes of the Lower Gawler Range Volcanics. Note the more complex stratigraphy and suite of felsic-mafic rocks at Kokatha and Lake Everard compared to the Southern Gawler Ranges Area. Compiled from descriptions by Allen et al 2003; Allen et al 2008; Blissett 1975; Blissett 1986; Branch 1978; Ferris 2003. .. 12
Figure 3. A simplified graphic log of the observed lithologies across the SGRA. BR-Bittali Rhyolite, WD - Waganny Dacite, UR – 'Unnamed Rhyolite', ER – Eucarro Rhyolite, b.s.p.d – brown sparsely porphyritic dacite, r.s.p.d – red sparsely porphyritic dacite..... 17
Figure 4. Left: A simplified geological map of the Toondulya Bluff area. Sample numbers in red. Right: The different lithofacies of the Waganny Dacite at Toondulya Bluff (modified from Jagodzinski (1985)). ..... 18
Figure 5. Lithologies at Toondulya Bluff. A) Porphyritic Bittali Rhyolite with subhedral potassium feldspars and quartz crystals. B) Brown dacite at the base of the Waganny Dacite. C) Clasts within the brown dacite. D) Microcrystalline, homogenous groundmass textures of the brown dacite, suggesting a lava-like emplacement method. E) Isoclinal flow-folding within the rhyodacitic unit of the Bittali Rhyolite. ..... 19
Figure 6. Rock features at Narlaby Well. A) Elongated amygdales aligned in a vertical orientation. B) Alternating flow-bands defined by phenocryst-rich/phenocryst-poor layers. C) Polished block exposing a large fluorite (Fl) filled amygdale. Dominant k-spar and minor quartz as phenocrysts. D) Thin section - spherical amygdale infilled by quartz and surrounded by a homogenous, microcrystalline groundmass (crossed polars). ..... 20
Figure 7. Locality maps of Narlaby Well (left) and Waganny Dam (right). Sample numbers in red (can be cross-referenced to field observations in Appendix A). ..... 21
Figure 8. Lithologies at Waganny Dam. Polished blocks of: A) Ignimbritic Bittali Rhyolite B) Waganny Dacite; D) 'Unnamed Rhyolite'. C) Thin section – ignimbritic BR displaying lenticular fiamme and broken crystals. E) Weathered surface of the BR displaying its eutaxitic texure. F) Thin section – patchy, altered groundmass of the Waganny Dacite. ..... 21
Figure 9. Lithologies at Thurlga. Polished blocks of: A) Waganny Dacite; B) Bittali Rhyolite. C) Rhyodacite with possible layering, relating to a pyroclastic origin. D) Thin

section – BR displaying well-preserved phenocrysts throughout a homogenous, microcrystalline groundmass (crossed polars). ..... 22
Figure 10. Lithologies at Buckleboo. A) Very-fine grained porphyritic rhyolite. B) Porphyritic rhyolite with angular phenocrysts. C) Highly porphyritic dacite dykes containing xenolith clasts of underlying basement rocks. D) Thin section – BR displaying angular phenocrysts. ..... 23
Figure 11. Locality maps of Thurlga (left) and Buckleboo (right). Sample numbers in red (can be cross-referenced to field observations in Appendix A). ..... 24
Figure 12. Lithologies at Menninnie Dam. A) Crystal rich, coherent rhyolite. B) Fiamme-bearing ignimbrite. C) Thin section – occasional broken crystals within the crystal-rich rhyolite may be fragments of the underlying Warrow Quartzite. D) Well defined hexagonal jointing in the crystal-rich rhyolite. E) Steep bedding orientations of the seriticized ignimbrite at Tank Hill. F) Seriticed ash-tuff..... 25
Figure 13. A) Pumiceous tuff. B) Crystal-rich rhyolite with large phenocrysts of quartz and k-feldspar. C) Porphyritic rhyolite. D) Thin section – vitriclastic texture within a tuff unit. E) Thin section – flow banded rhyolite. F) Thin section – porphyritic rhyolite. ..... 26
Figure 14. Locality maps for Wartaka (left) and Menninnie Dam (right). Sample numbers in red (can be cross-referenced to field observations in Appendix A). ..... 27
Figure 15. Structural measurements collected at various localities. WD – Waganny Dam, MD - Menninnie Dam, TB – Toondulya Bluff, NW – Narlaby Well, FB – Flow banding, APFF – Axial plane of flow folds..... 29
Figure 16. Classification scheme for the SGRAV where total alkalis ($Na_2O + K_2O$) are plotted against silica ($SiO_2$) (TAS diagram)(Le Maitre 1984, Doyle and McPhie 2000). Colours correspond to different rock units: Bittali Rhyolite – pink; Waganny Dacite - purple; unnamed rhyolite - green. Shapes correspond to the different SGRA localities: Toondulya Bluff – solid circles; Narlaby Well – 3-line crosses; Waganny Dam – triangles; Thurlga – squares; Buckleboo – crosses; Menninnie Dam – diamonds; Wartaka – hollow circles. ..... 30
Figure 17. Major oxides vs $SiO_2$. Inflection points occur at $SiO_2$ ~ 72% in $K_2O$ and $Na_2O$ plots. Other elements show continual depletion. Colours correspond to different rock units: Bittali Rhyolite – pink; Waganny Dacite - purple; unnamed rhyolite - green. Shapes correspond to the different SGRA localities: Toondulya Bluff – solid circles; Narlaby Well – 3-line crosses; Waganny Dam – triangles; Thurlga – squares; Buckleboo – crosses; Menninnie Dam – diamonds; Wartaka – hollow circles. ..... 32
Figure 18. Trace elements vs $SiO_2$. Inflection points marking changes from enrichment to decline occur at a common $SiO_2$ level of ~72% in many of the plots (Y, Zr, Nb, Nd). Colours correspond to different rock units: Bittali Rhyolite – pink; Waganny Dacite - purple; unnamed rhyolite - green. Shapes correspond to the different SGRA localities: Toondulya Bluff – solid circles; Narlaby Well – 3-line crosses; Waganny Dam – triangles; Thurlga – squares; Buckleboo – crosses; Menninnie Dam – diamonds; Wartaka – hollow circles. ..... 33
Figure 19. Epsilon Nd at 1592Ma versus MgO (wt%) for the SGRAV, other LGRV areas and the UGRV. The SGRAV samples from this study have been differentiated from the existing data from Stewart (1994). Each of the other LGRV areas broadly conform to individual trends. The most magnesian sample comes from the Chitanilga Volcanic Complex (CVC) at Kokatha. Greater variation in εNd values are seen in the

LGRV (SGRAV in blue, and other areas in grey) compared to the UGRV as a result of assimilation fractional crystallization (AFC) processes. ..... 34
Figure 20. The point at which zircon is just saturated is marked by the red line in diagram 'A'. This correlates to zircon saturation temperature calculations which indicate a magma temperature ranging from 850 ˚C – 920˚C, shown in 'B'. Calibrations and formulations for the zircon saturation temperature from Hanchar and Watson (2003) and Watson and Harrison (1983)..... 37
Figure 21. Major oxides vs $SiO_2$, comparing the Chitanilga Volcanic Complex, Glyde Hill Volcanic Complex, SGRAV and Wartaka area. ..... 38
Figure 22. Nd(ppm) versus $SiO_2$(wt%) highlighting the change in the distribution coefficient (D) to become greater than 1 after $SiO_2$>72%. ..... 41
Figure 23. The relationship between $SiO_2$(wt%) and the percentage of melt remaining through a pure fractonal crystallization model using the Rhyolite MELTs program (Ghiorso and Sack 1995, Gualda et al. 2012). Modelling started from the most primative GRV basalt composition (from Kokatha, sample K8) and fractionated at 3kbar up to a dacitic composition ($SiO_2$ – 63%). The more rhyolitic compositions were then fractionated at 1kbar. This model suggests that the UGRV would be the products of about 80% crystallization. From Tregeagle (2014). ..... 41
Figure 24. Calculated pressures for the SGRAV using the normative albite barometer of Blundy and Cashman (2008). The transition to rhyolitic compostions (>70% $SiO_2$) correlates to a decrease in pressure. Shapes correspond to the different SGRA localities: Toondulya Bluff – solid circles; Narlaby Well – 3-line crosses; Waganny Dam – triangles; Thurlga – squares; Buckleboo – crosses; Menninnie Dam – diamonds. ..... 42
Figure 25. Annotated εNd versus MgO (wt%) chart showing the possibility for mantle source variation associated with the GRV. Trendline A broadly fits the SGRAV dataset and shows relation to both MORB and K8, indicating some variation between the two endmembers, Trendlines B and C correlate better to the LGRV areas: Chitanilga Volcanic Complex (CVC), Glyde Hill Volcanic Complex (GHVC), and Tarcoola. ..... 44
Figure 26. AFC modelling (red line) to best fit the observed εNd and Nd data of the SGRAV (left) and other LGRV areas (right). Each model is occurs in two stages, a first stage before the inflection point and a second stage after the inflection point. Blue circles – SGRAV, red squares – other LGRV (GHVC, CVC and Tarcoola), yellow diamonds – UGRV. The SGRAV fit to a trend (left) where in the first stage Nd Kd – 0.15, r – 0.12 and in the second stage Nd Kd – 2, r – 0.3. The other LGRV data fits to a trend where in the first stage Nd Kd – 0.2, r – 0.55, and in the second stage Nd Kd – 3, r – 0.3. Modelling uses the equation of Powell (1984). ..... 46
Figure 27. Annotated epsilon Nd versus Nd(ppm) showng the two contrasting trends associated with differences in AFC processes. The two AFC models are associated with the SGRAV (shown in red, model 'A') and the other LGRV areas and UGRV (shown in blue, model 'B'). ..... 48

## INTRODUCTION

Large Igneous Provinces (LIPs) represent anomalous igneous events in Earth's history that emplace areally extensive (>0.1 $Mkm^2$) and highly voluminous magmas (>0.1 $Mkm^3$) over relatively short time periods (<50 Ma), and which are dominantly mafic in composition (Bryan and Ernst 2008). Across the world, LIPs are represented by flood basalt provinces (eg. Deccan Traps, Columbia River), flood basalts with large volume silicic units (eg. quartz latites of the Paraná- Etendeka province, Snake River Plain in Yellowstone) and felsic-dominated large igneous provinces (eg. Gawler Range Volcanics) (Bryan et al. 2010, Pankhurst et al. 2011). Emplacement of widespread felsic units in Silicic Large Igneous Provinces (SLIPs) is controlled by the style of eruption (explosive or effusive) and viscosity. In most cases, extensive areal coverage of felsic material is achieved through surge flows and ash falls associated with explosive eruptions (Bryan et al. 2010). However, in some LIPs across the world such as the Paraná-Etendeka province, Yellowstone volcanic field, and Gawler Range Volcanics, the dominant silicic units are lavas that have viscosities comparable to that of flood basalts (Giordano et al. 2008, Pankhurst et al. 2011). The low viscosities of these felsic lavas are controlled primarily by their high temperatures (800 °C - 1100 °C) and elevated fluorine contents (>1000ppm) (Agangi et al. 2012).

The Mesoproterozoic Gawler Range Volcanics (GRV) have been widely described as a Silicic Large Igneous Province (SLIP) that has an outcrop extent of ~25,000 $km^2$ and comprises a younger upper sequence and an older lower sequence (Blissett 1993). Research has primarily been focussed on the extensive rhyolitic-dacitic lava flows of the upper sequence or Upper Gawler Range Volcanics (UGRV) due the atypical nature of its felsic magma emplacement (Agangi 2011, Allen et al. 2008, Allen et al. 2003,

Creaser and White 1991, McPhie et al. 2008). Much less discussed is the lower sequence or Lower Gawler Range Volcanics (LGRV), which locally appear as discrete volcanic centres in the north west of the Gawler Ranges (e.g. the Chitanilga and Glyde Hill volcanic complexes) (Allen et al. 2008, Stewart 1994). The Bittali Rhyolite (BR) and Waganny Dacite (WD) are exposed discontinuously along the south and south western margins of the GRV. Unlike other LGRV units, the BR and WD of the Southern Gawler Ranges Area (SGRA) are not as easily attributed to a specific volcanic centre because of their curvilinear spatial distribution (Blissett 1993, Stewart 1994). The Bittali Rhyolite and Waganny Dacite are part of the 'developmental phase' of volcanism according to Stewart (1994), where numerous small volume magma systems assimilate crustal rocks to varying degrees while fractionation occurs, producing isotopic and compositional heterogeneity in the felsic volcanic deposits.

In this paper, the BR and WD are petrologically and geochemically characterised, through field observations and laboratory work on samples taken along the 200km E-W extent of discontinuous outcrop from Toondulya Bluff in the west to Wartaka in the east. These observations/analytical techniques will aim to uncover: 1) characteristics of the BR and WD, and if they are part of one volcanic sequence; 2) relationships to the other LGRV areas and the GRV as a whole; 3) methods of emplacement (effusive, explosive?) and the type(s) of source (point source, fissure); 4) petrogenesis (using isotope and geochemical analysis).

## REGIONAL GEOLOGY

The Mesoproterozoic Gawler Range Volcanics and co-magmatic Hiltaba Suite granites are an extensive Silicic Large Igneous Province (SLIP) covering ~25,000 $km^2$ in the central Gawler Craton, north of the Eyre Peninsula (Allen et al. 2008, Phillips 2006).

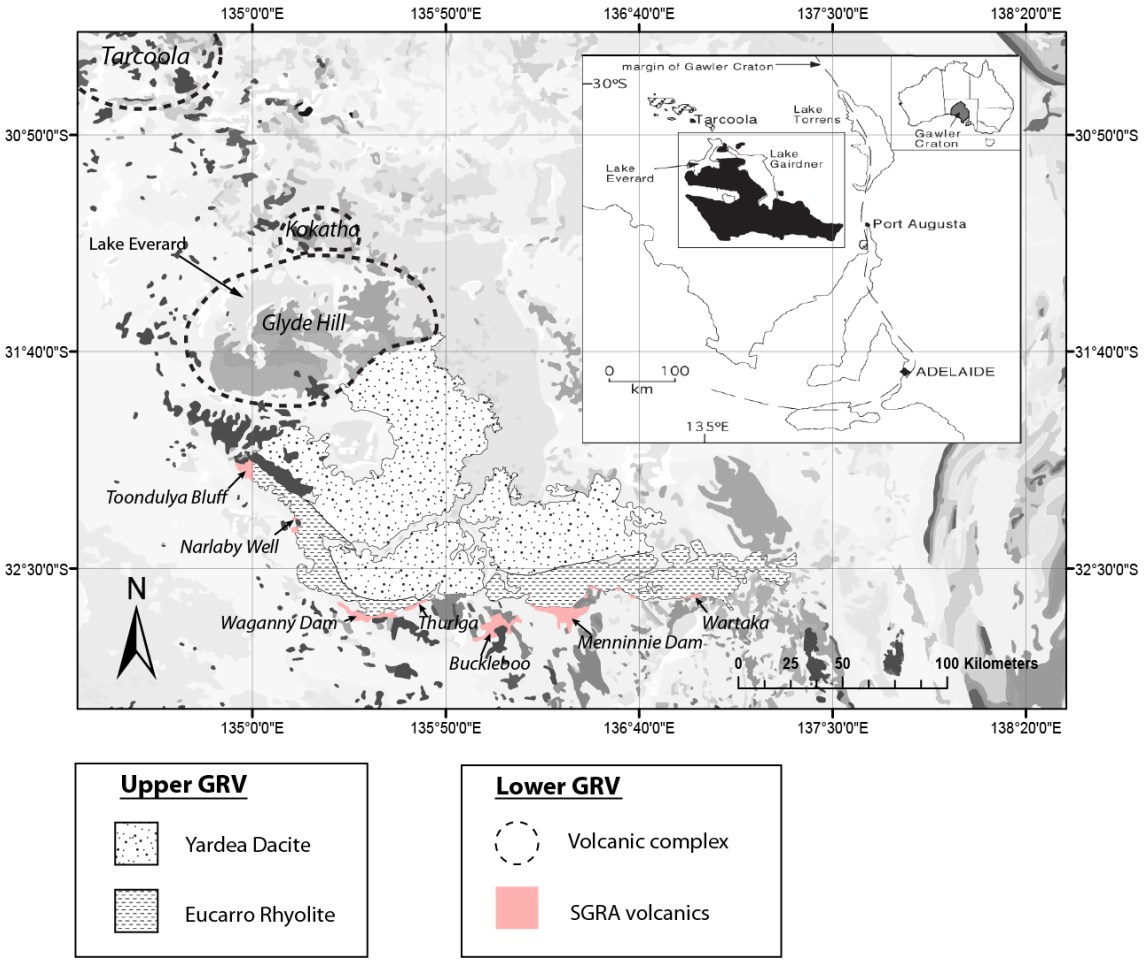


**Figure 1. Regional geological map (2M scale) of the Gawler Range Volcanics located north of the Eyre Peninsula in the central Gawler Craton, South Australia. Sub-circular dashed lines denote each of the 3 other areas in which the LGRV crops out; the Ealbara Rhyolite and Konkaby Basalt at Tarcoola (in the north-western corner of the map), the Chitanilga Volcanic Complex at Kokatha, and the Glyde Hill Volcanic Complex at Lake Everard. The Bittali Rhyolite and Waganny Dacite crop out along the southern margin of the Gawler Ranges (coloured in pink) at 7 main localities. As labelled on the map they are referred to in this paper by the following locality names (from west to east); Toondulya Bluff, Narlaby Well, Waganny Dam, Thurlga, Buckleboo, Menninnie Dam and Wartaka. Note the contrasting outcrop distribution between rocks of the LGRV; the linear-like Southern Gawler Ranges Area Volcanics in the south and the volcanic centres in the north-west. Inset map from Allen et al. 2003.**

Magma volumes of the GRV are estimated as being greater than 25,000km$^3$ with at least 90% of felsic composition (McPhie et al. 2008, Phillips 2006). The GRV also extends in the subsurface to the north east where it is overlain by Neoproterozoic sedimentary rocks of the Stuart Shelf as well as Phanerozoic cover, with an estimated total areal extent of ~ 90, 000km$^2$ (McPhie et al. 2008, Turner 1975). Combined with the Hiltaba Suite granites, the volume of felsic magma in the province exceeds 100,000 km$^3$

(McPhie et al. 2008). However, these figures are only minimum estimates as the GRV has been partly eroded (Agangi 2011, Blissett 1993). In fact, the igneous province is suggested to have extended well beyond the current area, supported by 1.6 Ga felsic volcanic clasts interpreted to be GRV found in Antarctica, and the temporally, geochemically, and isotopically related Benagerie Volcanic Suite (BVS) in the Curnamona Province (NE of the Flinders Rangers) (Peucat et al. 2002, Wade et al. 2012). In outcrop, they mostly appear a brick-red colour due to oxidation (Allen et al. 2003).

The most recent deformational event, the Kararan Orogeny (1570 – 1540Ma), has been largely restricted to the central-northern part of the Gawler Craton and as such the rocks remain almost entirely undeformed (Daly et al. 1998, Hand et al. 2007). Ages for the oldest and youngest volcanic units of the GRV (U-Pb zircon dating) are 1592 ± 3 Ma and 1591 ± 3 Ma, indicating that volcanism occurred over a relatively short time interval (Allen et al. 2008, Fanning et al. 1988). The bimodal Hiltaba Suite granites are considered to be coeval with the GRV due to an overlap in age estimates (1590 – 1575 Ma for the Hiltaba Suite)(Flint 1993).

The upper flow units of the GRV were originally thought to represent extensive welded ashflow tuffs but have since been interpreted as widescale lava flows based on field observations characteristic of effusive eruptions such as amygdaloidal upper parts, an evenly porphyritic texture, and presence of compostitional flow bands and mingled domains (Blissett 1975, Garner and McPhie 1999, Giles 1977, McPhie et al. 2008, Morrow and McPhie 2000). The GRV overlies and intrudes ortho- and paragneiss of the Neoarchaean Sleaford Complex (2555 – 2480 Ma) and metasediment of the

Palaeoproterozoic Hutchison Group (2000 – 1790 Ma), which were locally intruded by granite and gneisses during the Kimban Orogeny.

The LGRV are expressed as discrete volcanic centres such as the Chitanilga Volcanic Complex (CVC) at Kokatha, Glyde Hill Volcanic Complex (GHVC) at Lake Everard, Menninnie Dam Volcanic Complex at Nonning, the Roopena Basalt at Roopena and the Ealbara Rhyolite and Konkaby Basalt at Tarcoola (Allen et al. 2008, Wade et al. 2012). The best exposed are at Kokatha and Lake Everard, which each comprise a suite of volcanics from low silica (basalt) to high silica (rhyolite) and distributed as numerous interleaved lava flows and pyroclastic units (Blissett 1986).

## Southern Gawler Ranges Area Volcanics (SGRAV)

The stratigraphy of the Southern Gawler Ranges Area Volcanics (SGRAV) is much less complex than the Glyde Hill Volcanic Complex and Chitanilga Volcanic Complex as it is represented by only two volcanic units, the older Waganny Dacite (WD) and younger Bittali Rhyolite (BR). A highly weathered, sparsely porphyritic rhyolite underlies the WD at in the Paney area and is referred to herein as the 'Unnamed Rhyolite' (UR) (Figure 2) (Blissett 1986).

The WD has been described previously as a dacitic-rhyodacitic unit comprised of lava flows, crystal rich volcaniclastic facies and monomictic breccias that have been intruded by brecciated dykes (Allen et al. 2008). It is overlain by the BR, a composite unit of rhyolites and rhyodacites manifest as lava flows, ignimbrites, welded ash flows, lava domes, breccias and feeder dykes (Allen et al. 2008, Blissett 1986). The BR is characterised by abundant rounded quartz crystals (2mm in size) in the rhyolites and lesser amounts in the rhyodacites (Allen et al. 2008, Blissett 1986).

Previous investigations into the SGRA volcanics have focussed on exposures at Toondulya Bluff, Menninnie Dam and Wartaka (Jagodzinski 1985, Roache 1996, Turner 1975). At Toondulya Bluff Jagodzinski (1985) described a sequence of sparsely porphyritic dacites and rhyolites overlain by the Yardea Dacite. These dacites have since been equated with the WD and BR (Blissett 1987).

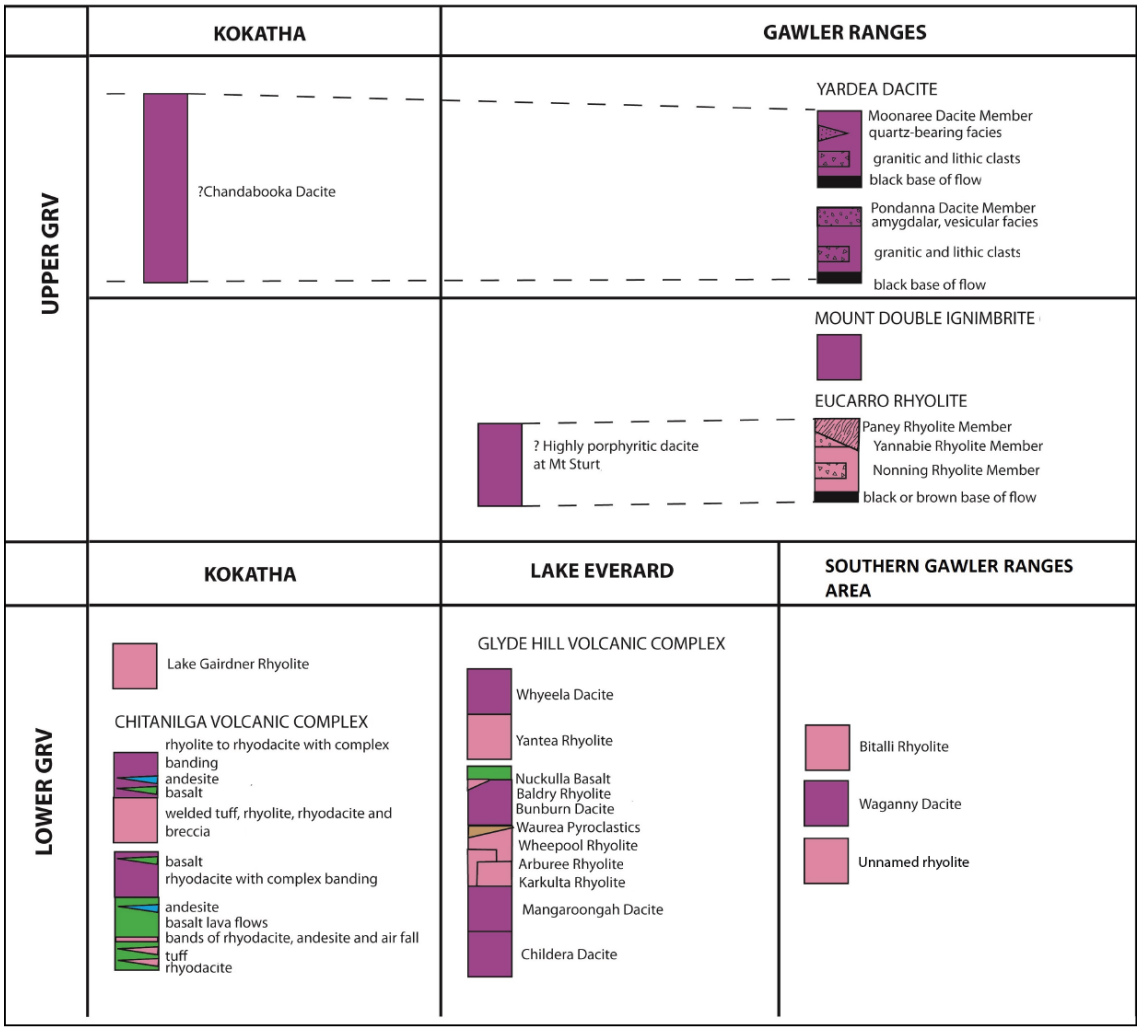


**Figure 2. An outline of the stratigraphy of the Upper Gawler Range Volcanics and prominent volcanic complexes of the Lower Gawler Range Volcanics. Note the more complex stratigraphy and suite of felsic-mafic rocks at Kokatha and Lake Everard compared to the Southern Gawler Ranges Area. Compiled from descriptions by Allen et al 2003; Allen et al 2008; Blissett 1975; Blissett 1986; Branch 1978; Ferris 2003.**

Diamond core drilling into the Bittali Rhyolite at Menninnie Dam revealed a small volume (<1km$^3$) hydroexplosive rhyolitic centre (Roache et al. 2000). The Menninnie

Dam area hosts Zn-Pb-Ag mineralization in breccias, and has been subject to 32 exploration drill holes (Roache 1996). Roache et al. (2000) interpreted 3 main rock types from drill core; a coherent rhyolite, a polymictic breccia, and a lithic-rich welded ignimbrite. From textural, compositional and stratigraphic relationships between the different lithologies, Roache et al (2000) suggested that the rocks are products of a single eruptive cycle that shifted from "wet" explosive phreatomagmatic eruptions to "dry" effusive lava flows.

In the Wartaka area, Turner (1975) identified an interbedded volcanic sequence of lithic/lapilli/crystal/pumiceous tuffs and porphyritic rhyolites bounded by the E-W trending Uno Fault to the south. A potential subsidence type structure was described to the north which may be a possible source (Turner 1975).

# BACKGROUND

## Petrogenetic models

The GRV was first suggested to have evolved from lithospheric extension in an anorogenic setting (Giles 1988). Later reconstructions place the GRV (and BVS) magmatics in an intra-continental setting adjacent to a subduction zone (Wade et al. 2012). In this model, major crustal melting was as a result of lithospheric extension (due to slab roll back) and subsequent upwelling asthenosphere (higher heat flow). At a more regional scale the GRV have been suggested to be the initial stages of a hot spot track from the Gawler Craton to the Mount Isa Inlier in north eastern Australia, based on isotopic/geochemical indicators of mantle plume interaction with the continental lithosphere along with the spatial and temporal distribution of A-type magmas (Betts and Giles 2006, Betts et al. 2009, Stewart 1994).

Stewart (1994) proposed a two-stage model for the genesis of the GRV represented by 'developmental phase' and 'mature phase' volcanism associated with the LGRV and UGRV respectively. According to Stewart (1994), the 'developmental phase' involved lithophile element enriched mafic melts that underwent crustal assimilation and fractional crystallization (AFC processes), producing a chemically heterogeneous magma. Continual supply of mafic melts to the small developmental magma systems caused an overall increase in volume, leading to the coalescence of these small chambers into one larger magma chamber. Convective flows in the large magma chamber caused by this event promoted mixing, creating a chemically homogeneous magma as reflected by the UGRV (Stewart 1994). The thick (<1km) felsic rocks of the developmental phase trapped the underlying mafic melts from extruding to the surface (explaining the absence of mafics in the UGRV) (Betts et al. 2009, Stewart 1994).

## Emplacement methods

Discerning the method(s) of emplacement associated with the rock types of the SGRAV is achieved through petrographical observations, which allow for a distinction between pyroclastic flows (particulate) and lava flows (non-particulate). In general, silicic volcanism in LIPs has occurred through explosive eruptions depositing areally extensive ignimbrite/welded-tuff sheets. However, in some instances in the geologic record, these widespread silicic units have been emplaced effusively through low viscosity, high temperature lava flows eg. Snake River Plain in Yellowstone, quartz latities of the Paraná-Etendeka province in Namibia, Rooiberg Felsite in South Africa (Ewart et al. 1998, Hildreth et al. 1991, Twist and French 1983). In some cases, pyroclastic flows that are manifest as rheoignimbrites (eg. Trans-Pecos volcanic field)

possess many shared characteristic with extensive lava flows which makes distinguishing the two very difficult (Henry et al. 1988).

Typically lava flows are distinguished on features such as an evenly porphyritic texture, intact crystals, flow banding, elongate vesicles and mingled domains, whereas pyroclastic flows are generally characterized by broken crystals, unevenly distributed phenocrysts, fiamme textures, and lithic fragments (Garner and McPhie 1999, McPhie 1993, Morrow and McPhie 2000). As previously mentioned, these identification tools are not mutually exclusive and can occur both in pyroclastics (rheoignimbrites) and lava flows.

## METHODS

Field work was undertaken in the southern Gawler Ranges at a set of localities where the WD and BR had been previously mapped by A. H Blissett (1975). The target localities for collecting rock samples and making field observations that were chosen provided an even geographic spread of the BR and WD. Across the 200km lateral extent of field area, rock samples showing the least amount of alteration and weathering were chosen for geochemical analysis, with an eventual total of 19 samples collected; 4 from Toondulya Bluff, 2 from Narlaby Well, 4 from Waganny Dam, 3 from Thurlga, 4 from Buckleboo and 3 from Menninnie Dam. Geochemical data, field observations and rock samples from the Wartaka area were acquired from the Geological Survey of South Australia.

Laboratory work was conducted at Adelaide University and Adelaide Microscopy. Rock samples were first crushed and milled to a fine powder to provide a base for

geochemical analysis. Sample powders were made into fused discs and pressed pellets before being sent to the CSIRO for analysis of major oxides and trace elements using X-ray fluorescence (XRF).

Isotope analysis of five samples from Waganny Dam, Thurlga and Buckleboo aimed to build on existing Nd-Sm data from Toondulya Bluff, Menninie Dam and Wartaka . The selected samples of Bittali Rhyolite, Waganny Dacite and 'unnamed rhyolite' were chosen to give a reasonably even spread across the central SGRA up to the existing data points (Toondulya Bluff in the west, Menninnie Dam/Wartaka in the east).

Polished thin sections facilitated in determining emplacement methods (lava/pyroclastic) and were analyzed for feldspar and quartz-hosted melt inclusions compositions using the electron microprobe at Adelaide Microscopy. The aim of which was to use the 2-feldspar geothermometer of Putirka (2008) by inputting plagioclase and alkali feldspar compositions for temperature estimates. Unfortunately, the majority of feldspars had completely unmixed into pure endmembers and were unusable. A small amount of alkali feldspars showed compositions which suggested they were well mixed and were therefore used in temperature calculations, with the groundmass composition substituted for plagioclase.

## OBSERVATIONS AND RESULTS

### Petrography

#### STRATIGRAPHY AND INTERPRETATION

In this section, field observations made on the Bittali Rhyolite, Waganny Dacite, and 'Unnamed Rhyolite' at 7 different localities across the SGRA are compiled and used to form an interpretation. Previous work in several areas (Toondulya Bluff, Menninnie

Dam, Wartaka) is acknowledged and used in conjunction with observations made in this study (Jagodzinski 1985, Roache 1996, Turner 1975). A simplified stratigraphic section of observed rock types at each of the SGRA localities is presented in Figure 3. For full rock and thin section descriptions, see Appendices A and B.

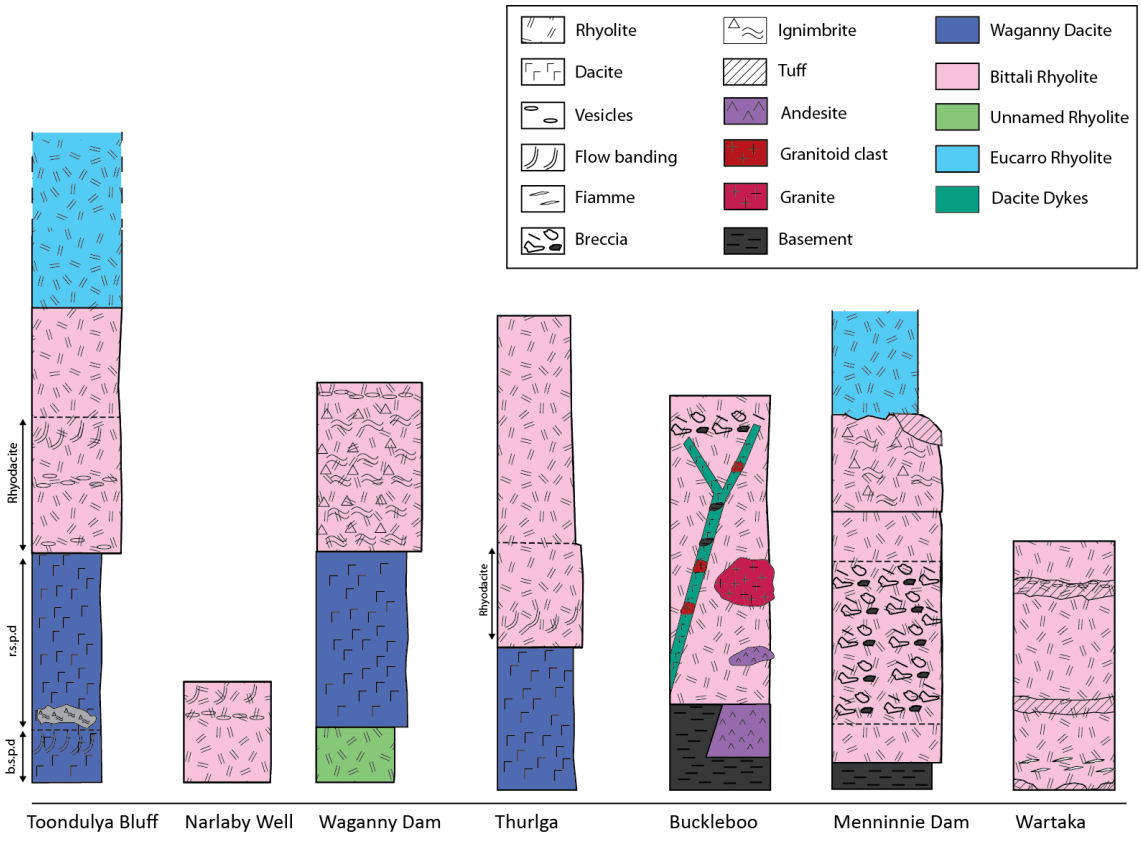


**Figure 3. A simplified graphic log of the observed lithologies across the SGRA. BR- Bittali Rhyolite, WD - Waganny Dacite, UR – 'Unnamed Rhyolite', ER – Eucarro Rhyolite, b.s.p.d – brown sparsely porphyritic dacite, r.s.p.d – red sparsely porphyritic dacite.**

## Toondulya Bluff

At Toondulya Bluff, rock types are characterised by a sparsely porphyritic texture, small phenocryst sizes (<2.5mm) and for the most part have a brick-red groundmass colour (Figure 5). The Waganny Dacite represents the immature, early stages of volcanism in the area with different lithofacies marking changes in eruption styles and/or magma chamber conditions. The basal unit, referred to here as 'brown dacite', is distinguished

by a paucity of phenocrysts, and largely aphyric texture, representing the earliest stages of crystal fractionation. Jagodzinski (1985) noted several lenticular-shaped units overlying the brown dacite that were highly porphyritic and contained clasts of the underlying volcanics. These were interpreted to be pyroclastics that deposited at the start of the second phase of volcanism after a short hiatus in which the main vent was closed. The second sequence is represented by a relatively voluminous lava flow (homogenous texture throughout, evenly porphyritic), termed the 'red dacite' (Figure 4). The BR in this area is a composite unit of rhyodacite overlain by a rhyolite (Figure 4). Observations in the rhyodacite such as complex geometries of flow-bands/ flow folds that associate with high viscosity magmas and bedding orientations that differ from the overall easterly dip in the area led Jagodzinski (1985) to interpret the unit as a lava dome. The overlying rhyolite possesses characteristics that would favour a lava-like emplacement such as a coherent texture, flow-banding, and rounded/well preserved phenocrysts (Henry and Wolff 1992, McPhie 1993).

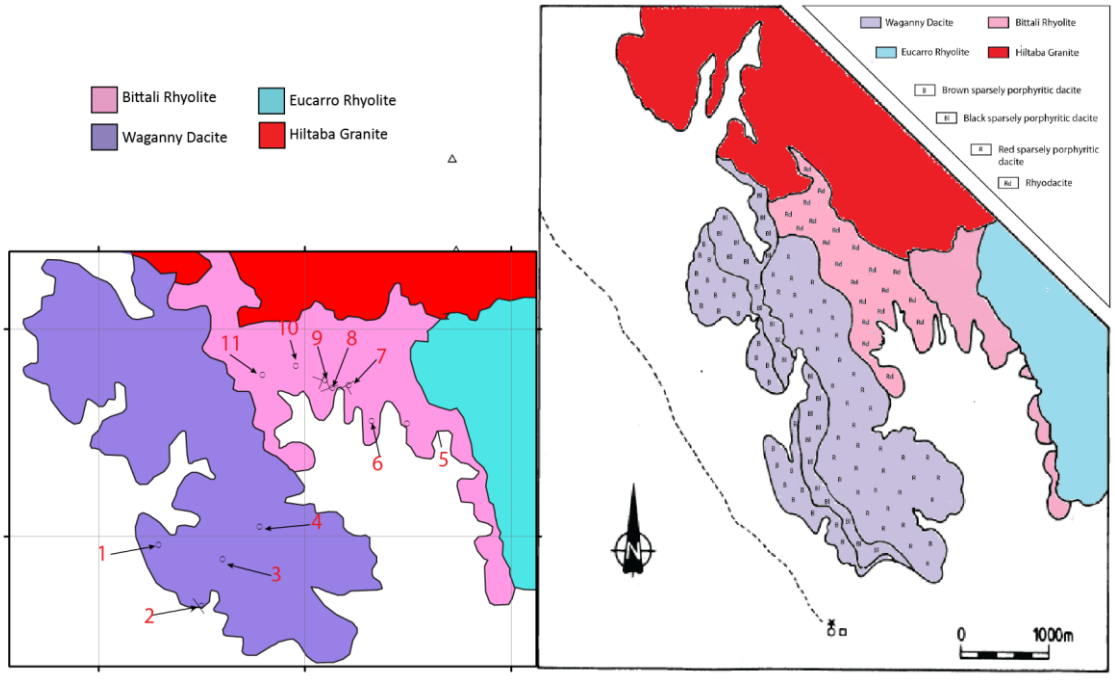


**Figure 4. Left: A simplified geological map of the Toondulya Bluff area. Sample numbers in red. Right: The different lithofacies of the Waganny Dacite at Toondulya Bluff (modified from Jagodzinski (1985)).**

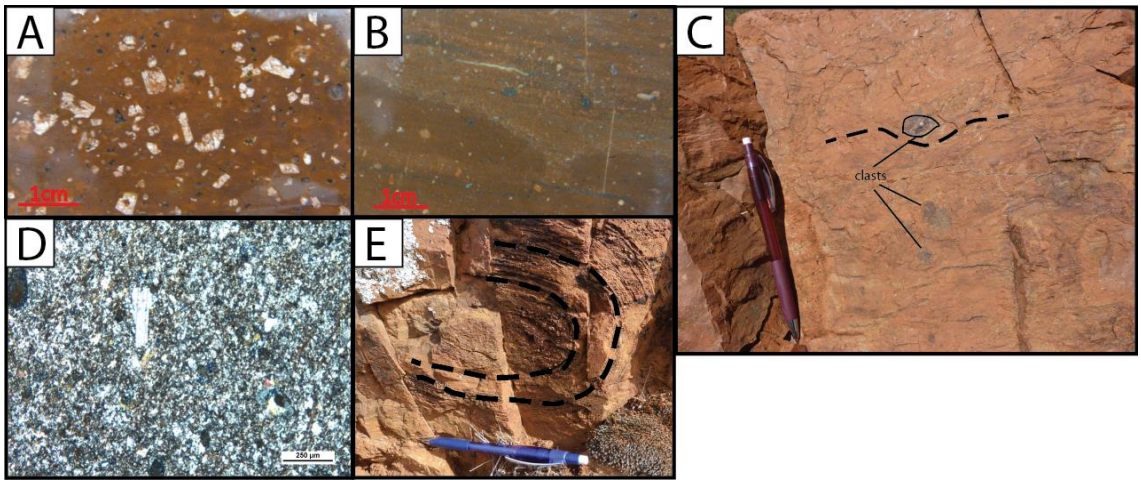


**Figure 5. Lithologies at Toondulya Bluff. A) Porphyritic Bittali Rhyolite with subhedral potassium feldspars and quartz crystals. B) Brown dacite at the base of the Waganny Dacite. C) Clasts within the brown dacite. D) Microcrystalline, homogenous groundmass textures of the brown dacite, suggesting a lava-like emplacement method. E) Isoclinal flow-folding within the rhyodacitic unit of the Bittali Rhyolite.**

## Narlaby Well

The rhyolite at Narlaby Well displays features that suggest this small outcrop represents the upper section of a lava-flow including; amygdales, flow-banding, evenly porphyritic texture, and immediate stratigraphic position below the Eucarro Rhyolite. Vertically aligned amygdales that were noted in one place may suggest emplacement as a dyke or that they are pipe-amygdales (common in lava flows). The latter interpretation is preferred given observations of contorted flow banding in the overlying section. Minor amounts of quartz phenocrysts in the rock make a clear distinction as BR difficult, given that a key characteristic of the BR are abundant round quartz crystals. The absence of WD in the area could be attributed to the flat-lying topography to the west under which it may be buried.

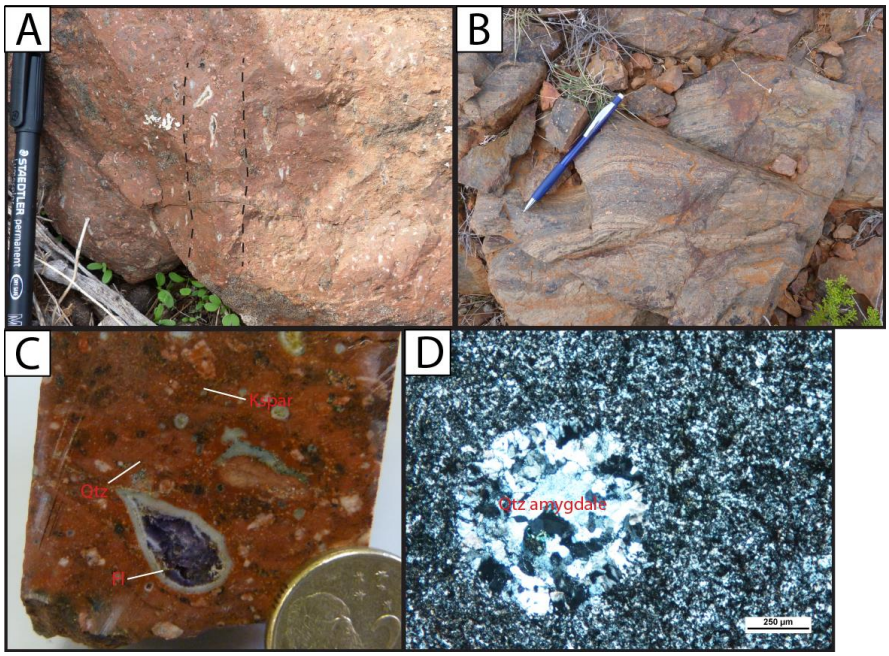


**Figure 6. Rock features at Narlaby Well. A) Elongated amygdales aligned in a vertical orientation. B) Alternating flow-bands defined by phenocryst-rich/phenocryst-poor layers. C) Polished block exposing a large fluorite (Fl) filled amygdale. Dominant k-spar and minor quartz as phenocrysts. D) Thin section - spherical amygdale infilled by quartz and surrounded by a homogenous, microcrystalline groundmass (crossed polars).**

## Waganny Dam

The stratigraphy at Waganny Dam is unlike other localities as it is represented by a third unit, the 'Unnamed Rhyolite' (UR). The relative position of the 'UR' is seemingly ambiguous as the main outcrop is small and positioned between outcrops of WD (Figure 7). However, it has been is interpreted to lie at the base of the stratigraphic pile due to its slightly northward dipping beds and topographic low position relative to the WD. A rhyolite sample found further south beyond the WD by Stewart (1994) also supports this. A narrow band of black rhyolite directly adjacent to the UR possesses a coarser groundmass which may suggest an intrusive origin (dyke). Although the WD shows some pyroclastic features (angular phenocrysts), more comprehensive evidence in thin section is lacking (broken crystals, glass shards). The BR to the north, exhibits

characteristic features of a pyroclastic deposit such as a eutaxitic texture and fiamme (Figure 8) (McPhie 1993).

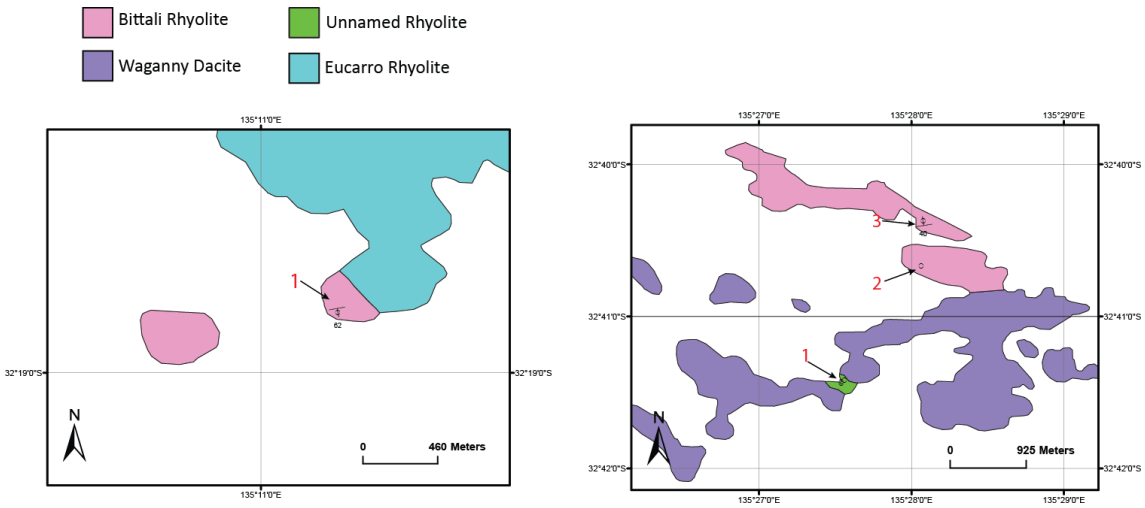


**Figure 7. Locality maps of Narlaby Well (left) and Waganny Dam (right). Sample numbers in red (can be cross-referenced to field observations in Appendix A).**

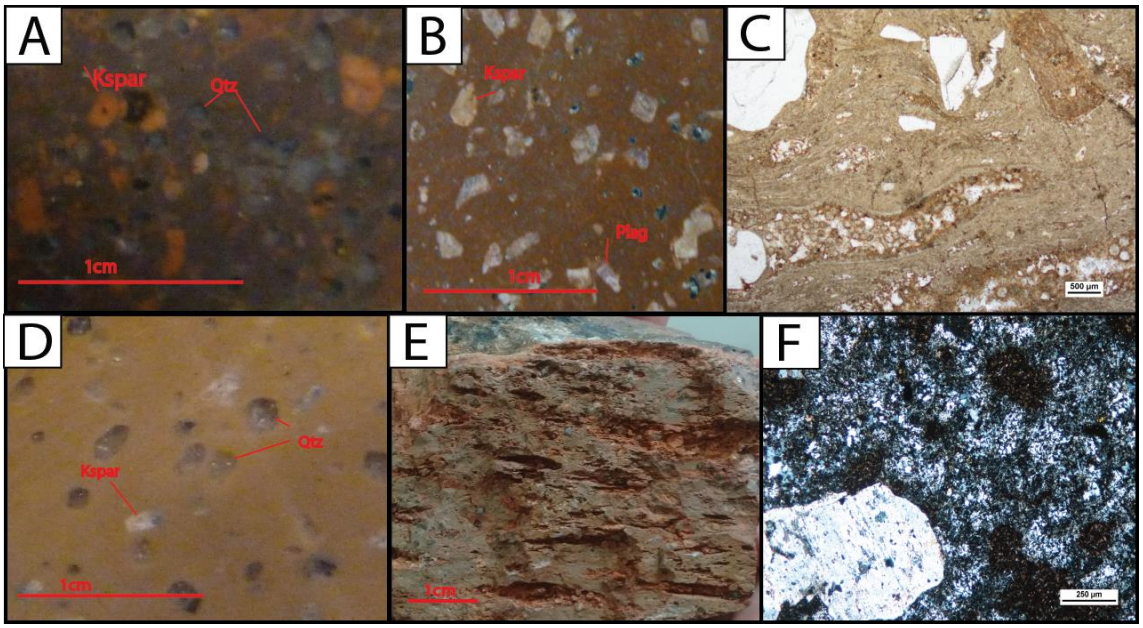


**Figure 8. Lithologies at Waganny Dam. Polished blocks of: A) Ignimbritic Bittali Rhyolite B) Waganny Dacite; D) 'Unnamed Rhyolite'. C) Thin section – ignimbritic BR displaying lenticular fiamme and broken crystals. E) Weathered surface of the BR displaying its eutaxitic texure. F) Thin section – patchy, altered groundmass of the Waganny Dacite.**

## Thurlga

The WD and BR exposed at Thurlga are more readily distinguished as products of an effusive eruption based on features such as well preserved, euhedral phenocrysts, a glassy groundmass and an evenly porphyritic texture (Figure 9). An intermediate rhyodacite unit crops out between the exposures of WD and BR, and possesses a coarser groundmass, and whispy streaks (fiamme?) in the interstitial space between crystals which may allude to a pyroclastic origin. As the rhyodacite contains abundant ~2mm quartz crystals, it is classified here as BR rather than WD as it has been previously assigned (Blissett 1987). The BR lies on an adjacent hillside to the west (Figure 11) and shows typical features of a lava-like method of emplacement (evenly porphyritic, well preserved phenocrysts, homogenous). Thurlga marks the farthest point to the east in which WD is observed.

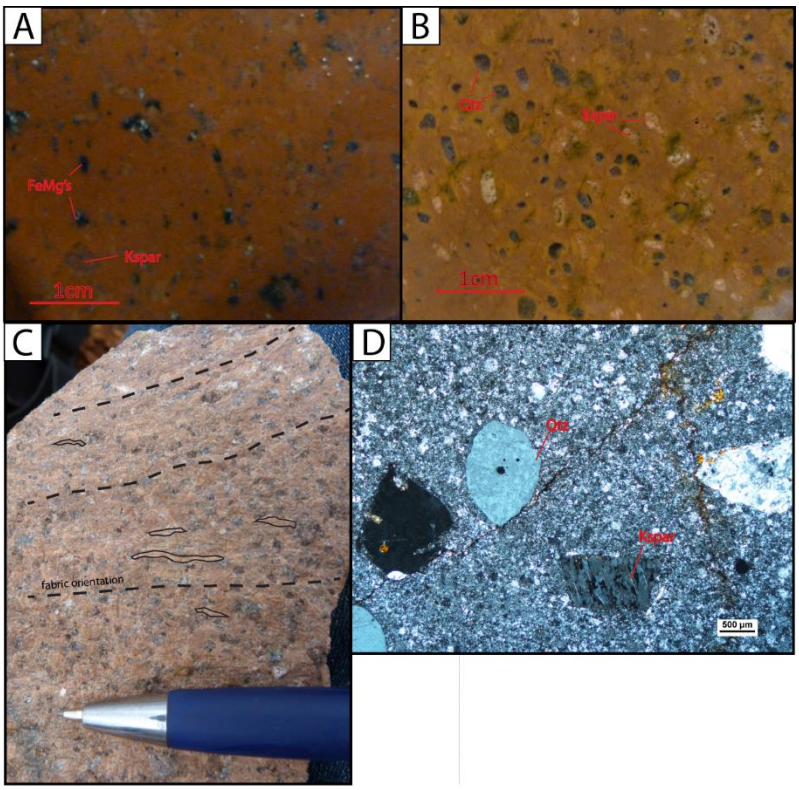


**Figure 9. Lithologies at Thurlga. Polished blocks of: A) Waganny Dacite; B) Bittali Rhyolite. C) Rhyodacite with possible layering, relating to a pyroclastic origin. D) Thin section – BR displaying well-preserved phenocrysts throughout a homogenous, microcrystalline groundmass (crossed polars).**

## Buckleboo

Greater lithological variation is seen at Buckleboo (60km north-west of Kimba) with andesitic-rhyolitic rocks, breccias, and exposed basement rocks at the surface (Warrow Quartzite of the Hutchison Group). As noted by Blissett (1986), the WD is not present in the area, and as such the BR appears to overlie an aphanitic andesitic unit (which is mapped as WD, assumingly due to its similar stratigraphic position) and basement rocks of the Hutchison Group. It seems apparent that the area has predominately undergone explosive volcanic activity from observations of highly angular quartz phenocrysts and presence of xenolith clasts in the rhyolites (Figure 10). Highly porphyritic dacite dykes intrude the BR, and contain xenoliths of underlying rock units which suggests they intruded later in the geologic history. They also appear petrographically similar (only differ in porphyritic texture, and lack of quartz phenocrysts) to the Hiltaba Suite granite, which may suggest that the two are genetically (and temporally?) related.

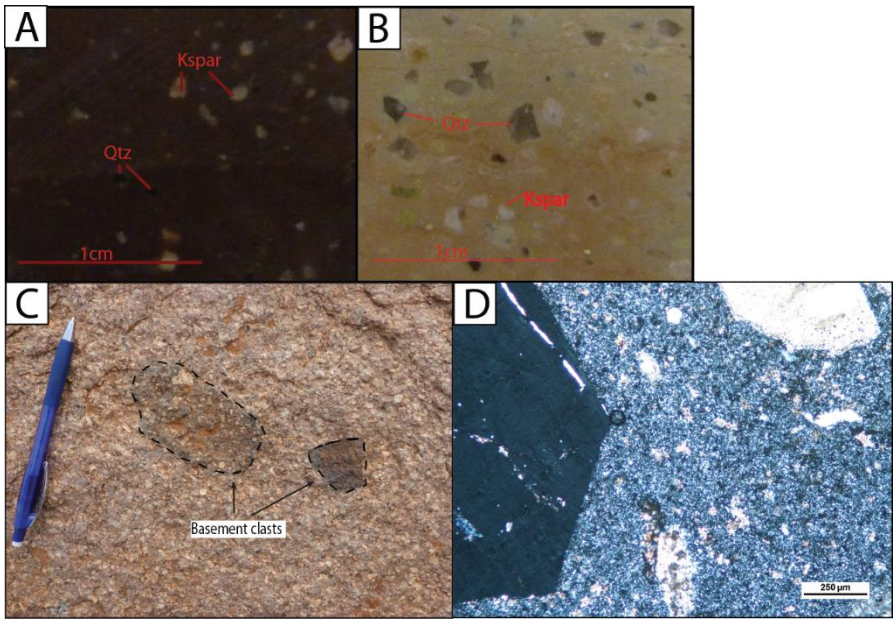


**Figure 10. Lithologies at Buckleboo. A) Very-fine grained porphyritic rhyolite. B) Porphyritic rhyolite with angular phenocrysts. C) Highly porphyritic dacite dykes containing xenolith clasts of underlying basement rocks. D) Thin section – BR displaying angular phenocrysts.**

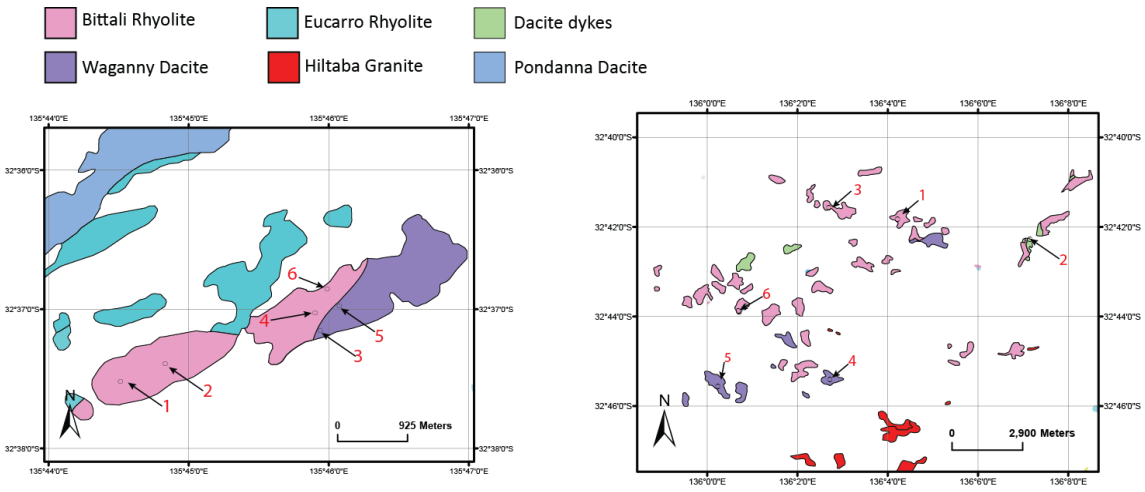


**Figure 11. Locality maps of Thurlga (left) and Buckleboo (right). Sample numbers in red (can be cross-referenced to field observations in Appendix A).**

## Menninnie Dam

Lithologies at Menninnie Dam identify mainly with explosive volcanism and compositions that are exclusively rhyolitic. The BR is exposed at the surface as 3 main lithofacies; a crystal-rich rhyolite, an ash tuff, and a widespread ignimbrite unit that has been deeply seriticized in places. Several drill cores (MD25=192459, MD31=192444, MD32=192464) from the area intersect polymict/monomict breccias and rhyolites correlated with the GRV. Drill hole MD 31 comprises an evenly porphyritic rhyolite in the upper sections (146.9m – 174.5m) which has similar appearance to the crystal-rich rhyolite. If the crystal-rich rhyolite is interpreted as a lava-flow (evenly porphyritic texture, well preserved phenocrysts) its distribution is surprisingly widespread (near identical lithologies separated N-S by ~4.5km) considering the association of higher crystallite contents with higher viscosities (Giordano et al. 2008). This observation, along with the scattered distribution of outcrops and a relatively large areal extent (12km E-W) suggest that the volcanics have erupted via multiple vents (Figure 14). The ignimbrite unit, termed the ‘Menninnie Dam ignimbrite’ shows a eutaxitic texture on

weathered surfaces and continual exposures towards the north east where it transitions to a seriticized ash tuff (Figure 12).

Potential mechanisms proposed for the emplacement of various units at Menninnie Dam have been described by Roache (1996), who suggests that interactions of rising rhyolitic magma with fault-hosted groundwater deposited a polymict breccia unit, which was then followed by the eruption of the main magma body (crystal-rich rhyolite). A younger lithic-rich welded ignimbrite overlies the rhyolite (Roache et al. 2000). Tank Hill (635268E, 6391495N) is likely one of multiple sources for the younger ignimbrite unit, supported by steeply-dipping beds and stronger sericite alteration. In the north east, the well sorted ash tuff may represent a low energy aqueous environment (pond?) and the final phase in BR volcanism prior to deposition of the Eucarro Rhyolite.

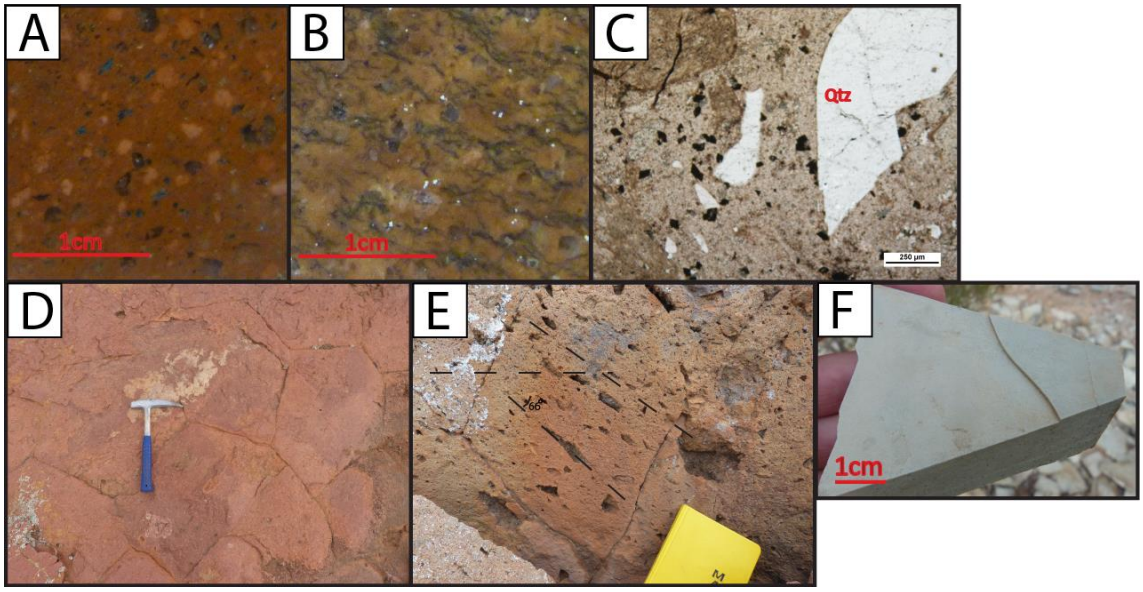


**Figure 12. Lithologies at Menninnie Dam. A) Crystal rich, coherent rhyolite. B) Fiamme-bearing ignimbrite. C) Thin section – occasional broken crystals within the crystal-rich rhyolite may be fragments of the underlying Warrow Quartzite. D) Well defined hexagonal jointing in the crystal-rich rhyolite. E) Steep bedding orientations of the seriticized ignimbrite at Tank Hill. F) Seriticed ash-tuff.**

## WARTAKA

The volcanics at Wartaka comprise a sequence of interbedded rhyolitic tuffs and lavas exposed as a narrow band ouctrop (1km N-S, 7km E-W) and are bound by the E-W trending Uno Fault at the southern margin (Figure 14). The volcanics display steep northward dipping beds, likely as a result of a ramp type structure associated which the Uno Fault. The units observed at Wartaka correlate to many of the rock units identified by Turner (1975). The array of distinct lithologies intercalated within a relatively narrow (1km) zone of outcrop may suggest close proximity to a source vent. The deposition of a highly crystal-rich and viscous lava (?) in the area adds to this claim. Moreover, notably large phenocrysts which appear to be aggregates of smaller crystals in the crystal-rich rhyolite may suggest a slower rate of cooling or closer proximity to a heat source (vent) (Figure 13). The sequence was classified as a single volcanic unit by (Turner 1975) based on geochemical observations.

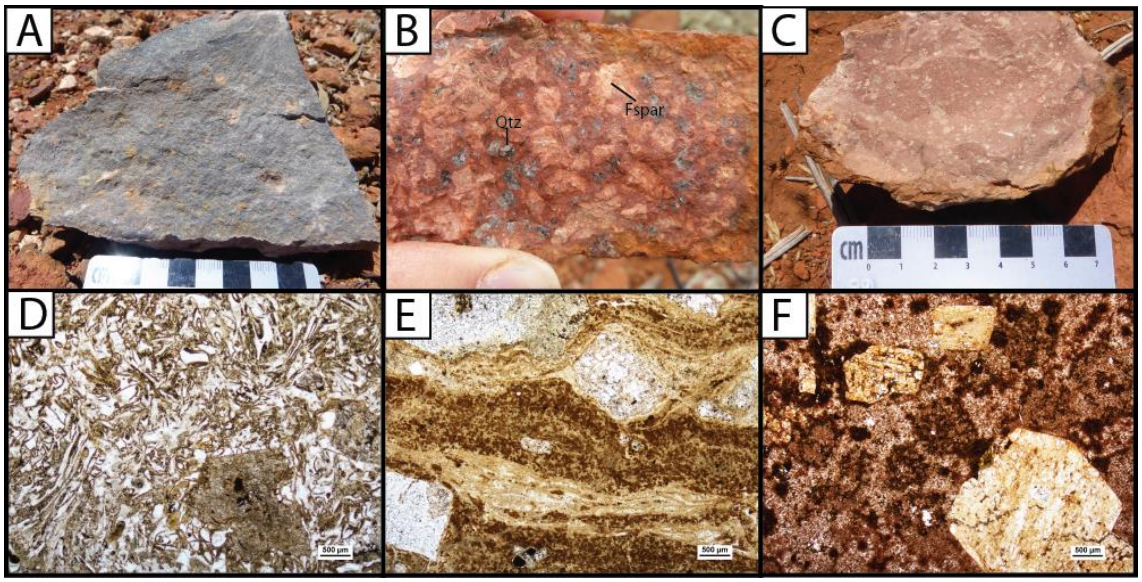


**Figure 13. A) Pumiceous tuff. B) Crystal-rich rhyolite with large phenocrysts of quartz and k-feldspar. C) Porphyritic rhyolite. D) Thin section – vitriclastic texture within a tuff unit. E) Thin section – flow banded rhyolite. F) Thin section – porphyritic rhyolite.**

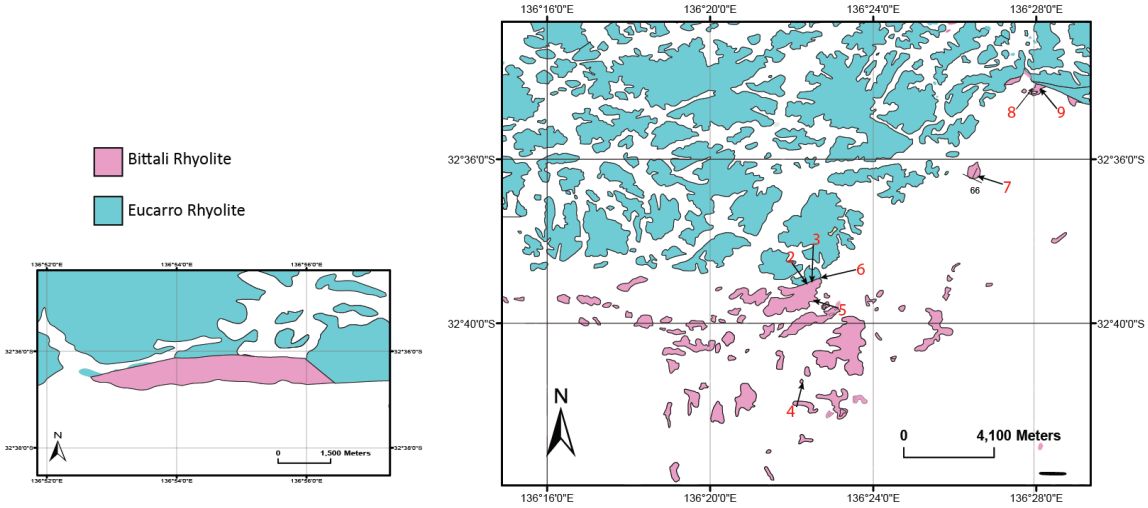


**Figure 14. Locality maps for Wartaka (left) and Menninnie Dam (right). Sample numbers in red (can be cross-referenced to field observations in Appendix A).**

## COMPARISONS

In Table 1, the different lithologies observed at each of the SGRA localities have been categorized into an emplacement method as interpreted from lava-like or pyroclastic features. In Table 2, the SGRAV are summarized at each locality based on their methods of emplacement, texture, mineralogy, groundmass, phenocryst percentage, and outcrop features.

Across the SGRA comparisons can be drawn between individual rock samples based on appearance in hand sample and from rock descriptions from other sources. These include: 1) the dacites at Toondulya Bluff, which bear resemblance both to the dacite at Waganny Dam (differ in decreased phenocryst abundance and size at the latter) and the Childera Dacite at Lake Everard; 2) the 'Unnamed Rhyolite' and the rhyolite at Thurlga (differ in groundmass colour, pale brown and brick-red respectively); 3) the BR at Narlaby Well and Eucarro Rhyolite at the same locality described by Allen et al. (2003). As Thurlga and Waganny Dam are in close proximity to each and display a similar spatial distribution, the BR and WD could be expected to show strong petrographic

similarities, however, this is not what is observed. The WD at Thurlga is different from that at Waganny Dam primarily by its mineralogy, as it comprises a ferromagnesic phenocryst phase. The BR is difficult to correlate between the two areas given that the explosive eruptive style at Waganny Dam may have immediately destroyed any original textural similarities there may have been. It is also possible that other lithofacies exist at these localities but were not found.

| Area | Rock sample | Emplacement method | Basis for distinction |
|---|---|---|---|
| *Toondulya Bluff* | Brown dacite (WD) | Pyroclastic flow | Compaction layering, presence of lithics, depressions in fine layering beneath lithic clasts |
| | Red dacite (WD) | Lava flow | Homegenous/massive texture, evenly porphyritic |
| | Rhyodacite (BR) | Lava dome | Complex flow banding/folding geometries, domal bedding orientations |
| | Rhyolite (BR) | Lava flow | Flow banding, evenly porphyritic, rounded/intact phenocrysts |
| | | | |
| *Narlaby Well* | Rhyolite (BR?) | Lava flow | Alligned amygdales, flow banding, evenly porphyritic |
| | | | |
| *Waganny Dam* | Rhyolite (UR) | Lava flow | Evenly porphyritic, rounded/intact phenocrysts, homogenous/massive |
| | Rhyolite (UR) | Dyke? | Coarser groundmass, contrast with adjacent rocks |
| | Dacite (WD) | Pyroclastic flow? | Thin section shows some crystal fragments in groundmass |
| | Rhyolite (BR) | Pyroclastic flow | Eutaxtic texture, fiamme |
| | | | |
| *Thurga* | Dacite (WD) | Lava flow | Evenly porpyritic, euhedral/intact phenocrysts |
| | Rhyodacite (BR) | Pyroclastic flow? | Possible fiamme (whispy pink streaks) |
| | Rhyodacite (BR) | Lava flow | Evenly porphyritic, massive, euhedral crystal habit |
| | | | |
| *Buckleboo* | Dark brown rhyolite (BR) | Pyroclastic flow | Angular quartz phenocrysts, glassy groundmass, xenoliths |
| | Pale brown rhyolite (BR) | Pyroclastic flow | Angular quartz phenocrysts |
| | | | |
| *Menninnie Dam* | Crystal rich-rhyolite (BR) | Lava flow | Evenly porphyritic, intact phenocrysts, hexagonal jointing |
| | Fiamme-bearing rhyolite (BR) | Pyroclastic flow | Anhedral/angular crystals, fiamme |
| | Seriticized ignimbrite (BR) | " " | " " |
| | Seriticized tuff (BR) | Pyroclastic fall | Fine ash layers |
| | | | |
| *Wartaka* | Tuffs | Pyoclastic fall | Fine ash layers |
| | | Pyroclastic flow | Crystal-rich, pumiceous clasts, lithics |
| | Porphyritic rhyolites | Lava flows | Evenly porphyritic, intact phenocrysts |

**Table 1. Overview of the emplacement mechanisms for the observed rock types in the SGRA. BR- Bittali Rhyolite, WD - Waganny Dacite, UR – Unnamed Rhyolite**

| | | Toondulya Bluff | Narlaby Well | Waganny Dam | Thurlga | Buckleboo | Menninnie Dam | Wartaka |
|---|---|---|---|---|---|---|---|---|
| | **Volcanic units** | Bittali Rhyolite, Waganny Dacite | Bittali Rhyolite? | Bittali Rhyolite, Waganny Dacite, Unnamed Rhyolite | Bittali Rhyolite, Waganny Dacite | Bittali Rhyolite, Waganny Dacite?, unnamed andesite | Bittali Rhyolite | Bittali Rhyolite? |
| | **Outcrop Features** | Flow-banding/folding, amygdales, lithics | Flow banding/folding, amygdales | Lithics, fiamme | Fiamme?, blocky, highly jointed | Basement rock xenoliths, scattered outcrop distribution | Basement rock xenoliths, scattered outcrop distribution, hexagonal jointing | Amygdales, geodes, pumice clasts, fiamme, flow banding |
| ***Bittali Rhyolite*** | **Texture** | Sparsely porphyritic, evenly porphyritic, flow banded | Porphyritic, flow banded | Eutaxitic, fiamme-bearing, porphyritic | Evenly porphyritic, massive | Evenly porphyitic, brecciated | Porphyitic, brecciated, eutaxitic, fiamme-bearing | Porphyritic, massive |
| | **Phenocryst %** | 5 - 10% | 22% | 32% | 10% | 15 - 27% | 35 - 50% | 17 - 25% |
| | **Mineralogy** | Quartz, k-feldpar, plagioclase, hornblende | Quartz. orthoclase, calcite, chlorite | Quartz, k-feldspar, chlorite, calcite, zircon | Quartz, k-feldspar, pyrite | Quartz, k-feldpar, plagioclase, epidote | Quartz, k-feldspar, chlorite, zircon, epidote, ilmenite | Quartz, k-feldpar, plagioclase |
| | **Groundmass** | Reddish-brown to black, microcrystalline, granophyric | Dark brown, fine-medium grained, spherulites | Dark brown, fine-medium grained, | Pale brown, microcrystalline, homogenous, finely recrystallized | Cream-pale brown, dark brown, microcrystalline finely recrystallized | Brick-red, pale brown, fine-medium grained | Brick red, grey, fine-medium grained, fiamme, glass shards |
| ***Waganny Dacite*** | **Texture** | Sparsely porphyritic, flow banded | | Porphyritic | Porphyritic | | | |
| | **Phenocryst %** | 5% | | 15% | 15 - 25% | | | |
| | **Mineralogy** | K-feldspar, minor quartz | | K-feldspar, chlorite, calcite, augite, apatite, zircon, | K-feldspar, ferromagnesic phase | | | |
| | **Groundmass** | Reddish brown, microcrystalline | | Dark brown, microcrystalline | Brick red, fine-grained | | | |
| ***Unnamed Rhyolite*** | **Texture** | | | Sparsely porphyritic | | | | |
| | **Phenocryst %** | | | 8% | | | | |
| | **Mineralogy** | | | Quartz, k-feldspar | | | | |
| | **Groundmass** | | | Pale-brown, fine-grained | | | | |

**Table 2. Lithological overview of the Bittali Rhyolite, Waganny Dacite and 'Unnamed Rhyolite' across the 7 main SGRA localities.**

## STRUCTURAL DATA

Flow banding geometries will differ between methods of extrusion eg. radiating flow bands related to a circular conduit or point source, and flow bands which orient perpendicular to a linear, fissure type source (Ashwell et al. 2013). The collection of structural measurements of flow banding obtained across are SGRA has been plotted in Figure 15. Although the data is sparse, it generally plots in the southern hemisphere of the stereonet in relatively close proximity, which may suggest these are radiating flow bands indicative of a point source. Anomalous data points are at Toondulya Bluff and Narlaby Well which plot away from the general trend.

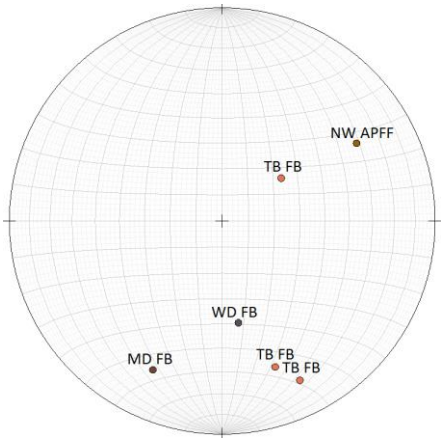


**Figure 15. Structural measurements collected at various localities. WD – Waganny Dam, MD - Menninnie Dam, TB – Toondulya Bluff, NW – Narlaby Well, FB – Flow banding, APFF – Axial plane of flow folds**

## Geochemistry

The Southern Gawler Ranges Area Volcanics (SGRAV) are predominantly peraluminous to metaluminous and rhyolitic-rhyodacitic in composition, but also fall into the dacite and andesite fields when total alkalis ($Na_2O + K_2O$) are plotted against silica (Figure 16). Broader ranges in silica content are seen at Toondulya Bluff and Buckleboo. Both the Waganny Dacite and Bittali Rhyolite are composite units overlapping in the rhyodacite silica range of 69 – 73% suggested for rocks of the GRV (Branch 1978).

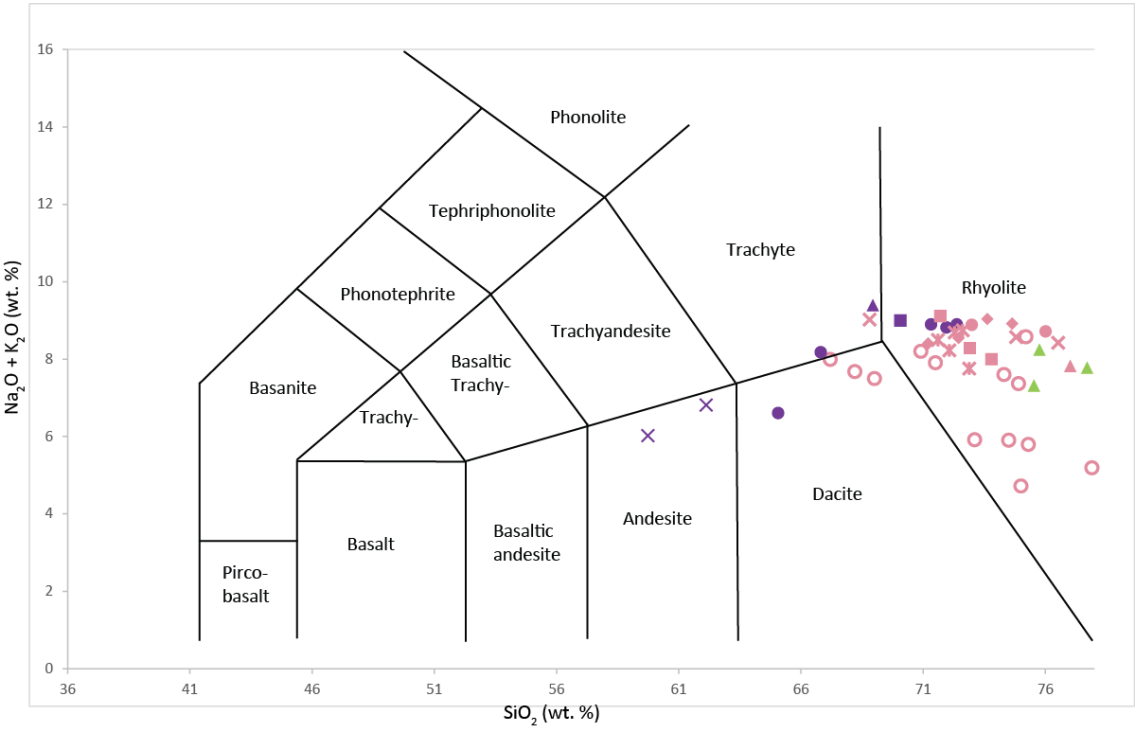


**Figure 16. Classification scheme for the SGRAV where total alkalis ($Na_2O + K_2O$) are plotted against silica ($SiO_2$) (TAS diagram)(Le Maitre 1984, Doyle and McPhie 2000). Colours correspond to different rock units: Bittali Rhyolite – pink; Waganny Dacite - purple; unnamed rhyolite - green. Shapes correspond to the different SGRA localities: Toondulya Bluff – solid circles; Narlaby Well – 3-line crosses; Waganny Dam – triangles; Thurlga – squares; Buckleboo – crosses; Menninnie Dam – diamonds; Wartaka – hollow circles.**

Harker diagrams allow for a graphical representation of fractionation trends within an igneous province by plotting major and trace elements against silica. Figures 17 and 18 include all available data for the SGRAV (including data obtained from this study). Sample data points generally tend to conform to broad trends, but anomalies are observed in the low silica TB sample (65%) and highly siliceous samples from Wartaka (>80%). These anomalous samples show depletions in mobile elements ($Na_2O$) and high normative corundum values suggesting they have been subject to alteration and loss of $Na_2O$. In the $TiO_2$ plot (an element more resistant to immobilization/alteration) the TB anomaly shows a strong fit to the rest of the dataset, however, Wartaka samples (at more appreciable $SiO_2$ levels <78%) show slight deviation from the general trend. Narlaby Well samples all plot with narrow limits of each other as is expected of its smaller outcrop area, but also in close proximity to several Toondulya Bluff samples. Inflection points that occur in plots of $K_2O$ and Ba mark the onset of K-feldspar crystallization at $SiO_2$ of ~72%. Other inflection points occur in Y, Zr, Nb, Nd, $Na_2O$ at a similar $SiO_2$ (72%) also mark a change in crystallizing mineral assemblages. Continual depletions in Sc and Sr are likely as a result of incorporation into pyroxene/hornblende and plagioclase respectively.

## ISOTOPES

Neodymium and samarium analysis of five samples from the SGRA volcanics as well as existing data from Toondulya Bluff and Menninnie Dam are presented as a function of epsilon Nd at 1592Ma versus MgO (as a fractionation controlled parameter) in Figure 19 (Stewart 1994). Bittali Rhyolite tends to associate with lower εNd values, whereas Waganny Dacite associates with higher εNd values. The ‘unnamed rhyolite’ shows the highest εNd value of the rhyolite samples, which may be a reflection of its lower

stratigraphic position. Narrow ranges in εNd data can be seen in samples from Toondulya Bluff (from -0.8 to 0.8) and Waganny Dam (-2.9 to -1.9). In comparison,

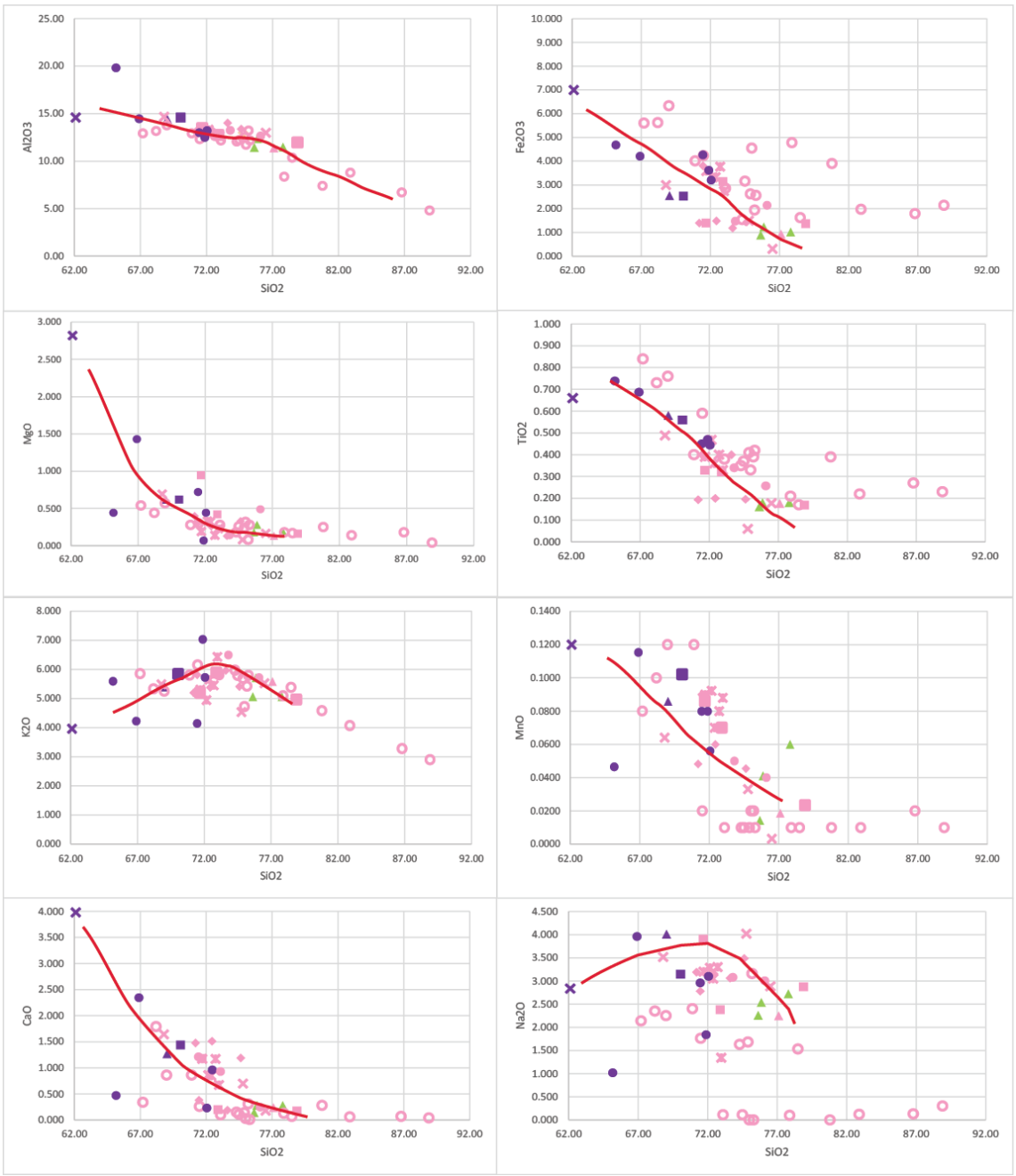


**Figure 17. Major oxides vs $SiO_2$. Inflection points occur at $SiO_2$ ~ 72% in $K_2O$ and $Na_2O$ plots. Other elements show continual depletion. Colours correspond to different rock units: Bittali Rhyolite – pink; Waganny Dacite - purple; unnamed rhyolite - green. Shapes correspond to the different SGRA localities: Toondulya Bluff – solid circles; Narlaby Well – 3-line crosses; Waganny Dam – triangles; Thurlga – squares; Buckleboo – crosses; Menninnie Dam – diamonds; Wartaka – hollow circles.**

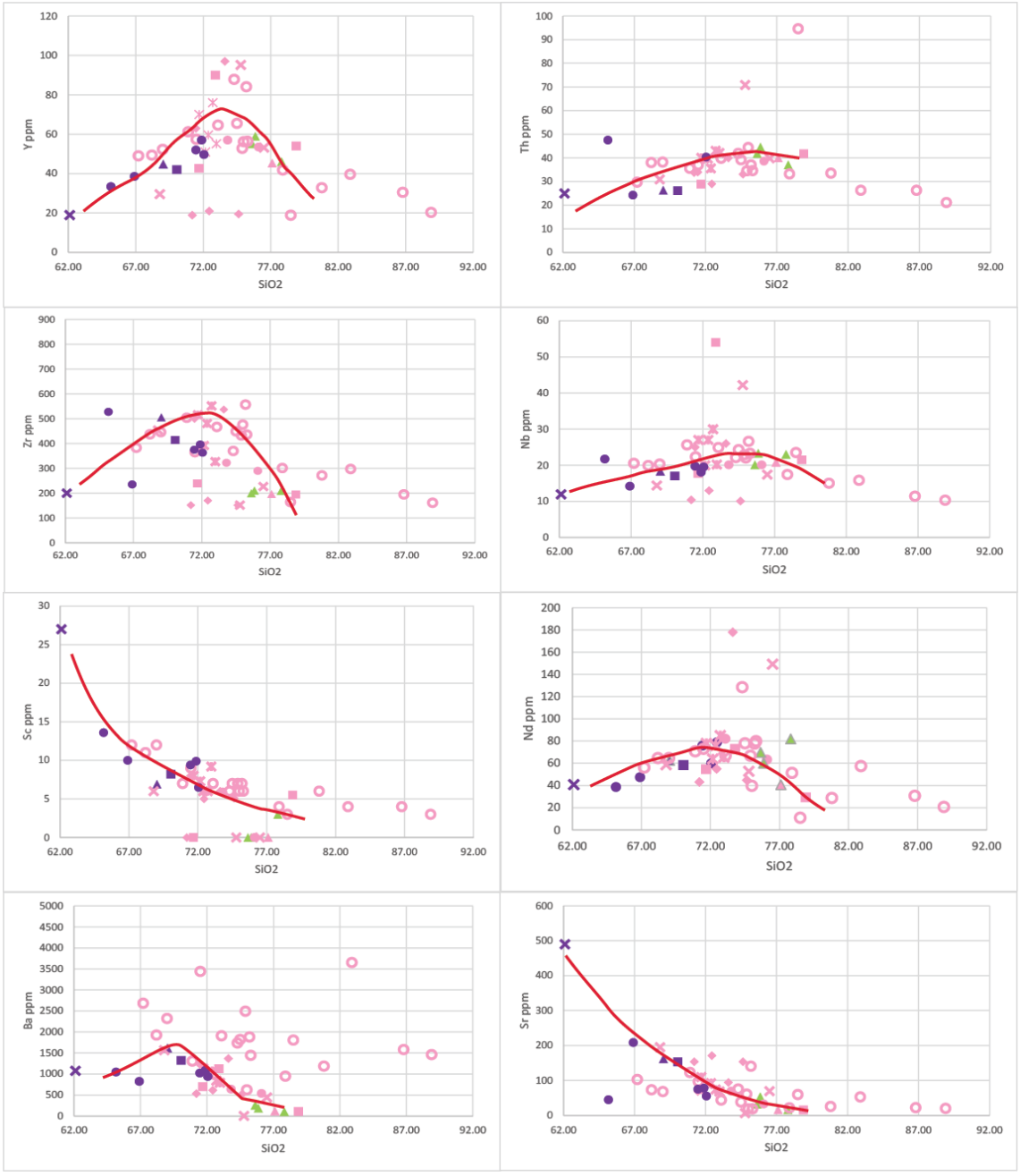


**Figure 18. Trace elements vs $SiO_2$. Inflection points marking changes from enrichment to decline occur at a common $SiO_2$ level of ~72% in many of the plots (Y, Zr, Nb, Nd). Colours correspond to different rock units: Bittali Rhyolite – pink; Waganny Dacite - purple; unnamed rhyolite - green. Shapes correspond to the different SGRA localities: Toondulya Bluff – solid circles; Narlaby Well – 3-line crosses; Waganny Dam – triangles; Thurlga – squares; Buckleboo – crosses; Menninnie Dam – diamonds; Wartaka – hollow circles.**

Thurlga shows a much greater range in εNd (-5.6 to -0.79) which is surprising considering these samples are in close proximity to each other (within 2km). A paucity of data lowers confidence in identifying trends. Nevertheless, a reasonably coherent

trend line can be fit to the Toondulya Bluff samples. Waganny Dam and Thurlga samples also show increasing εNd with higher MgO. The andesite from Buckleboo falls away from the broad trend of the SGRAV, indicating a difference in crustal residence. Each of the other LGRV areas tend to conform to sharper trends with increasing MgO.

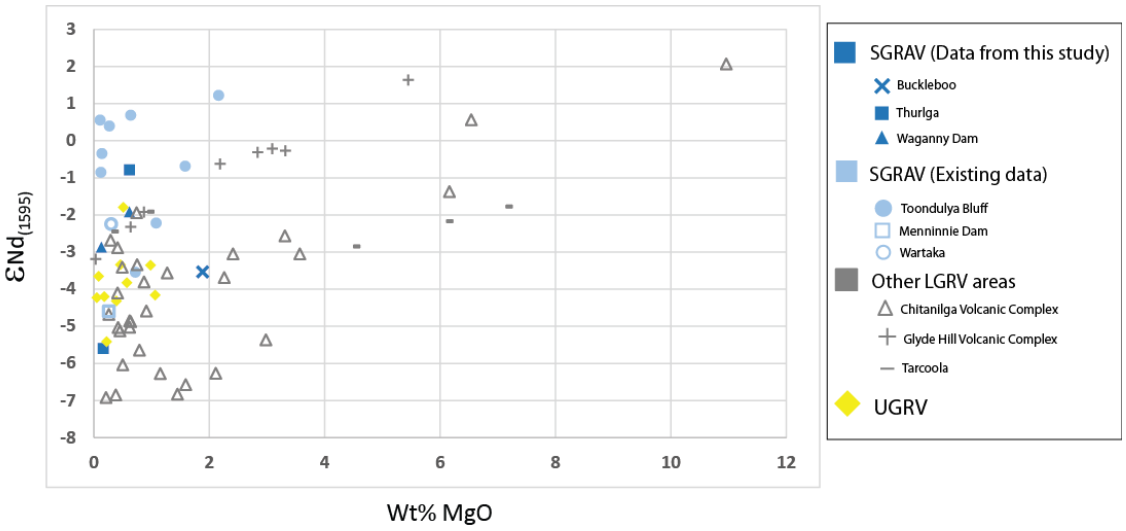


**Figure 19. Epsilon Nd at 1592Ma versus MgO (wt%) for the SGRAV, other LGRV areas and the UGRV. The SGRAV samples from this study have been differentiated from the existing data from Stewart (1994). Each of the other LGRV areas broadly conform to individual trends. The most magnesian sample comes from the Chitanilga Volcanic Complex (CVC) at Kokatha. Greater variation in εNd values are seen in the LGRV (SGRAV in blue, and other areas in grey) compared to the UGRV as a result of assimilation fractional crystallization (AFC) processes.**

## DISCUSSION

A primary aim of this study was to determine how alike the Bittali Rhyolite and Waganny Dacite are to each other and whether or not they are genetically related. As is discussed earlier on the basis of petrographic features, the BR and WD not only represent different phases of volcanism, but also comprise different lithofacies within them. The clarity in discerning trends for the SGRAV becomes skewed due to the chemical heterogeneity of the LGRV (Stewart 1994). Nevertheless, the rocks of Toondulya Bluff, Narlaby Well, Waganny Dam, Thurlga, Buckleboo and Menninnie Dam do tend to conform to a common trend in most harker diagrams, suggesting they

are related. Between Waganny Dam and Thurlga, the BR and WD show strong similarities in major/trace element values suggesting that the two areas are analogous, despite lithological variations previously discussed. Wartaka samples are difficult to correlate due to the effects of alteration, however, because of slight differences in geochemical data ($Fe_2O_3$, $Ti_2O$) and the dissimilarity of lithologies (compared to other localities) seen in the area, it could be argued that this is a previously unrecognized volcanic sequence of the LGRV. Although, recent TIMS U-Pb dating on a rhyolite from Wartaka yielded an age of 1588.5 ± 0.5 Ma (A Reid, pers. comm.), which overlaps with previous age estimates of 1592 ± 5 Ma (WD at Toondulya Bluff) and implies the volcanics are indeed synchronous with the rest of the SGRAV.

## Halogen contents and temperature

As the BR is observed to cover 200km – 150km (whether or not Wartaka is considered), this poses questions into the methods of magma emplacement and associated viscosities. Enriched fluorine values have been recorded in the rocks at Toondulya Bluff (WD, 1800ppm) and Waganny Dam (UR, 1500 – 1750ppm) which is significant considering Fl is known to depolymerise melts and therefore reduce viscosity (Pankhurst 2006, Stewart 1994). Primary mineralization of fluorite at Narlaby Well suggests the original melt was also Fl saturated. Other Fl values in the SGRA at Menninnie Dam (680ppm) and Wartaka (<1160ppm) are more typical of felsic magmas, however, these values are probably underestimates considering the loss of volatiles through exsolution, which may have had greater effects in these particular areas due to the dominance of explosive volcanism. The contrast in Fl values also coincides with a difference in emplacement methods between Toondulya Bluff-Waganny Dam-Thurlga (TB-WD-Th) where effusive eruptive styles are dominant and Buckleboo-Menninnie

Dam (B-MD) which represent a zone of explosive volcanism (Table 1). Given that anhydrous mineral assemblages are observed across the SGRAV, the change in eruptive styles from effusive (TB-WD-Th) to phreatomagmatic (B-MD) indicates the magma must have interacted with an external water source. This is supported by high degrees of seritization and peperitic margins in rock units from drill core at Menninnie Dam (Roache 1996).

Temperature is also a primary control on melt viscosity, where increases in T cause viscosity to decrease. Using the 2-feldspar thermometer (requires inputs of pressure, alkali feldspar and plagioclase compositions) of Putirka (2008), a temperature range of 930 ˚C – 1100 ˚C for the BR at Waganny Dam was obtained. However it must be noted that there is error associated with this temperature as the plagioclase feldspars were found to be of pure albite composition, and because of this, the required plagioclase composition input was substituted with the bulk rock composition. Moreover, of the five samples which were analyzed (using the electron microprobe), only one showed alkali feldspar compositions which were well-mixed, and predicted through modelling programs. Nevertheless, the temperature range is very similar to that previously calculated for the Upper GRV (950 ˚C – 1110˚C), rocks which are considerably high temperature given their dacitic-rhyolitic composition (Creaser and White 1991, Stewart 1994). This observation supports the idea of an areally extensive zone of high Fl and high temperature effusive volcanism in the west represented by TB-WD-Th.

Zircon saturation temperatures have been calculated for the GRV previously by Tregeagle (2014), the results of which are shown in Figure 20. The change from Zr enrichment to decline occurs at the exact on-set of zircon crystallization and therefore the zircon saturation temperature is equal to the magma temperature. Before the

inflection point, zircon is undersaturated and therefore the saturation temperature is less than the magma temperature. After the inflection point, zircon is oversaturated

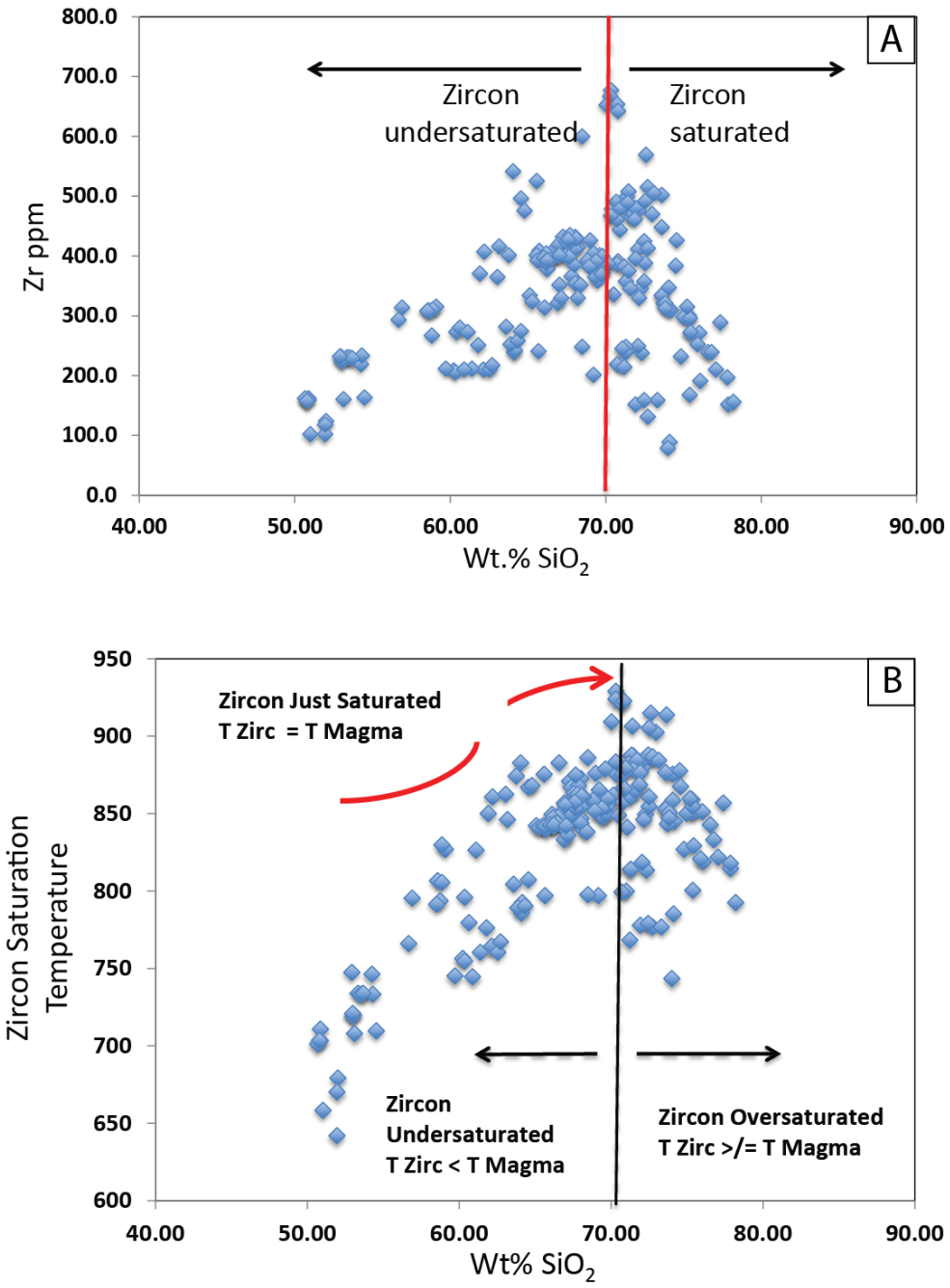


**Figure 20. The point at which zircon is just saturated is marked by the red line in diagram 'A'. This correlates to zircon saturation temperature calculations which indicate a magma temperature ranging from 850 ˚C – 920˚C, shown in 'B'. Calibrations and formulations for the zircon saturation temperature from Hanchar and Watson (2003) and Watson and Harrison (1983)**

and saturation temperature is less than the magma temperature. At the inflection point (where zircon saturation temperature equals magma temperature) the indicated magma

temperature is in the range of 850 ˚C – 920˚C, which is similar to the previous temperature estimates discussed prior.


**Figure 21. Major oxides vs $SiO_2$, comparing the Chitanilga Volcanic Complex, Glyde Hill Volcanic Complex, SGRAV and Wartaka area.**

## Relation to the rest of the GRV

When considering the SGRA volcanics as distinct zones, the areal extent of silicic units becomes more realistic. The distance of lava coverage from Toondulya Bluff to Thurlga is ~95km, which is not unreasonable considering the Yantea Rhyodacite of the GHVC also possesses textural characteristics of a lava flow and has a similar lateral extent (~90km) and enriched Fl contents (1500ppm) (Agangi 2011, Stewart 1994). Another unit of the GHVC which warrants comparison is the Childera Dacite which sits at the base of the Glyde Hill Volcanic Complex and has been noted to be similar in appearance to the lower dacitic units at Toondulya Bluff (Blissett 1986). On geochemical grounds, the Childera shows significant differences in major/trace element values at similar $SiO_2$ levels to that of the TB dacites, and as such is not considered equivalent. When compared to other regions of the LGRV, the SGRA are easier to distinguish from the CVC (more mafic compositions) than the GHVC, however, they tend to show lower $TiO_2$ and $Na_2O$ at a given $SiO_2$ level (Figure 21).

## Petrogenesis

A-type magmas are derived through fractional crystallization of either a mantle-derived source, partial melts of felsic crust, or mafic melts that have undergone assimilation of crustal material ie. assimilation fractional crystallization processes (AFC). Tregeagle (2014) showed that the entire GRV can be derived from the most primitive GRV basalt (from Kokatha) in two-stages through pure fractional crystallization in which basalt-dacites crystallize at low pressures (~3kb) followed by the fractionation of siliceous rhyolites shallower in the crust (~1kb). This was modelled using the Rhyolite MELTs program (Gualda et al. 2012). However, it was noted that this would not be able to explain the relationship of lower epsilon neodymium values with increased

differentiation, which suggests crustal contamination (AFC processes). Furthermore, modelling predicted that the mature phase would be reached after ~80% crystallization (Figure 23), which seems unrealistic considering that the main magma body would therefore need to be 4 times as large as the extruded volume. The high variability in εNd values for the SGRAV indicates AFC processes are present with high amounts of late stage crustal assimilation at more felsic compositions.

There are notable changes in the geochemistry of the SGRAV during the transition from dacite to rhyolite (or WD to BR) that occurs at $SiO_2$ ~72%: 1) inflections points marking changes from enrichment to depletion, or distribution coefficients (Kd or D) becoming greater than 1 in the trace elements eg. Nd (Figures 17, 18 & 22); 2) discontinuities between data points in the CaO and MgO plots (Figure 17); 3) the rapid decline in εNd values (Figure 19). It is highly likely that these observations are not coincidental, and are likely related to a change in magma conditions. The increases in crystallization (after inflection points at ~72%) and sudden depletions in CaO/MgO may suggest that he magma body has moved to shallower crustal levels, causing exsolution of volatiles and the sudden on-set of crystallization (plagioclase and pyroxenes). This transitional stage also coincides with increased crustal assimilation (Figure 19), in which the felsic contaminant may be CaO and MgO depleted (to account for discontinuities), causing a dilutional effect on the magma.

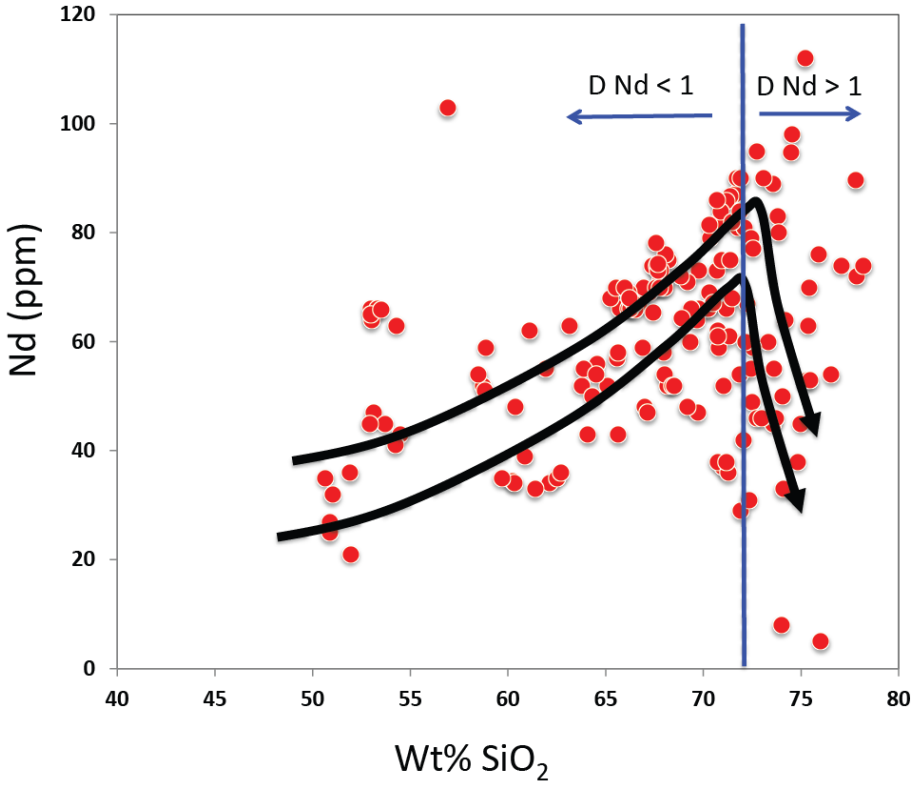


**Figure 22. Nd(ppm) versus $SiO_2$(wt%) highlighting the change in the distribution coefficient (D) to become greater than 1 after $SiO_2$>72%.**

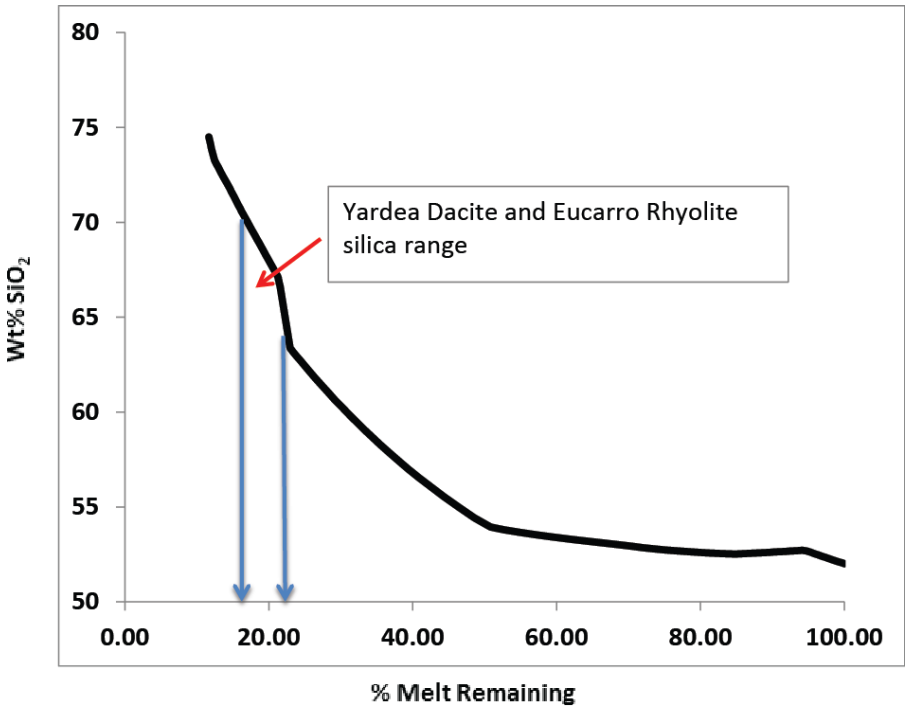


**Figure 23. The relationship between $SiO_2$(wt%) and the percentage of melt remaining through a pure fractonal crystallization model using the Rhyolite MELTs program (Ghiorso and Sack 1995, Gualda et al. 2012). Modelling started from the most primative GRV basalt composition (from Kokatha, sample K8) and fractionated at 3kbar up to a dacitic composition ($SiO_2$ – 63%). The more rhyolitic compositions were then fractionated at 1kbar. This model suggests that the UGRV would be the products of about 80% crystallization. From Tregeagle (2014).**

Using the normative albite barometer of Blundy and Cashman (2008), an estimate of the pressures at which the SGRAV formed was calculated. This is shown in Figure 24, where a clustering of samples occurs at the transition from dacite to rhyolite (~73%), and where the saturation point is reached for many trace/major elements. The calculated pressure range of 100 – 50 MPas (1 – 0.5 kb) for the rhyolites is quite low, and supports the idea of a rising magma body to a shallower crustal level.

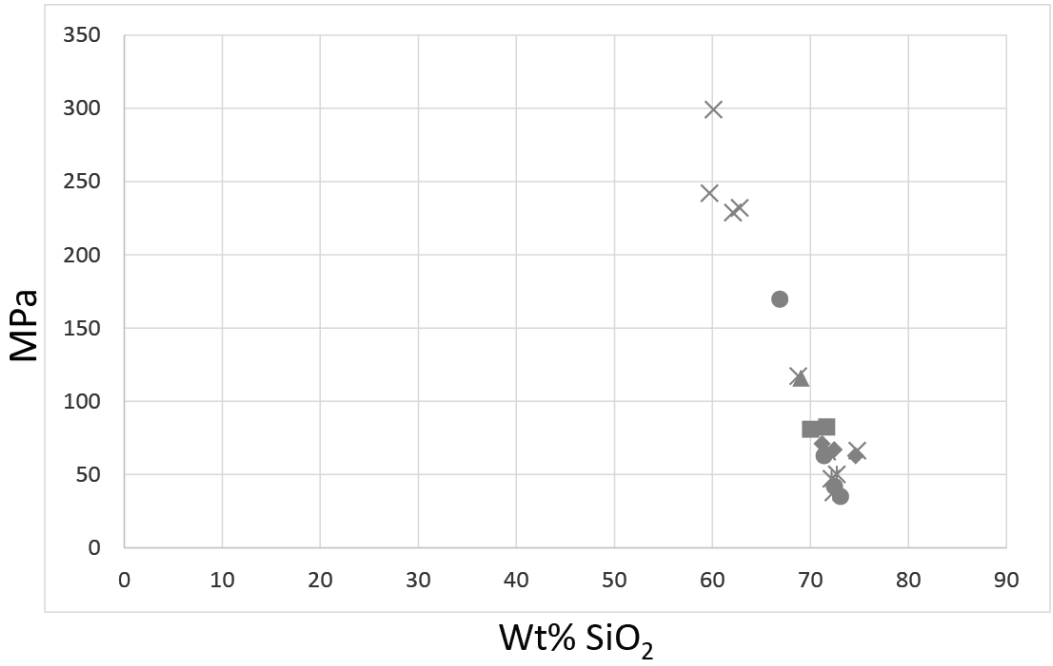


**Figure 24. Calculated pressures for the SGRAV using the normative albite barometer of Blundy and Cashman (2008). The transition to rhyolitic compostions (>70% $SiO_2$) correlates to a decrease in pressure. Shapes correspond to the different SGRA localities: Toondulya Bluff – solid circles; Narlaby Well – 3-line crosses; Waganny Dam – triangles; Thurlga – squares; Buckleboo – crosses; Menninnie Dam – diamonds.**

## SOURCE

Assimilation fractional crystallization (AFC) may be involved with two end-member source compositions: 1) crustal melts; 2) mantle melts. In a two-stage model of assimilation fractional crystallization processes, Tregeagle (2014) showed that the GRV

may be derived from two mantle end-member starting compositions, a MORB-like parental magma and an enriched mantle. The correlation between the GRV and these two parent sources can be seen in εNd versus MgO as is shown in Figure 25. The most primitive GRV basalt comes from Kokatha (sample K8) and shows enrichments in incompatible trace elements compared to MORB (eg. Nd of MORB- 9ppm, Nd of K8 – 25ppm). Given that K8 has undergone little fractionation since leaving the mantle (high Cr, Ni and MgO), this implies that the GRV has partly been derived from an incompatible element enriched source. This may be due to a mantle plume interacting with the sub-continental lithospheric mantle (SCLM). The variation between the two sources is indicated by individual trends lines which can be fit to the SGRA volcanics (trendline A) and the other LGRV areas (trendlines B & C) (Figure 25).

A recently revised εNd value of K8 from -2 to +2 shifts the two parent sources closer together, however, it should be remembered that the true end member composition could plot beyond K8 (as indicated by the black arrow in Figure 25). The shallower gradient of trendline ‘A’ associated with the SGRAV in Figure 25 suggests dominant fractional crystallization but with late stage crustal assimilation. Trendlines ‘B’ and ‘C’ associate with the other LGRV areas, and reflect earlier and continual crustal assimilation with increasing differentiation. These observation imply different crustal residences for each of the LGRV successions, which is of course expected of their regional spread. Some consideration should be taken in the effect of sampling bias at lower MgO levels in the SGRAV.

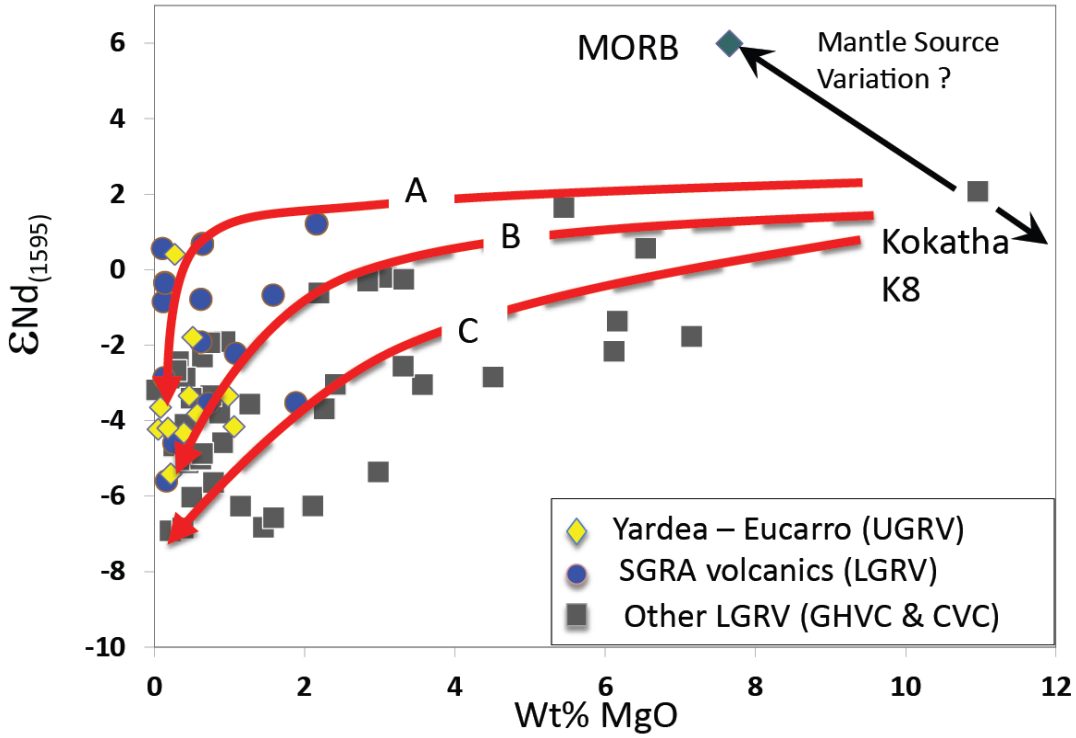


**Figure 25. Annotated εNd versus MgO (wt%) chart showing the possibility for mantle source variation associated with the GRV. Trendline 'A' broadly fits the SGRAV dataset and shows relation to both MORB and K8, indicating some variation between the two endmembers, Trendlines 'B' and 'C' correlate better to the other LGRV areas: Chitanilga Volcanic Complex (CVC), Glyde Hill Volcanic Complex (GHVC), and Tarcoola.**

## AFC Modelling

The AFC processes associated with the SGRAV and other rocks of the GRV have been modelled using the programs of DePaolo (1981) and Powell (1984). This is seen in Figure 26, where there are two types of AFC models which better account for the observed differences between the SGRA volcanics and other LGRV areas on an εNd versus Nd (ppm) plot. The model is primary controlled by several parameters: 1) The distribution coefficient (Kd) of a trace element, which in this case is Nd (as it shows an inflection point marking enrichment to decline); 2) The ratio between the rate of

assimilation and rate of crystallization, termed the ‘r’ value; 3) Isotopic compositions of the parent magma and contaminant.

For the SGRAV, the model best fits the dataset in a two stage process where the second stage begins at the inflection point at which point Nd is saturated in the melt (Figure 26A). The first stage is characterised by a slight decrease in εNd with increasing Nd concentration (Kd<1), suggesting a low rate of crustal assimilation (r = 0.12). The second stage occurs after the inflection point, where the magma undergoes a steep decline in both Nd concentration (Kd>1) and εNd. The rapid decline in εNd occurs very late in the fractionation process and suggests contamination by an assimilant with highly negative εNd values (-25).

The other GRV data (Figure 26B), which mostly comes from the LGRV (GHVC & CVC) and a small amount from the UGRV is also characterized by a two stage AFC process showing contrasting trends to the SGRAV (Figure 26B). They reach the inflection point at a lower εNd, implying earlier crustal assimilation since fractionation from the parental magma, as is consistent with trendlines ‘B’ and ‘C’ in εNd versus MgO (Figure 25). The magma temperature is likely to have been substantially high in the first stage to assimilate larger amounts of felsic crust (r = 0.55). In the second stage, there is a sharp decrease in Nd (Kd>1) but with a relatively slight decline in εNd, suggesting lower amounts of crustal assimilation (at a cooler temperature) and a contaminant with relatively higher εNd values (-11) than that associated with the SGRA volcanics. Lower amounts of crustal contamination in this later stage is consistent with magma chambers in the upper crust which are in contact with colder material and hence a lower rate of assimilation. The UGRV data clusters together as expected due to the highly voluminous and homogenous magma from which it is derived.

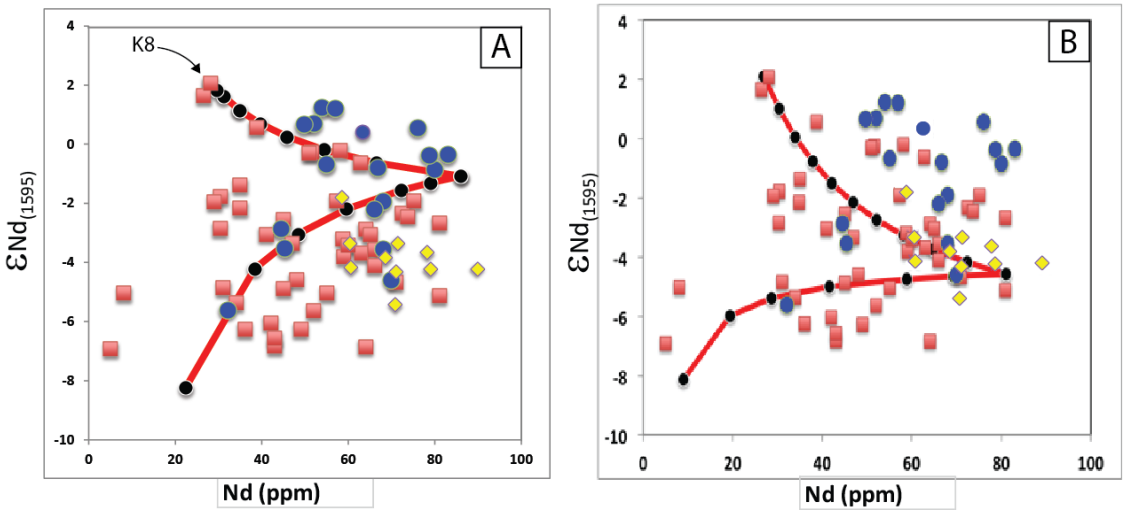


**Figure 26. AFC modelling (red line) to best fit the observed εNd and Nd data of the SGRAV (A) and other LGRV areas (B). Each model occurs in two stages, a first stage before the inflection point and a second stage after the inflection point. Blue circles – SGRAV, red squares – other LGRV (GHVC, CVC and Tarcoola), yellow diamonds – UGRV. The SGRAV fit to a trend (left) where in the first stage Nd Kd – 0.15, r – 0.12 and in the second stage Nd Kd – 2, r – 0.3. The other LGRV data fits to a trend where in the first stage Nd Kd – 0.2, r – 0.55, and in the second stage Nd Kd – 3, r – 0.3. Modelling uses the equation of Powell (1984).**

The two AFC models are summarised in Figure 27, showing the contrast between the SGRAV and other GRV data. There are different types of assimilants associated with the two models. The SGRAV has been contaminated by a highly negative εNd source which may be older Archean rocks, whereas the other GRV areas have assimilated lower εNd rocks which may be younger Paleoproterozoic rocks. As discussed earlier, a pure fractional crystallization process to produce the GRV faces a problem in very large volumes of the lower differential gabbroic and peridotitic intrusives that would be present in the lower crust (4 times that of the extruded UGRV). However, this becomes more realistic through AFC modelling whereby the final magma mass may represent 45% (r = 0.55) of the parent mafic magma, due to addition of material.

As alluded to in the prior discussion, BR volcanism seems to have been associated with magma bodies that were stored at shallower crustal levels. At deeper levels the WD may have been stored as a singular magma body which gave rise to multiple shallower magma chambers associated with the BR. This may help explain the continuation of the

BR further east than the WD. Furthermore, during this transition, the rising magma likely assimilated wall rocks of Archean age, which helps explain the lower εNd values of the BR compared to the WD.

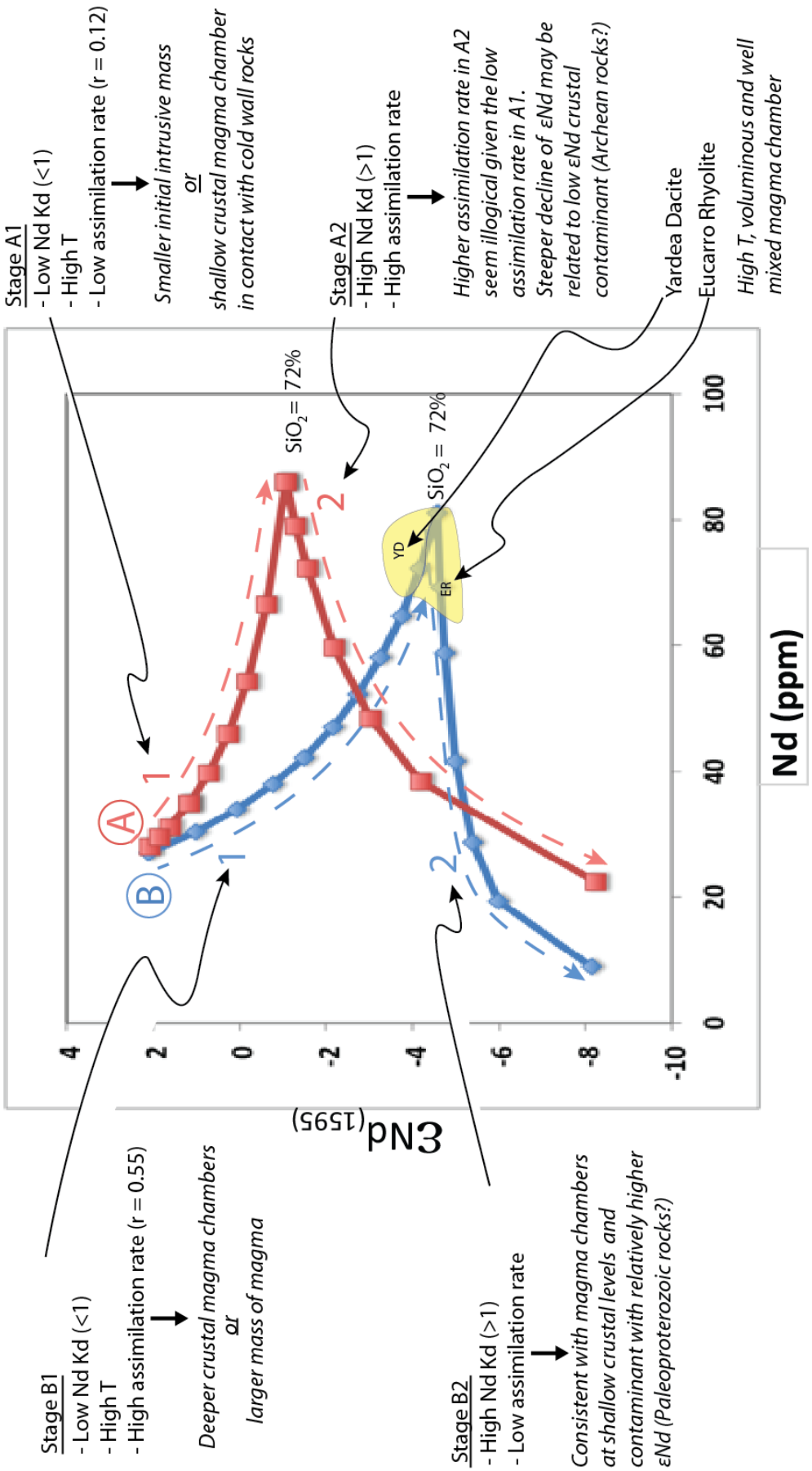


**Figure 27. Annotated epsilon Nd versus Nd(ppm) showng the two contrasting trends associated with differences in AFC processes. The two AFC models are associated with the SGRAV (shown in red, model 'A') and the other LGRV areas and UGRV (shown in blue, model 'B').**

## CONCLUSION

The Southern Gawler Ranges Area Volcanics (SGRAV) are considered here to be geochemically related rocks exposed along the extensive southern margin of the GRV. The SGRA may be divided into a western zone of dominantly effusive volcanism (Toondulya Bluff, Waganny Dam, Thurlga) characterized by high magma temperatures and high Fl values, (which are key contributing factors to lowering viscosity) and an explosive zone of magmatism in the central region (Buckleboo, Menninnie Dam). The outcrop of Bittali Rhyolite in the eastern margin (Wartaka), is more difficult to correlate to the rest of the SGRAV due to highly altered samples, however, there are subtle differences in fractionation trends of the more immobile elements ($TiO_2$) which may suggest it is an entirely separate volcanic sequence. It is likely that the effusive zone in the west represents an areally extensive lava flow not unlike the Yantea Rhyodacite of the GHVC.

Petrogenetic modelling seems to suggest that the Waganny Dacite developed in the middle crust which gave rise to the Bittali Rhyolite at shallower crustal levels. The later stage of fractionation involved higher assimilation rates of wall rock material, likely to be older Archean age rocks. Compared to the rest of the GRV, including the other LGRV areas such as the GHVC and CVC, the SGRA volcanics were associated with dominant fractional crystallization early in the genetic history until the transition to rhyolite, where greater amounts of crustal assimilation and increased crystallization occurred. The volume problem associated with large amounts of mafic parents in the lower crust if the GRV was derived through pure fractional crystallizaton is lessened through AFC modelling where the main magma mass may represent 45% of the extruded amount which is more realistic.

The GRV can be modelled through a two stage AFC process to derive directly from the most primitive basalt, which represents a separate endmember source that is enriched in incompatible elements. There is also some evidence that the GRV shows affinities with a MORB type source.

Locations for sources of the SGRA volcanics are still mostly uncertain, with the exception of the Menninnie Dam hydroexplosive centre. A source in the Paney area (north of Waganny Dam) has previously been suggested based on the given outcrop distribution and presence of a ring structure (Ferris 2003, Turner 1975). This may indeed be possible given the very similar geochemistry between rock units of Waganny Dam and Thurlga and structural data which may suggest a point source eruption.

## ACKNOWLEDGMENTS

I would like to thank my supervisor John Foden for his mentorship, guidance and support throughout the year. I'd also like to give a big thanks to Stacey McAvaney for her companionship and assistance during fieldwork, and constant support and advice. For sample preparation, many thanks go to David Bruce, Ben Wade, Ben Cooke, and Funny Meeuws. Also, thankyou to Katie Howard for her moral support and advice throughout the year.

## REFERENCES

AGANGI A. 2011. Magmatic and volcanic evolution of a silicic large ignous province (SLIP): the Gawler Range Volcanics and Hiltaba Suite, South Australia. p.203.

AGANGI A., KAMENETSKY V. S. & MCPHIE J. 2012. Evolution and emplacement of high fluorine rhyolites in the Mesoproterozoic Gawler silicic large igneous province, South Australia. *Precambrian Research* **208 211**, p.124.

ALLEN S. R., MCPHIE J., FERRIS G. & SIMPSON C. 2008. Evolution and architecture of a large felsic Igneous Province in western Laurentia: The 1.6 Ga Gawler Range Volcanics, South Australia. *Journal of Volcanology and Geothermal Research* **172**, 132-147.

ALLEN S. R., SIMPSON C. J., MCPHIE J. & DALY S. J. 2003. Stratigraphy, distribution and geochemistry of widespread felsic volcanic units in the Mesoproterozoic Gawler Range Volcanics, South Australia. *Aust. J. Earth Sci.* **50**, 97-112.

ASHWELL P. A., KENNEDY B. M., GRAVLEY D. M., VON AULOCK F. W. & COLE J. W. 2013. Insights into caldera and regional structures and magma body distribution from lava domes at Rotorua Caldera, New Zealand. *Journal of Volcanology and Geothermal Research* **258**, 187-202.

BETTS P. G. & GILES D. 2006. The 1800-1100 Ma tectonic evolution of Australia. *Precambrian Research* **144**, 92-125.

BETTS P. G., SCHAEFER B. F., MARK G., PANKHURST M. J., WILLIAMS H. A., HILLS Q., FODEN J., CHALMERS N. C., GILES D. & FORBES C. J. 2009. Mesoproterozoic plume-modified orogenesis in eastern Precambrian Australia. *Tectonics* **28**.

BLISSETT A. H. 1975. Rock units in the Gawler Range Volcanics. *Quarterly Geological Notes.* pp. 2-14. Geological Survey Of South Australia.

BLISSETT A. H. 1986. Subdivisions of the Gawler Range Volcanics in the Gawler Ranges. *Quarterly Geological Notes.* pp. 2-11.

BLISSETT A. H. 1987 Geological Setting of the Gawler Range Volcanics. Geological Atlas Special Series. S. Aust. Dept. Mines and Energy.

BLISSETT A. H. C., R. A.; DALY, S. J.; FLINT, R. B.; PARKER, A. J.; 1993. Gawler Range Volcanics. *Bulletin 54.* Geological Survey of South Australia.

BLUNDY L. & CASHMAN K. 2008. Petrological reconstruction of magmatic system variables and processes. *Reviews in Mineralogy and Geochemistry* **69**, 179-239.

BRANCH C. D. 1978. Evolution of the Middle Proterozoic Chandabook Caldera, Gawler Range acid volcano-plutonic province, South Australia. *Geological Society of Australia*, 199-218.

BRYAN S. E. & ERNST R. E. 2008. Revised definition of Large Igneous Provinces (LIPs). *Earth-Science Reviews* **86**, 175-202.

BRYAN S. E., PEATE I. U., PEATE D. W., SELF S., JERRAM D. A., MAWBY M. R., MARSH J. S. & MILLER J. A. 2010. The largest volcanic eruptions on Earth. *Earth Science Reviews* **102**, 207-229.

CREASER R. A. & WHITE A. J. R. 1991. Yardea Dacite -large-volume, high-temperature felsic volcanism from the Middle Proterozoic of South Australia. *Geology* **19**.

DALY S. J., FANNING C. M. & FAIRCLOUGH M. C. 1998. Tectonic evolution and exploration potential of the Gawler Craton, South Australia. *Journal of Australian Geology & Geophysics* **17 (3)**, 145-168.

DEPAOLO D. J. 1981. Trace element and isotopic effects of combined wallrock assimilation and fractional crystallization. *Earth and Planetary Science Letters* **53**, 189-202.

DOYLE M. G. & MCPHIE J. 2000. Facies architecture of a silicic intrusion-dominated volcanic centre at Highway–Reward, Queensland, Australia. *Journal of Volcanology and Geothermal Research* **99**, 79-96.

EWART A., MILNER S. C., ARMSTRONG R. A. & DUNCAN A. R. 1998. Etendeka Volcanism of the Goboboseb Mountains and Messum Igneous Complex, Namibia. Part II: Voluminous Quartz Latite Volcanism of the Awahab Magma System. *Journal of Petrology* **39**, 227-253.

FANNING C. M., FLINT R. B., PARKER A. J., BLISSETT K. R. & LUDWIG A. H. 1988. Refined Proterozoic evolution of the Gawler Craton, South Australia, through U-Pb zircon geochronology. *Precambrian Research* **40-41**, 363-386.

FERRIS G. 2003. Volcanic textures within the Glyde Hill Volcanic Complex. *Mesa Journal* **29**, 36 - 41.

FLINT R. B. 1993. The Geology of South Australia, Volume 1. The Precambrian. *Geological Survey of South Australia Bulletin.* pp. 107-169.

GARNER A. & MCPHIE J. 1999. Partially melted lithic megablocks in the Yardea Dacite, Gawler Range Volcanics, Australia: Implications for eruption and emplacement mechanisms. *Bulletin of Volcanology* **61**, 396-410.

GHIORSO M. & SACK R. 1995. Chemical mass transfer in magmatic processes. IV. A revised and internally consistent thermodynamic model for the interpolation and extrapolation of liquid-solid equilibria in magmatic systems at elevated temperatures and pressures. *Contributions to Mineralogy and Petrology* **119**, 197-212.

GILES C. W. 1977. Rock units in the Gawler Range Volcanics, Lake Everard area, South Australia. *Quarterly Geology Notes.* pp. 7-16. Geological Survey of South Australia.

GILES C. W. 1988. Petrogenesis of the Proterozoic Gawler Range Volcanics, South Australia. *Precambrian Research* **40**, 407-427.

GIORDANO D., RUSSELL J. K. & DINGWELL D. B. 2008. Viscosity of magmatic liquids: A model. *Earth and Planetary Science Letters* **271**, 123-134.

GUALDA G. A. R., GHIORSO M. S., LEMONS R. V. & CARLEY T. L. 2012. Rhyolite-MELTS: A modified calibration of MELTS optimized for silica-rich fluid-bearing magmatic systems. *Journal of Petrology* **53**, 875-890.

HANCHAR J. M. & WATSON E. B. 2003. Zircon saturation thermometry. *Reviews in Mineralogy and Geochemistry* **53**, 89-112.

HAND M., REID A. & JAGODZINSKI L. 2007. Tectonic framework and evolution of the Gawler Craton, southern Australia. *Economic Geology and the Bulletin of the Society of Economic Geologists* **102**, 1377-1395.

HENRY C. & WOLFF J. 1992. Distinguishing strongly rheomorphic tuffs from extensive silicic lavas. *Bulletin of Volcanology* **54**, 171-186.

HENRY C. D., PRICE J. G., RUBIN J. N., PARKER D. F., WOLFF J. A., SELF S., FRANKLIN R. & BARKER D. S. 1988. Widespread, lavalike silicic volcanic rocks of Trans-Pecos Texas. *Geology (Boulder)* **16**, 509-512.

HILDRETH W., CHRISTIANSEN R. L. & HALLIDAY A. N. 1991. Isotopic and chemical evidence concerning the genesis and contamination of basaltic and rhyolitic magma beneath the yellowstone plateau volcanic field. *Journal of Petrology* **32**, 63-138.

JAGODZINSKI E. A. 1985 The Geology of the Gawler Range Volcanics in the Toondulya Bluff Area and U-Pb dating of the Yardea Dacite at Lake Acraman., The University of Adelaide.

LE MAITRE R. W. 1984. A proposal by the IUGS Subcommission on the Systematics of Igneous Rocks for a chemical classification of volcanic rocks based on the total alkali silica (TAS) diagram: (on behalf of the IUGS Subcommission on the Systematics of Igneous Rocks). *An International Geoscience Journal of the Geological Society of Australia* **31**, 243-255.

MCPHIE J., DELLAPASQUA F., ALLEN S. R. & LACKIE M. A. 2008. Extreme effusive eruptions: Palaeoflow data on an extensive felsic lava in the Mesoproterozoic Gawler Range Volcanics. *Journal of Volcanology and Geothermal Research* **172**, 148-161.

MCPHIE J. D., M.

ALLEN, R. 1993 Volcanic textures: a guide to the interpretation of textures in volcanic rocks. University of Tasmania Centre for Ore Deposit and Exploration Studies.

MORROW N. & MCPHIE J. 2000. Mingled silicic lavas in the Mesoproterozoic Gawler Range Volcanics, South Australia. *Journal of Volcanology and Geothermal Research* **96**, 1-13.

PANKHURST M. J. 2006 The World's only shield volcano: geodynamical constraints of the Mesoproterozoic Felsic Large Igneous Province, South Australia. Monash University.

PANKHURST M. J., SCHAEFER B. F., PANKHURST P. G., SCHAEFER N., BETTS M., PHILLIPS M. & HAND M. 2011. A Mesoproterozoic continental flood rhyolite province, the Gawler Ranges, Australia: The end member example of the Large Igneous Province clan. *Solid Earth* **2**, 25-33.

PEUCAT J. J., CAPDEVILA R., FANNING C. M., MÉNOT R. P., PÉCORA L. & TESTUT L. 2002 1.60 Ga felsic volcanic blocks in the moraines of the Terre Adélie Craton, Antarctica: comparisons with the Gawler Range Volcanics, South Australia. pp. 831-845. Oxford, UK.

PHILLIPS N. 2006 Geophysical mapping of the Hutchison Group beneath the Gawler Range Volcanics, Gawler Craton, Australia. Monash University.

POWELL R. 1984. Inversion of the assimilation and fractional crystallization (AFC) equations: Characterisation of contaminants from isotope and trace element relationships in volcanic suites. *J. Geol Soc Lond.* **141**, 447 -52.

PUTIRKA K. D. 2008. Thermometers and Barometers for Volcanic Systems. *Reviews in Mineralogy and Geochemistry* **69**, 61-120.

ROACHE M. W. 1996 The geology, timing of mineralization and genesis of the Menninnie Dam Zn-Pb-Ag deposit, Eyre Peninsula, South Australia. The University of Tasmania.

ROACHE M. W., ALLEN S. R. & MCPHIE J. 2000. Surface and subsurface facies architecture of a small hydroexplosive, rhyolitic centre in the Mesoproterozoic Gawler Range Volcanics, South Australia. *Journal of Volcanology and Geothermal Research* **104**, 237-259.

STEWART K. P. 1994 High temperature felsic volcanism and the role of mantle magmas in Proterozoic crustal growth: The Gawler Range Volcanic Province. The University of Adelaide.

TREGEAGLE J. 2014 Petrogenesis and magma chamber evolution of the Gawler Range Volcanics. The University of Adelaide.

TURNER A. R. 1975. The petrology of the eastern Gawler Ranges Volcanic Complex. *Bulletin 45.* The Geological Survey of South Australia.

TWIST D. & FRENCH B. 1983. Voluminous acid volcanism in the Busheveld Complex: A review of the Rooiberg Felsite. *Bulletin Volcanologique* **46**, 225-242.

WADE C. E., REID A. J., WINGATE M. T. D., JAGODZINSKI E. A. & BAROVICH K. 2012. Geochemistry and geochronology of the c. 1585Ma Benagerie Volcanic Suite, southern Australia: Relationship to the Gawler Range Volcanics and implications for the petrogenesis of a Mesoproterozoic silicic large igneous province. *Precambrian Research* **206-207**, 17-35.

WATSON E. B. & HARRISON T. M. 1983. Zircon saturation revisited: temperature and composition effects in a variety of crustal magma types. *Earth and Planetary Science Letters* **64**, 295-304.

# APPENDIX A: GPS COORDS, ROCK/THIN SECTION DESCRIPTS.

| Area | Sample # | Lithology | E | N | Brief comment | Dip | Strike | Measurement type | Rock Descript. | Thin Section Descipt. |
|---|---|---|---|---|---|---|---|---|---|---|
| Toondulya Bluff | 1 | Dacite | 494146 | 6446557 | Flow-banded | | | | Highly weathered sparsely porphyritic dacite with 2-5% feldspar phenocrysts set in a fine-grained red-brown groundmass. Subhedral feldspars are circular/angular, cream-pink and no larger than 2mm. Some have been completely altered to sericite, giving a dull green appearance. The rock shows other signs of alteration in the presence of discontinuous black laminar layers along fractures and black specks throughout the groundmass giving a mottled texture. Minor amounts of magnetic minerals are present. | Rock is notable for its paucity of phenocrysts and where they are seen are small and anhedral in crystal habit. The feldspars are represented by potassium feldspar and plagioclase with the latter in slightly less abundance. Quartz occurs only in the groundmass as small circular and sub-circular crystals. The groundmass is microcrystalline, homogenous and consists of randomly oriented grains giving a felty texture. Overall the rock has a very homogenous composition and coherent texture |
| Toondulya Bluff | 2 | Dacite | 494474 | 6446014 | Flow-banded, lithic clasts ellipsoidal shaped 1-5cm, flow banding wraps around | 28 | 144 | flow bands | See sample 1 | |
| Toondulya Bluff | 3 | Dacite | 494635 | 6446427 | Quartz present | | | | Reasonably fresh sample of feldspar-phyric rhyodacite. Rock has an evenly porphyritic texture comprising phenocrysts of k-feldspar and quartz. Potassium feldspar crystals are deep pink, <3mm, some partially sericitised, subhedral and tabular, and often hard to distinguish from the similarly coloured brick-red fine-grained groundmass. Quartz is present in small quantities as circular/subcircular crystals ≈1mm and rarely greater than 2mm. Although the rock closely resembles samples 1&2, subtle differences can be seen in its groundmass colour and mineralogy (presence of quartz). | |
| Toondulya Bluff | 4 | Dacite | 494916 | 6446718 | Same lithology as stop 4 | | | | See sample 3 | |
| Toondulya Bluff | 11 | Dacite | 494937 | 6448069 | Near columnar jointed, sparsely porphyritic | | | | See sample 3 | |
| Toondulya Bluff | 5 | Rhyolite | 496040 | 6447635 | Porphyritic rhyolite | | | | Sparsely porphyritic rhyolite containing feldspar and quartz phenocrysts in a fine-grained dark red/brown groundmass. Quartz and feldspars are evenly distributed and occur in roughly equal amounts. Euhedral feldspars are white-cream coloured with partial hematite staining and are relatively large up to 5mm. They commonly display well defined edges and square-tabular shapes. Quartz occur mostly as subrounded, glassy crystals sized from 1mm to 2mm. | Dominant phenocryst phases of quartz and potassium feldspar set in a microcrystalline, moderately-highly weathered groundmass. Quartz crystals are all of similar size (1-2.5mm) and subcircular shape. Potassium feldspars are highly weathered, euhedral to subhedral in shape and up to 4mm. Less amounts of plagioclase also present, showing polysynthetic twinning, sometimes occurring in amalgamations with k-feldspar. Locally seen is a hornblende phenocryst distinguished by its cleavage planes, and has been replaced by many small opaques. Patches of granophyric textured domains are common, which may be remnants of the original, less altered groundmass. |

| | | | | | | | | | | | | | |
|---|---|---|---|---|---|---|---|---|---|---|---|---|---|
| Toondulya Bluff | 6 | Rhyolite | 495768 | 6447660 | Same rock as stop 5 | | | | | See sample 5 | | | |
| Toondulya Bluff | 7 | Rhyodacite | 495595 | 6447976 | Flow bands, flow folds, black groundmass | | 72 | 60 | flow bands | Sparsely porphyritic dacite with abundant pink-red potassium feldspar phenocrysts. Feldspars vary in size (<2mm) and are mostly angular fragments with a scattered distribution. They vary in a colour spectrum from cream to red, which may be from different degrees of iron staining. The rock is easily distinguished by its fine-grained black groundmass. | | | |
| Toondulya Bluff | 10 | Rhyodacite | 495193 | 6448154 | Flow bands, some amygdales, black/dark brown groundmass | | | | | Same lithology as sample 7, except amygdales are present and groundmass is dark-brown. | | | |
| Toondulya Bluff | 8 | Rhyodacite | 495470 | 6447953 | Flow bands, flow folds, black groundmass | | 62 | 250 | flow bands | See sample 7 | | | |
| Toondulya Bluff | 9 | Dacite | 495414 | 6448028 | Amygdales, some alligned. Coarser groundmass. | | | 200 | amydale alligment | | | | |
| | | | | | | | | | | | | | |
| Narlaby Well | 1 | Rhyolite | 517658 | 6424821 | Flourite crystals, moderately coarse-grained | | | | | Porphyritic rock with approximately 22% phenocryst population comprising pink euhedral feldspars and rounded glassy quartz crystals. Quartz are mostly circular crystals up to 2mm. Potassium feldspars are anhedral, pink and sized up to 4mm. The groundmass appears mottled due to a scattered distribution of quartz/feldspar fragments. Minor amounts of fluorite are also present. | | | |
| Narlaby Well | 2 | Rhyolite | | | Flourite in some amygdales higher up hill | | | | | The rock only differs to sample 1 in the presence of amygdales. The amygdales are abundant, commonly <2.5mm, but are locally seen up to 1.5cm, and characterized by their quartz rims and spherical/tear shapes. In many amygdales fluorite has precipitated, giving them a purple glassy appearance. Feldspars are pink, euhedral and angular, evenly distributed and less than 4mm. | Rock is quite homogenous, containing only amygdales and k-feldspar phenocrysts among a recrystallized altered groundmass. Amygdales appear as almost perfectly spherical aggregates of quartz, and are commonly partly chloritized. K-feldspar have a reddish tinge and many have been partially altered by chlorite, occurring as small irregular green patches within the crystals. | |
| Narlaby Well | 3 | Rhyolite | | | Further up-hill, flow bands, flow folds | | 62 | 80 | axial plane of flow folds | Overlying the amygdaloidal rhyolite and only differs from previous samples in having a flow banded texture. Flow banding is wavy and defined by alternating pale brown and dark brown bands. Potassium feldspar phenocrysts tend to align in the direction of flow. | | | |
| Waganny Dam | 1 | Rhyolite | 543057 | 6382947 | Very quartz rich, pale-brown groundmass | | | | | Sparsely porphyritic rhyolite with an even distribution of rounded quartz crystals (<2mm) and euhedral cream feldspars (2.5mm). Phenocryst population is dominated by feldspars and quartz with a ratio of 3:7. A distinctive feature of the rock is its pale brown groundmass. | | | |

| | | | | | | | | | | |
|---|---|---|---|---|---|---|---|---|---|---|
| Waganny Dam | 1.4 | Rhyodacite | 543026 | | 6382928 | 50/50 quartz:fspar, dark brown-black | | | | Porphyritic 'rhyodacite' with phenocrysts dominated by feldspar and quartz. Euhedral feldspars are milky white with partial iron staining, tabular and angular shaped, sized up to 3mm and are unevenly distributed. Sub-rounded, glassy quartz are evenly distributed among the dark grey fine-medium grained groundmass and sized up to 2mm. Feldspar and quartz are equally abundant, representing 2% of the total rock amount each. |
| Waganny Dam | 1.8 | Dacite | 543025 | | 6382914 | | | | | Porphyritic dacite with phenocrysts of k-feldspar and plagioclase set in a fine grained dark brown groundmass. Majority of feldspars are plagioclase, quite randomly distributed and of all sizes up to 6mm. Occasional small (<1mm) laths of feldspars, aswell as crystal fragments can be seen. Similar appearance to the dacite at Toondulya Bluff (samples 3, 4, 11), but mostly differs in a higher percentage of phenocrysts. | Massive texture throughout with dominant phenocryst phases of potassium feldspar and plagioclase. Quartz is less common, occurring as small (<0.1mm) sub-circular to irregular shaped crystals. There are significant amounts of alteration, reflected by a patchy matrix of light and dark shades of brown as well as secondary carbonate mineralization in the feldspars. Phenocrysts occupy app. 15% of the total rock and are set in a finely recrystallized groundmass composed of thin, discontinuous bands of quartz intergrowths and smaller crystal fragments. Plagioclase feldspar appears tabular/euhedral, and as intergrowths of smaller crystals giving it an irregular shape. Polysynthetic twinning is common and most crystals have been breached with alteration. Crystal sizes are up to 3mm. Potassium feldspar appears in slightly less amounts than plagioclase but is similar sized and shows the same degrees of alteration. |
| Waganny Dam | 2 | Rhyolite | 543852 | | 6384335 | Crystal-rich | | | | Crystal-rich ignimbrite containing a random distribution of pink feldspars and glassy quartz crystals of equal amounts. Feldspars are commonly euhedral and no larger than 2.5mm. Quartz crystals are rounded and 1-2mm. Crystal aggregates occur in some places where k-spar and quartz are concentrated in distinct subcircular zones (possible xenoliths). Groundmass is fine-medium grained, dark brown and contains many small fragments of quartz crystals and feldspars (may allude to a pyroclastic origin). | The rock has distinctive flow banding or compaction layering with many lenticular clasts of quartz (flattened pumice?). Fiamme are seen as orange-brown coloured altered zones of quartz showing undulose extinction. Phenocrysts are unevenly distributed and are 'wrapped' by the dominant layering indicating they are pre or syn-depostional. Many quartz phenocrysts have been broken with crystal fragments scattered throughout the groundmass. The groundmass itself is microscrystalline, composed mosly of quartz and k-feldspar and has a moderate amount of shard-like quartz crystals. Quartz also has melt inclusions, some are better preserved than others. Of the k-feldspars, some show single twinning and a heterogeneous composition due to unmixing of the solid solution. |

| | | | | | | | | | | | |
|---|---|---|---|---|---|---|---|---|---|---|---|
| Waganny Dam | | 3 | Rhyolite | 543876 | 6384881 | Crystal-rich, flow bands, pink clasts | | 40 | 261 | flow bands | |
| | | | | | | | | | | | Sample 3 is petrographically identical to sample 2 with an exception to its more pronounced pyroclastic features, such as eutaxitic texture exposed on weathered surfaces where remnants of whispy shaped fiamme (<3cm) can be seen. Groundmass slightly differs in colour as a pale brown. |
| | | | | | | | | | | | |
| Thurlga | | 1 | Rhyolite | 569597 | 6390005 | Sparsely porphyritic, highly jointed | | | | | |
| | | | | | | | | | | | Sparsely porphyritic rhyolite with a well preserved phenocrysts of quartz and potassium feldspar. Quartz is rounded to subrounded, glassy, <2mm while k-spar is pink, euhedral and less than 2.5mm. Phenocrysts are set in a fine grained brick red groundmass. Minor amounts of pyrite. |
| | | | | | | | | | | | Rock has a massive texture with no signs of flow banding. Major phenocrysts are quartz and k-feldspar distributed quite unevenly throughout a microcrystalline groundmass.Quartz grains appear mostly sub-circular with some showing signs of fracturing and broken edges. Size of quartz phenocrysts varies from 0.1mm up to 3mm. Melt inclusions are common, distinguished by their pale brown colour and black rimmed edges within quartz grains. Potassium feldspar are slightly less common than quartz, some showing a perthitic texture and are mostly tabular and fragmented, sized from 2mm – 6mm. Inclusions of opaques are common. |
| Thurlga | | 2 | Rhyolite | 570097 | 6390243 | Sparsely porphyritic, highly jointed | | | | | |
| | | | | | | | | | | | See sample 1 |
| Thurlga | | 6 | Rhyolite | 571904 | 6391198 | Possible lithics, potentially volcaniclastic/ignimbrite | | | | | |
| | | | | | | | | | | | Weakly flow-banded crystal rich porphyritic rhyolite with even distribution of quartz and k-spar phenocrysts. Relatively abundant crystal amounts with app. 3 – 5% quartz and 6 – 8% k-spar. Phenocrysts set in a fine-medium grained pink-red groundmass with occasional small whispy streaks (possible fiamme?). |
| | | | | | | | | | | | Highly weathered rock with many crystals either entirely or partially recrystallized Phenocrysts in order of abundance are quartz, plagioclase and k-feldspar. Melt inclusions are common in the subhedral, angular quartz crystals, less than 2mm in size. Plagioclase displays polysynthetic twinning, is commonly subhedral with broken edges and sized up to 3mm. Potassium feldspar is slightly less abundant with sharp edges, some fragmented and of similar size to k-feldspar. Both feldspar phases contain spotty inclusions of opaques, and have been partially or completed altered. The groundmass is relatively coarse in comparison to other areas and has an equigranular, texture showing alteration in secondary mineralization of carbonates. Much of the groundmass is dominated by quartz which appears irregular shaped and overprints much of the finer-grained material. |

| | | | | | | | | | | |
|---|---|---|---|---|---|---|---|---|---|---|
| Thurlga | 4 | Rhyolite | 571778 | 6390922 | Quartz more abundant, and bigger | | | | See sample 6 | |
| Thurlga | 3 | Dacite | 571772 | 6390701 | Evenly porphyritic, highly weathered | | | | Porphyritic dacite comprising potassium feldspar and quartz, which respectively make up approximately 4% and 2% of the rock. Feldspars are euhedral and anhedral, <3mm, and hard to distinguish against the similarly coloured fine-medium grained brick groundmass. Some have been partially sericitized. Quartz crystals vary in size up to 3mm, rounded/egg-shaped and randomly distributed. Minor amounts of mustard coloured limonite and blue-grey hematite occur along fractures and in some crystals. The groundmass appears relatively heterogenous due to an abundance of scattered crystal(?) fragments. | |
| Thurlga | 5 | Dacite | 572033 | 6390997 | Fresher, quartz absent | | | | See sample 3 | |
| Buckleboo | 1 | Rhyolite | 600326 | 6381782 | | | | | Sparsely porphyritic rhyolite with an even texture containing small amounts of quartz and feldspar phenocrysts ≈ 3% and 5% respectively. Quartz crystals are rounded and sub-rounded, glassy and commonly 2mm but locally seen up to 5mm. Pink potassium feldspars are rounded and square shaped up to 2mm. Rock has a very fine-grained mud brown groundmass. Rounded pink clasts (≈2cm) are slightly more crystal rich and have a eutaxitic texture defined by light brown streaks (fiamme) within the groundmass. Minor amounts of pyrite. | |
| Buckleboo | 2 | Dacite | 604890 | 6380905 | Coarse-grained rock, high phenocryst abundance in fine groundmass | | | | | |
| Buckleboo | 3 | Rhyolite | 597949 | 6382256 | Angular crystals | | | | Sparsely porphyritic rhyolite containing phenocrysts of milky white potassium feldspar and glassy quartz. Both minerals are of equal abundance amounting to a total phenocryst population of 10%. Quartz is variable in size from larger (3mm) square/angular shaped crystals to smaller (1mm) sub-rounded/angular crystals. Potassium feldspar is smaller in size ranging from 0.5mm to 1.5mm, and displays similar crystal shapes (angular, square). The rock has a distinctive pale brown/cream coloured groundmass that is fine-grained with occasional light brown lenticular domains sizing from several mm's up to several cm's | Potassium feldspar and quartz have a moderately even crystal distribution set in a pale brown, microcrystalline groundmass. Of the feldspars, some show single twinning and most have been weathered, giving them a cloudy appearance. Some have been completely recrystallized with constituents from the groundmass. Phenocrysts are set in a pale brown, equigranular and distinct microcrystalline groundmass composed of a mosaic of quartz and k-feldspar crystals. |
| Buckleboo | 4 | Andesite | 597917 | 6375193 | | | | | Black andesite with small white phenocrysts, irregular shaped and commonly 1mm, rarely up to 1.5mm. Fine crystals of quartz, galena glisten on the surface along with minor amounts of pyrite. Rock has a fine-grained homogenous black/dark grey coloured groundmass. | Aphanitic and massive textured rock with an equigranular and microcrystalline groundmass. Many irregular shaped quartz filled vesicles, commonly 1mm appear throughout. |

| | | | | | | | | | | | |
|---|---|---|---|---|---|---|---|---|---|---|---|
| Buckleboo | 5 | Andesite | 594036 | 6374936 | | | | | See sample 4 | | |
| Buckleboo | 5.5 | Nil | 588951 | 6373157 | Regolith, mapped as Waganny, loose highly weatered volcanic nodules | | | | | | |
| Buckleboo | 6 | Rhyolite/Dac | 594773 | 6378039 | Porphyric black clasts 2-5cm, | | | | Crystal rich porphyritic rhyolite with phenocryst constituents of quartz (3%), cream coloured potassium feldspar (1-2%), and lithic clasts. Subhedral feldspar crystals show slight iron staining around the margins and partial-complete chloritization. They are no larger 4mm and are commonly seen scattered among the groundmass as smaller crystals (0.5mm). Quartz are quite large (3.5mm) and have a similar even distribution and crystal habit as the feldspars. Lithic clasts are minor and appear fine-grained and grey-green coloured sized up to 4mm. In the interstitial space between phenocrysts are occasional grey whisps/streaks, roughly aligned among the dark brown fine-grained groundmass | The rock has a massive texture with no signs of flow banding or any type of layering. Random distribution of phenocrysts with a spectrum of sizes and shapes. The lithics are mostly 4mm although locally appear up to 9mm, altered and containing an abundance of shard-like objects. The quartz crystals are sub-rounded and angular, some containing portions of the surrounding pale-brown microcrystalline groundmass. Partially altered k-feldspars appear cloudy and sized up to 4mm. Groundmass is mostly equigranular, but appears coarser grained in some places, represented by slightly larger quartz crystals. | | |
| Buckleboo | 7 | Rhyolite | 620673 | 6385990 | Highly weathered | | | | | | |
| Menninnie Dam | 2 | Rhyolite | 628825 | 6386621 | Very quartz rich, xenoliths of quartzite (Warrow) | | | | Porphyritic rhyolite with phenocrysts of quartz and potassium feldspar of 6% and 8% abundance respectively. Most of the quartz is interpreted to be fragments of the Warrow Quartzite (basement unit) which can be differentiated from the melt fractionated phenocrysts by a less glassy and translucent appearance. Quartz occurs as sub-rounded and angular phenocrysts, with a glassy appearance, sized up to 2mm. Subhedral potassium feldspar are pink, angular/sub-rounded/tabular, and no larger than 2mm. Minor amounts of pyrite. | Phenocrysts are abundant and mostly represented by fractured and broken crystals of quartz and k-feldspar. Many quartz possess recrystallized melt inclusions which appear similar to the surrounding groundmass. After quartz and k-feldspar in mineral abundance is a pale green mineral with high birefringence displaying pleochroism in light shades of green to dark green and rectangular shaped with sharp edges. The groundmass is fresh and not unlike that of the rhyolites found in Buckleboo (eg. sample 3), consisting of a mosaic of quartz and k-feldspar crystals. Within the groundmass are abundant crystal fragments, giving the groundmass a coarser appearance in some places. | | |
| Menninnie Dam | 3 | Dacite/Rhyo | 628772 | 6386670 | Brecciated contact, clasts of Eucarro | | | | | | |
| Menninnie Dam | 4 | Rhyolite | 628545 | 6382161 | Very quartz rich, basement xenoliths, black clasts 2cm | | | | Similar rock to stop 2 in its groundmass colour and mineralogy. Slight differences are seen in a higher abundance of phenocrysts (≈50% of total rock space), and a more coherent texture. The rock contains abundant potassium feldspar and quartz (in slightly less amounts). Pink and cream coloured potassium feldspars are tabular and sub-rounded shapes, commonly 2.5mm but also occurring as scattered smaller crystals with the fine-grained brick red groundmass. The rock has an evenly distributed phenocryst population. | | |

| | | | | | | | | | | | |
|---|---|---|---|---|---|---|---|---|---|---|---|
| Menninnie Dam | 5 | Rhyolite | 629035 | 6385916 | Sericite altered, green appearance | | | | | | |
| Menninnie Dam | 6 | Ignimbrite | 629440 | 6386860 | "Menninnie ignimbrite", large fiamme, sericticised | | | | | | |
| Menninnie Dam | 7 | Rhyolite | 635268 | 6391495 | Deeply altered/sericicised ignimbrite, en 66 | 295 | flow bands | | | | |
| Menninnie Dam | 8 | Tuff | 637666 | 6395401 | Slaty cleavage ,finely laminated ash and crystal rich layers, pale green | | | Pale green tuff with finely laminated layering abruptly changing to a more crystal rich zone. Groundmass is strongly altered to sericite, giving the rock its green appearance. The rock has near vertical slaty cleavage in outcrop. | | | |
| Menninnie Dam | 9 | Rhyolite | 637637 | 6395371 | Fiamme textures, adjacent to ash flow | | | Rhyolitic ignimbrite with a eutaxitic texture and phenocryst phases of quartz and potassium feldspar. Quartz are rounded and moderately evenly distributed, no larger than 1.5mm. Anhedral potassium feldspars are similar sized and the same colour as the pale red coloured, fine-grained groundmass. The fabric running throughout the rock is represented by discontinuous black streaks (2 – 5mm) wrapping around phenocrysts. Shard-like objects (<3mm) also align in the same orientation. | Whispy streaks weakly define a fabric that bends and wraps around phenocrysts of potassium feldspar and quartz. The streaks consist of aggregates of quartz and have been partially replaced by the groundmass. Potassium feldspars are quite altered and are all heavily fractured. In many quartz crystals are well preserved melt inclusions. Irregular shaped intergrowths of quartz (5mm) may have once been vesicles. The groundmass is finely recrystallized and quite heterogenous in grain size with some areas appearing as slightly coarser layers of quartz and potassium feldspar. | | |

# APPENDIX B: FIELD OBSERVATIONS

## Toondulya Bluff

At Toondulya Bluff in the SGRA's most western outcrop is a relatively simple stratigraphic sequence of Waganny Dacite and Bittali Rhyolite. To the northeast, the Eucarro Rhyolite overlies the Bittali Rhyolite, and is intruded by a Hiltaba Suite granite. A characteristic feature among the volcanics of the area is a sparsely porphyritic texture and phenocrysts sizes less than 2.5 mm (on average).
The Waganny Dacite can be divided into 2 different lithofacies; a brown sparsely porphyritic dacite and a red sparsely porphyritic dacite. A thin layer of black sparsely porphyritic dacite has also been described in the area overlying the brown dacite. Jagodzinski (1985) suggests that this unit is a dyke intruding the brown dacite as it shows vertical flow-banding. The Bittali Rhyolite overlies the rhyodacite and underlies the Eucarro Rhyolite to the east.
At the base of the Waganny Dacite is a highly weathered sparsely porphyritic dacite (samples 1 & 2) comprising scattered phenocrysts of subhedral cream plagioclase, 1-2 mm, set in a fine-grained brown groundmass. The unit is mostly massive in outcrop but locally shows layering of variable thickness from 2 mm to 10 cm. In some places it contains purplish-grey ellipsoidal clastsup to 3 cm in diameter and seemingly aligned in a horizontal orientation. The surrounding groundmass diverges around the clasts.
Overlying the brown dacite is a thick homogenous red sparsely porphyritic dacite unit (samples 3, 4, & 11) which can be discerned by its brick-red groundmass and presence of quartz phenocrysts. The rock has a massive texture throughout and is evenly porphyritic. Quartz occurs in small quantities as rounded, glassy crystals no larger than 1mm in diameter. Potassium feldspar is in greater abundance than plagioclase and occurs as deep pink, tabular-shaped crystal sized up to 3 mm in diameter. The unit is well jointed in places, closely resembling a columnar-jointed type cooling texture.
The lower portion of the Bittali Rhyolite is represented by a sparsely porphyritic rhyodacitic unit (samples 7, 8, 9 & 10) which is compositionally varied. In the basal section, amygdales occupy approximately 3% of the total rock volume and have been infilled with quartz and lesser amounts of secondary calcite and chlorite. Higher in stratigraphy at the crest of a hill, (towards the middle section) amygdales appear in higher abundance (~10%), are of larger size (up to 3 cm) and are set in a brick-red groundmass. In the upper section, the rock has a distinguishing fine-grained black groundmass with pink potassium feldspars (2 mm) and minor amounts of quartz. The rock displays flow banding and flow folding defined by mingled black- and brown-coloured domains. The banding has no preferential orientation and is of variable thickness from several millimetres to several centimetres.
The upper portion of Bittali Rhyolite starts to appear as scattered outcrop up the side of a hill (samples 5 & 6). It is quite easily distinguished from the underlying rocks by an increased abundance of phenocrysts (5 – 10% of total rock volume) and in particular rounded/sub-rounded quartz crystals of similar size (1.5 – 2 mm). Potassium feldspar occurs in slightly less amounts than quartz and is significantly large (<7 mm) towards the base of the unit. Outcrops of the Bittali are often well hidden amongst vegetation which makes it difficult to recognize any obvious textural features. As such, the Bittali is considered to be homogenous and massive, with no evidence of flow banding

## Narlaby Well

Located 32 km to the south east of Toondulya Bluff is a small outcrop of Bittali Rhyolite exposed on a hill (517658E, 6424821N) to the north of Mt Centre and west of Eurilla Hill. At the foot of the hill the rocks are porphyritic and contain a slightly higher phenocryst abundance (22%) than that observed in the rocks at Toondulya Bluff. Pink potassium feldspar (<4 mm) and a ferromagnesic phase dominate the phenocryst population. Minor amounts of rounded quartz crystals (<2 mm) and fluorite are also present less than 1mm in size. The lithology gradationally changes into an amygdaloidal rhyolite higher in stratigraphy in the middle section. Amygdales appear spherical and flattened (towards the top of the unit), with some seen to align in a vertical orientation. They have been infilled with secondary quartz and fluorite. Spherulites are also common in this section. Contorted flow-banding and flow-folding predominates the upper section and is defined by alternating black phenocryst-poor layers and brown phenocryst-rich layers.

## Waganny Dam

Although Waganny Dam is the type locality for the Waganny Dacite the unit is poorly exposed. The Bittali Rhyolite provides better exposures on a hill side to the north which is separated by a valley. The 'unnamed rhyolite' crops out as a thin band along a narrow saddle, bounded to the north and south by the Waganny Dacite.
The 'unnamed rhyolite' is sparsely porphyritic, containing euhedral cream potassium feldspars and rounded quartz crystals (average size 3 mm and 2 mm respectively), and evenly distributed throughout a distinct pale brown groundmass. To its immediate south is another rhyolite which is identical in its mineral phases, phenocrysts size, abundance and distribution but distinguished by a slightly coarser, dark-grey groundmass. Both rock types are visible as subcrop for ~ 30 m in a north – south direction (perpendicular to strike). The outcrop displays a massive texture and is highly weathered.
The Waganny Dacite is porphyritic with dominant phenocrysts of plagioclase and potassium feldspar sized up to 6mm. Both feldspar phases have unmixed completely to their alkali and plagioclase endmembers. Phenocrysts occupy a higher percentage of rock volume (15%) relative to the dacites seen at Toondulya Bluff and are set in a fine-grained brown groundmass.
Two crystal-rich rhyolitic units lying north of the dacite-rhyolite-dacite sequence exhibit a eutaxitic texture with flattened and aligned fiamme more clearly seen on the weathered surfaces. In both units, the phenocryst population is dominated by quartz and potassium feldspar which are quite unevenly distributed and set within a dark brown groundmass that is littered with crystal fragments. The basis for distinguishing the two rhyolites is subtle, and lies in a difference in groundmass colour (paler shade of brown).

## Thurlga

At Thurlga two conjoined low-lying hills have been mapped with a separate rock type for each; Bittali Rhyolite on the west hill, and Waganny Dacite on the east hill. It became apparent that the area hosted 3 different units distinguished by their silica content; dacite and rhyodacite where Waganny is mapped, and a single rhyolitic unit

where Bittali is mapped. The eastern hill has been subdivided into both WD and BR based on a quite immediate change and contrast in lithologies.
The dacite is sparsely and evenly porphyritic and highly weathered resulting in hematite alteration along fractures. Within the fresher interior are small (<2.5mm) phenocrysts of potassium feldspar and a ferromagnesic phase present in equal amounts. The groundmass is fine-grained and dark-red with minor amounts of quartz also present. Although the description above is reminiscent of the dacites (in particular the red dacite) at Toondulya Bluff, there are subtle differences in a slightly higher phenocryst percentage and coarser groundmass at Thurlga.
Although a visible boundary between the dacite and rhyodacite was not found, a change in lithology across a NE-SW trending line is interpreted as the boundary. The rhyodacite may be further broken down into two lithofacies that are distinguished only by crystal size and texture. Mineralogy of the two rock types are identical with quartz, plagioclase, potassium feldspar, and a ferromagnesian phase dominating the phenocryst assemblage. Whispy streaks occurring throughout one unit may define a weak form of layering. Thin flow bands are seen in outcrop occasionally wrapping around lenticular clast-like objects. Smaller-sized crystals and a slightly coarser groundmass also provide further distinction between the two units. The second rhyodacite shows no obvious signs of layering and has larger-sized crystals set in a fine-grained pale brown groundmass. The rhyolite cropping out on the adjacent hill is massive and porphyritic, comprising rounded/sub-rounded quartz (<2 mm) and pink potassium feldspars (<2.5mm) well distributed throughout a fine-grained brick red groundmass.

## Buckleboo

At Buckleboo (60 km north-west of Kimba), the SGRA volcanics are areally scattered across a large sub-circular zone. Basement rocks of the Warrow Quartzite (part of the Hutchison Group) are exposed at the surface as are intrusions of the Hiltaba Granite and highly porphyritic dacite dykes. The area has been a target for Cu-Au-Ag mineralization, which is hosted in hydrothermal and polymictic breccias of the GRV. Although Waganny Dacite has been mapped in the area, it is in fact an aphyric andesite unit that has been lumped into the Waganny nomenclature due to its similar stratigraphic position. The andesite was found as subcrop, well hidden by vegetation and highly weathered.
The rhyolites observed at Bittali outcrops show contrasting lithologies. To the north it is sparsely porphyritic with small (commonly 1mm, but locally up to 2.5mm) scattered phenocrysts of angular quartz and potassium feldspar throughout a very fine-grained mud brown groundmass. Ellipsoidal clasts are occasionally seen up to 2 cm in diameter with an identical phenocryst assemblage (size, shape and mineralogy), but in a coarser pinkish-brown groundmass. At outcrop 3, is a pale brown evenly porphyritic rock that is noticeably different by its colour and larger sized phenocrysts. Quartz and potassium feldspar again dominate, up to 2 mm in diameter, and have angular crystal edges. Approximately 5 km to the south west is a matrix-supported breccia where Bittali has been mapped. On exposed rock faces it appears similar to a crystal-rich lava flow of rhyolitic composition, however when cut open the rock presents abundant clasts and crystals of varying sizes with angular edges. Lithic clasts are green-coloured and fine-grained up to 4 mm. Quartz are a similar distribution and size among a fine-grained dark

brown matrix. In the interstitial space between clasts/crystals are faint pale brown whisp-shaped objects no larger than 3 mm.
Dacite dykes intrude the Bittali Rhyolite in several places, and appear petrographically similar to the Hiltaba Granite, although are distinguished by a highly porphyritic texture and lack of quartz. Xenolith clasts are common in the dykes and consist of Hutchison Group lithologies, andesite and autoliths.

### Menninnie Dam

At Menninnie Dam, rock units are exclusively rhyolitic and are scattered over a large area (~ 12 km E-W). Basement rocks of the Hutchison Group (predominantly Warrow Quartzite) are also scattered and exposed at the surface. In comparison to other SGRA localities, the rhyolites at Menninnie Dam area are substantially more crystal rich (>50% of total rock volume). At two outcrops in the central area (outcrops 2 & 4, Figure 13), a crystal rich rhyolite was found which appears almost identical, even though separated by a N-S distance of 4.5 km. The unit has an evenly porphyritic texture and contains xenoliths of underlying units (breccias, basement rocks). The top of the BR is represented by an autobreccia containing quartz-phyric rhyolite clasts of similar composition to the host rock. In some areas the unit has a green appearance due to sericite alteration.
Eutaxitic textures on weathered surfaces are prominent in several outcrop areas east of the crystal-rich rhyolite. In the north eastern most extent of the Menninnie Dam area is a fiamme-bearing rock with small (1mm) glassy, angular quartz crystals and anhedral potassium feldspars (1.5mm) set in a fine-grained dark-red/grey groundmass. Lateral variation occurs to the east where a finely layered sericite-altered ash tuff has been deposited. It curiously shows vertical, wavy slaty cleavage for up to 100 m along strike. At Tank Hill (635268E, 6391495N) a deeply sericite-altered ignimbrite displays moderate to steeply dipping layering orientations and contrasts the surrounding low-lying rocks in higher degrees of alteration.
Several drill cores (MD25=192459, MD31=192444, MD32=192464) from the area were found to intersect breccias and rhyolites correlated with the GRV. Drill hole MD 31 comprises an evenly porphyritic rhyolite in the upper sections (146.9m – 174.5m) which has similar appearance to the crystal-rich rhyolite described prior. It is potassium feldspar and quartz-phyric with average phenocrysts size no larger than 4 mm. Lithic fragments (<15mm) of the Hutchison Group and Kimban granitoids are present throughout. Below the rhyolite is a poorly sorted polymict breccia extending to the base of the drill core.

## WARTAKA

A sequence of interbedded rhyolitic tuffs and lavas are exposed as a narrow band (7 km E-W, 1 km N-S) of outcrop bound by the E-W trending Uno Fault at its southern margin. The volcanics have steep northward dipping beds (70 - 85˚) likely as a result of a ramp structure adjacent to the Uno Fault, which allows for N-S contrast in lithologies across the flat-lying topography (Turner 1975). Although the sequence displays lensing of units across its lateral extent, a generalized description of the stratigraphy is summarised below.

At the base of the sequence is a thin layer of greyish-green fine-grained banded tuff discontinuously in contact with and overlain by a purplish-red porphyritic rhyolite. Noted throughout the rock are whispy streaks (3-4mm) and phenocrysts of potassium feldspar and plagioclase (<1.5mm). In the upper sections of the sub-unit are abundant cavities (geodes sized from 5mm – 8cm) partially filled with quartz. The porphyritic rhyolite is overlain by a coarse crystal-rich rhyolite with anhedral quartz (<12mm) and potassium feldspar crystals (14mm) amounting to 40 % of the total rock volume. A thin crystal-rich tuff layer possessing much of the same petrographic characteristics (mineralogy, phenocryst distribution) as the underlying crystal-rich rhyolite but with smaller sized phenocrysts. Another tuff unit lies above the crystal-rich tuff and is distinctive by its greenish-grey groundmass containing randomly distributed pumiceous clasts. Further north is a flow banded rhyolite with a porphyritic texture predominantly comprising feldspar phenocrysts (4mm) and small amounts of quartz (1mm). Lateral variation is seen within the sub-unit in the presence of a discontinuous and lenticular amygdaloidal rhyolitic band. Flow banding becomes absent in overlying rhyolite and is distinguished by a sparsely porphyritic texture. The upper sequence comprises an aphyric black vitric tuff with weakly defined layering (flattened crystals) and a paucity of phenocrysts (<5%), a highly weathered banded tuff with quartz/feldspar phenocrysts (2-4mm) set in a purple-brown groundmass, and a coherent rhyolite containing euhedral feldspars (3mm) set in a reddish-brown groundmass.

# APPENDIX B: DRILL CORE DESCRIPTIONS

| Drill hole name | Drill hole no. | Depth from (m) | Depth to (m) | Lithology | Desciption |
|---|---|---|---|---|---|
| MD 25 | 192459 | 168.3 | 199.2 | Breccia | Polymict breccia, poorly sorted and composed of various lithic clasts;<br>whispy pale brown clasts (fiamme?) <5mm, large medium-grained granite (assemblage of qtz, plag and kspar) clasts up to 5m, foliated granodiorite, very fine grained chloritized rock. |
| | | 199.2 | 208 | | Crystalline, altered and unfoliated granodiorite clast in the polymict breccia unit. |
| | | 208 | 210.4 | | Polymict breccia as described before |
| | | 210.4 | 212 | | Fault breccia |
| | | 212 | 226.5 | | Clast-supported breccia composed of white qtz, altered yellow -green clasts, pegmatite fragments all of varying size and shapes. Groundmass is fine-grained dark grey-black with no volcaniclastic textures. |
| | | 226.5 | 232 | | Brecciated and fractured pink pegmatite set in a dark-grey groundmass. |
| | | 232 | 235.5 | | Metapelitic rock (Hutchison Group?) with a dark-grey matrix and layering progressively becoming discontinuous towards the base. Contains minor amounts of pyrite. |
| | | 235.5 | 237 | | Gradational contact into a matrix supported breccia with irregular to rounded clasts of granite in a dark grey and fine-grained matrix. |
| | | 237 | 239.2 | | Medium-grained brecciated and fractured granite in a dark grey and fine-grained matrix |
| | | | | | |
| MD 31 | 192444 | 146.9 | 174.7 | | Evenly porphyritic felsic volcanic rock with tabular to subhedral pink feldspars up to 10mm with partial green alteration (chloritized?) and making up 10% rock. Quartz are subrounded to rounded, <8mm and have similar abundance to the feldspars. Phenocrysts are set in a orange-brown to orange-green groundmass. Occasional xenoliths and white/green whispy shaped clasts are also present. |
| | | 174.7 | 180.7 | | Gradational contact into a polymict breccia (top of breccia reworked into the base of the lava flow). Breccia is poorly sorted and contains tabular quartzite, granite, sulphides and lithic clasts (shale). Clasts are dominantly quartzite nearer to the base. |
| | | | | | |
| MD 32 | 192464 | 114 | 202.1 | | Polymict matrix supported breccia. Clasts are composed of lithics, crystals (chloritized feldspar) Red and cream coloured thin, whispy volcanic clasts with pale brown rims and dark brown centres (flattened pumice?). Pegmatitic granite clasts pebble (3mm) to boulder size (35cm) containing k-spar, plag, quartz and biotite. Large (≈2m) black compositionally banded and sulphide (galena?) bearing metasediment clast present toward base. Quartzofeldspathic gneiss at the very base of the unit, texturally and compositionally alike the overlying rocks. |
| | | 202.1 | 204.5 | | Overlying polymict breccia intrudes the top of a dark grey and fine-grained psammite. |
| | | 204.5 | 217.4 | | Pelitic gneiss with a fabric defined by aligned black ferromagnesic mineral. Rock is folded and contains quartz veins. Gneiss banding becomes discontinuous towards the base. |
| | | 217.4 | 219.5 | | Dark grey fine-grained psammite. |
| | | 219.5 | 235 | | Medium-grained altered granite with abundant k-spar. |
| | | 235 | 246.9 | | Matrix-supported breccia with angular to sub-rounded granite clasts in a dark grey matrix |

## APPENDIX C: MICROPROBE DATA

Note: WD – Waganny Dam, D – Dacite, MD – Menninnie Dam, TB – Toondulya Bluff, PTS – Thurlga, S… - Sample number. GM – Groundmass, MI – Melt inclusion, Chl – Chlorite, Hbl – Hornblende, Apt – Apatite, Ilm – Ilmenite, Pl – Plagioclase, Kspar – K feldspar.

| Type | MI | MI | MI | MI | MI | MI | MI | MI | MI | MI | MI | MI | MI | MI | Apt | Apt | Apt | Chl |
|---|---|---|---|---|---|---|---|---|---|---|---|---|---|---|---|---|---|---|
| Sample ID | WDS2 | WDS2 | WDS2 | WDS2 | WDS2 | WDS2 | WDS2 | MDS2 | MDS2 | MDS2 | MDS2 | MDS2 | PTSS1 | PTSS1 | PTSS1 | WDD | WDD | WDD |
| SiO2 | 80.95 | 79.57 | 82.65 | 82.14 | 45.13 | 43.55 | 45.98 | 67.83 | 63.42 | 62.30 | 71.71 | 91.33 | 83.60 | 47.89 | 50.61 | 50.67 | 0.22 | 0.29 | 0.20 | 24.46 |
| TiO2 | 0.11 | 0.12 | 0.06 | 0.23 | 0.08 | 0.08 | 0.08 | 0.01 | 0.04 | 0.01 | 0.01 | 0.02 | 0.03 | 0.07 | 0.07 | 0.06 | 0.00 | 0.02 | 0.00 | 0.01 |
| Al2O3 | 10.19 | 10.95 | 9.92 | 9.28 | 27.33 | 26.01 | 28.96 | 17.72 | 17.96 | 17.19 | 16.80 | 5.86 | 9.07 | 26.60 | 30.11 | 29.05 | 0.01 | 0.02 | 0.00 | 19.21 |
| Cr2O3 | 0.00 | 0.00 | 0.00 | 0.00 | 0.03 | 0.01 | 0.02 | 0.00 | 0.00 | 0.00 | 0.03 | 0.00 | 0.02 | 0.00 | 0.00 | 0.01 | 0.01 | 0.00 | 0.01 | 0.00 |
| FeO | 0.82 | 0.27 | 0.55 | 0.35 | 8.46 | 8.26 | 7.58 | 1.87 | 2.09 | 5.19 | 0.34 | 0.02 | 1.31 | 8.54 | 4.05 | 4.34 | 0.28 | 0.40 | 0.31 | 25.97 |
| MnO | 0.02 | 0.01 | 0.03 | 0.01 | 0.16 | 0.20 | 0.12 | 0.05 | 0.03 | 0.16 | 0.03 | 0.00 | 0.00 | 0.11 | 0.08 | 0.11 | 0.19 | 0.19 | 0.17 | 1.37 |
| MgO | 0.05 | 0.02 | 0.03 | 0.01 | 0.82 | 0.81 | 0.71 | 0.32 | 0.58 | 1.48 | 0.02 | 0.00 | 0.19 | 0.98 | 1.05 | 1.39 | 0.18 | 0.15 | 0.15 | 11.80 |
| ZnO | 0.06 | 0.00 | 0.00 | 0.00 | 0.00 | 0.04 | 0.00 | 0.00 | 0.00 | 0.10 | 0.02 | 0.02 | 0.01 | 0.02 | 0.00 | 0.09 | 0.01 | 0.01 | 0.07 | 0.10 |
| CaO | 0.07 | 0.06 | 0.09 | 0.65 | 0.31 | 4.51 | 0.24 | 0.29 | 0.27 | 0.30 | 0.34 | 0.24 | 0.09 | 0.09 | 0.20 | 0.18 | 54.03 | 53.80 | 53.66 | 0.11 |
| Na2O | 0.41 | 0.56 | 1.25 | 0.59 | 0.28 | 0.24 | 0.23 | 9.23 | 2.74 | 4.94 | 7.92 | 3.47 | 1.11 | 0.20 | 0.24 | 0.19 | 0.27 | 0.27 | 0.25 | 0.00 |
| K2O | 7.69 | 9.03 | 6.77 | 7.42 | 7.44 | 7.36 | 8.53 | 0.70 | 8.28 | 4.09 | 2.63 | 0.17 | 4.37 | 8.58 | 7.58 | 7.68 | 0.01 | 0.01 | 0.01 | 0.02 |
| Cl | 0.00 | 0.01 | 0.00 | 0.01 | 0.07 | 0.01 | 0.01 | 0.05 | 0.07 | 0.02 | 0.02 | 0.02 | 0.05 | 0.06 | 0.03 | 0.04 | 0.06 | 0.09 | 0.19 | 0.00 |
| F | 0.00 | 0.00 | 0.00 | 0.35 | 0.77 | 2.99 | 0.97 | 0.00 | 0.00 | 0.00 | 0.00 | 0.00 | 0.03 | 0.23 | 0.13 | 0.16 | 3.59 | 3.59 | 3.04 | 0.11 |
| Total | 100.37 | 100.60 | 101.37 | 100.89 | 90.54 | 92.82 | 93.00 | 98.07 | 95.47 | 95.77 | 99.86 | 101.14 | 99.86 | 93.26 | 94.08 | 93.89 | 57.33 | 57.30 | 56.74 | 83.11 |
| Si | 2.695 | 2.649 | 2.751 | 2.734 | 1.502 | 1.450 | 1.530 | 2.258 | 2.111 | 2.074 | 2.387 | 3.040 | 2.783 | 1.594 | 1.685 | 1.687 | 0.007 | 0.010 | 0.007 | 0.814 |
| Ti | 0.003 | 0.003 | 0.002 | 0.006 | 0.002 | 0.002 | 0.002 | 0.000 | 0.001 | 0.000 | 0.000 | 0.000 | 0.001 | 0.002 | 0.002 | 0.002 | 0.000 | 0.000 | 0.000 | 0.000 |
| Al | 0.300 | 0.322 | 0.292 | 0.273 | 0.804 | 0.765 | 0.852 | 0.521 | 0.528 | 0.506 | 0.494 | 0.172 | 0.267 | 0.783 | 0.886 | 0.855 | 0.000 | 0.000 | 0.000 | 0.565 |
| Cr | 0.000 | 0.000 | 0.000 | 0.000 | 0.001 | 0.000 | 0.000 | 0.000 | 0.000 | 0.000 | 0.001 | 0.000 | 0.000 | 0.000 | 0.000 | 0.000 | 0.000 | 0.000 | 0.000 | 0.000 |
| Fe2+ | 0.011 | 0.004 | 0.008 | 0.005 | 0.118 | 0.115 | 0.105 | 0.026 | 0.029 | 0.072 | 0.005 | 0.000 | 0.018 | 0.119 | 0.056 | 0.060 | 0.004 | 0.006 | 0.004 | 0.361 |
| Mn2+ | 0.000 | 0.000 | 0.000 | 0.000 | 0.002 | 0.003 | 0.002 | 0.001 | 0.000 | 0.002 | 0.000 | 0.000 | 0.000 | 0.002 | 0.001 | 0.002 | 0.003 | 0.003 | 0.002 | 0.019 |
| Mg | 0.001 | 0.000 | 0.001 | 0.000 | 0.020 | 0.020 | 0.018 | 0.008 | 0.014 | 0.037 | 0.000 | 0.000 | 0.005 | 0.024 | 0.026 | 0.034 | 0.004 | 0.004 | 0.004 | 0.293 |
| Zn | 0.001 | 0.000 | 0.000 | 0.000 | 0.000 | 0.001 | 0.000 | 0.000 | 0.000 | 0.001 | 0.000 | 0.000 | 0.000 | 0.000 | 0.000 | 0.001 | 0.000 | 0.000 | 0.001 | 0.001 |
| Ca | 0.001 | 0.001 | 0.002 | 0.012 | 0.006 | 0.080 | 0.004 | 0.005 | 0.005 | 0.005 | 0.006 | 0.004 | 0.002 | 0.002 | 0.004 | 0.003 | 0.963 | 0.959 | 0.957 | 0.002 |
| Na | 0.007 | 0.009 | 0.020 | 0.010 | 0.004 | 0.004 | 0.004 | 0.149 | 0.044 | 0.080 | 0.128 | 0.056 | 0.018 | 0.003 | 0.004 | 0.003 | 0.004 | 0.004 | 0.004 | 0.000 |
| K | 0.082 | 0.096 | 0.072 | 0.079 | 0.079 | 0.078 | 0.091 | 0.007 | 0.088 | 0.043 | 0.028 | 0.002 | 0.046 | 0.091 | 0.080 | 0.081 | 0.000 | 0.000 | 0.000 | 0.000 |
| Ni | 0.000 | 0.000 | 0.000 | 0.000 | 0.000 | 0.000 | 0.000 | 0.000 | 0.000 | 0.000 | 0.000 | 0.000 | 0.000 | 0.000 | 0.000 | 0.000 | 0.000 | 0.000 | 0.000 | 0.000 |
| Cl | 0.000 | 0.000 | 0.000 | 0.000 | 0.002 | 0.000 | 0.000 | 0.002 | 0.002 | 0.001 | 0.001 | 0.001 | 0.002 | 0.002 | 0.001 | 0.001 | 0.002 | 0.002 | 0.005 | 0.000 |
| F | 0.000 | 0.000 | 0.000 | 0.019 | 0.040 | 0.157 | 0.051 | 0.000 | 0.000 | 0.000 | 0.000 | 0.000 | 0.002 | 0.012 | 0.007 | 0.008 | 0.189 | 0.189 | 0.160 | 0.006 |

| Type | Chl | Chl | Chl | Chl | Chl | Chl | Hbl | Hbl | Ilm | Ilm | GM | GM | GM | GM | GM | GM | GM | GM |
|---|---|---|---|---|---|---|---|---|---|---|---|---|---|---|---|---|---|---|
| Sample ID | WDD | WDD | WDD | WDD | WDD | WDD | MDS2 | MDS2 | MDS2 | MDS2 | WDS2 | WDS2 | WDS2 | WDS2 | WDS2 | WDS2 | WDD | WDD |
| SiO2 | 25.48 | 25.86 | 25.87 | 24.64 | 24.69 | 28.65 | 0.18 | 44.78 | 46.21 | 1.45 | 0.22 | 77.33 | 76.47 | 74.61 | 85.37 | 74.09 | 85.71 | 84.03 | 79.63 | 64.81 | 65.03 | 60.65 |
| TiO2 | 0.00 | 0.01 | 0.00 | 0.01 | 0.00 | 26.63 | 1.71 | 0.14 | 0.09 | 92.37 | 94.84 | 0.12 | 0.09 | 0.08 | 0.12 | 0.06 | 0.08 | 0.20 | 0.06 | 0.02 | 0.04 | 0.18 |
| Al2O3 | 19.52 | 19.26 | 21.07 | 19.41 | 19.34 | 6.77 | 0.47 | 28.19 | 31.11 | 0.84 | 0.22 | 11.04 | 11.31 | 12.63 | 7.22 | 12.16 | 7.04 | 8.16 | 10.68 | 18.53 | 18.41 | 18.59 |
| Cr2O3 | 0.00 | 0.00 | 0.00 | 0.00 | 0.00 | 0.00 | 0.17 | 0.00 | 0.00 | 0.00 | 0.00 | 0.00 | 0.01 | 0.00 | 0.00 | 0.00 | 0.00 | 0.00 | 0.00 | 0.00 | 0.02 | 0.00 |
| FeO | 27.03 | 25.91 | 26.98 | 26.71 | 26.80 | 2.70 | 2.88 | 6.28 | 3.10 | 0.91 | 0.76 | 0.63 | 0.24 | 0.60 | 0.54 | 0.70 | 0.36 | 0.42 | 0.36 | 0.66 | 0.97 | 6.53 |
| MnO | 1.42 | 1.36 | 1.49 | 1.44 | 1.48 | 0.13 | 0.33 | 0.15 | 0.00 | 0.00 | 0.00 | 0.00 | 0.02 | 0.00 | 0.00 | 0.01 | 0.00 | 0.01 | 0.00 | 0.01 | 0.00 | 0.04 |
| MgO | 12.47 | 13.09 | 12.14 | 11.56 | 11.87 | 0.64 | 0.10 | 2.02 | 1.26 | 0.09 | 0.08 | 0.07 | 0.02 | 0.07 | 0.04 | 0.03 | 0.01 | 0.01 | 0.05 | 0.01 | 0.01 | 0.29 |
| ZnO | 0.07 | 0.09 | 0.15 | 0.08 | 0.10 | 0.00 | 0.46 | 0.04 | 0.00 | 0.00 | 0.00 | 0.01 | 0.04 | 0.00 | 0.00 | 0.05 | 0.05 | 0.01 | 0.00 | 0.00 | 0.00 | 0.00 |
| CaO | 0.09 | 0.09 | 0.09 | 0.07 | 0.06 | 27.57 | 12.75 | 0.09 | 0.03 | 0.05 | 0.21 | 0.11 | 0.11 | 0.15 | 0.05 | 0.06 | 0.07 | 0.06 | 0.12 | 0.22 | 0.17 | 0.24 |
| Na2O | 0.05 | 0.00 | 0.00 | 0.06 | 0.03 | 0.06 | 0.08 | 0.07 | 0.08 | 0.01 | 0.00 | 1.06 | 0.80 | 1.01 | 0.48 | 1.12 | 0.56 | 0.82 | 1.18 | 3.69 | 3.56 | 6.75 |
| K2O | 0.02 | 0.03 | 0.03 | 0.02 | 0.03 | 0.01 | 0.05 | 9.48 | 10.89 | 0.46 | 0.13 | 7.79 | 9.20 | 8.92 | 5.23 | 9.47 | 5.18 | 6.24 | 6.51 | 11.27 | 11.35 | 5.97 |
| Cl | 0.00 | 0.02 | 0.01 | 0.00 | 0.02 | 0.00 | 0.08 | 0.01 | 0.00 | 0.00 | 0.00 | 0.00 | 0.00 | 0.01 | 0.01 | 0.01 | 0.01 | 0.00 | 0.01 | 0.04 | 0.03 | 0.02 |
| F | 0.12 | 0.10 | 0.06 | 0.11 | 0.07 | 1.73 | 7.31 | 0.26 | 0.23 | 0.01 | 0.00 | 0.00 | 0.00 | 0.00 | 0.00 | 0.00 | 0.00 | 0.00 | 0.00 | 0.00 | 0.00 | 0.00 |
| Total | 86.22 | 85.77 | 87.86 | 84.08 | 84.46 | 94.16 | 23.48 | 91.40 | 92.91 | 96.19 | 96.46 | 98.17 | 98.30 | 98.08 | 99.07 | 97.74 | 99.08 | 99.97 | 98.61 | 99.24 | 99.58 | 99.26 |
| Si | 0.848 | 0.861 | 0.861 | 0.820 | 0.822 | 0.954 | 0.006 | 1.491 | 1.538 | 0.048 | 0.007 | 2.574 | 2.545 | 2.484 | 2.842 | 2.466 | 2.853 | 2.797 | 2.651 | 2.157 | 2.165 | 2.019 |
| Ti | 0.000 | 0.000 | 0.000 | 0.000 | 0.000 | 0.667 | 0.043 | 0.003 | 0.002 | 2.313 | 2.375 | 0.003 | 0.002 | 0.002 | 0.003 | 0.001 | 0.002 | 0.005 | 0.001 | 0.000 | 0.001 | 0.004 |
| Al | 0.574 | 0.567 | 0.620 | 0.571 | 0.569 | 0.199 | 0.014 | 0.830 | 0.915 | 0.025 | 0.006 | 0.325 | 0.333 | 0.372 | 0.213 | 0.358 | 0.207 | 0.240 | 0.314 | 0.545 | 0.542 | 0.547 |
| Cr | 0.000 | 0.000 | 0.000 | 0.000 | 0.000 | 0.000 | 0.003 | 0.000 | 0.000 | 0.000 | 0.000 | 0.000 | 0.000 | 0.000 | 0.000 | 0.000 | 0.000 | 0.000 | 0.000 | 0.000 | 0.000 | 0.000 |
| Fe2+ | 0.376 | 0.361 | 0.375 | 0.372 | 0.373 | 0.038 | 0.040 | 0.087 | 0.043 | 0.013 | 0.011 | 0.009 | 0.003 | 0.008 | 0.008 | 0.010 | 0.005 | 0.006 | 0.005 | 0.009 | 0.014 | 0.091 |
| Mn2+ | 0.020 | 0.019 | 0.021 | 0.020 | 0.021 | 0.002 | 0.005 | 0.002 | 0.000 | 0.000 | 0.000 | 0.000 | 0.000 | 0.000 | 0.000 | 0.000 | 0.000 | 0.000 | 0.000 | 0.000 | 0.000 | 0.001 |
| Mg | 0.309 | 0.325 | 0.301 | 0.287 | 0.294 | 0.016 | 0.003 | 0.050 | 0.031 | 0.002 | 0.002 | 0.002 | 0.000 | 0.002 | 0.001 | 0.001 | 0.000 | 0.000 | 0.001 | 0.000 | 0.000 | 0.007 |
| Zn | 0.001 | 0.001 | 0.002 | 0.001 | 0.001 | 0.000 | 0.006 | 0.000 | 0.000 | 0.000 | 0.000 | 0.000 | 0.000 | 0.000 | 0.000 | 0.001 | 0.001 | 0.000 | 0.000 | 0.000 | 0.000 | 0.000 |
| Ca | 0.002 | 0.002 | 0.002 | 0.001 | 0.001 | 0.492 | 0.227 | 0.002 | 0.001 | 0.001 | 0.004 | 0.002 | 0.002 | 0.003 | 0.001 | 0.001 | 0.001 | 0.001 | 0.002 | 0.004 | 0.003 | 0.004 |
| Na | 0.001 | 0.000 | 0.000 | 0.001 | 0.000 | 0.001 | 0.001 | 0.001 | 0.001 | 0.000 | 0.000 | 0.017 | 0.013 | 0.016 | 0.008 | 0.018 | 0.009 | 0.013 | 0.019 | 0.060 | 0.057 | 0.109 |
| K | 0.000 | 0.000 | 0.000 | 0.000 | 0.000 | 0.000 | 0.000 | 0.101 | 0.116 | 0.005 | 0.001 | 0.083 | 0.098 | 0.095 | 0.056 | 0.101 | 0.055 | 0.066 | 0.069 | 0.120 | 0.120 | 0.063 |
| Ni | 0.000 | 0.000 | 0.000 | 0.000 | 0.000 | 0.000 | 0.000 | 0.000 | 0.000 | 0.000 | 0.000 | 0.000 | 0.000 | 0.000 | 0.000 | 0.000 | 0.000 | 0.000 | 0.000 | 0.000 | 0.000 | 0.000 |
| Cl | 0.000 | 0.000 | 0.000 | 0.000 | 0.000 | 0.000 | 0.002 | 0.000 | 0.000 | 0.000 | 0.000 | 0.000 | 0.000 | 0.000 | 0.000 | 0.000 | 0.000 | 0.000 | 0.000 | 0.001 | 0.001 | 0.001 |
| F | 0.007 | 0.005 | 0.003 | 0.006 | 0.004 | 0.091 | 0.385 | 0.014 | 0.012 | 0.001 | 0.000 | 0.000 | 0.000 | 0.000 | 0.000 | 0.000 | 0.000 | 0.000 | 0.000 | 0.000 | 0.000 | 0.000 |

| Type | GM | GM | GM | GM | GM | GM | GM | GM | GM | GM | GM | GM | GM | GM | GM | GM | GM | GM | GM | GM | GM | GM |
|---|---|---|---|---|---|---|---|---|---|---|---|---|---|---|---|---|---|---|---|---|---|---|
| Sample ID | WDD | WDD | MDS2 | MDS2 | MDS2 | MDS2 | MDS2 | TBS2 | TBS2 | TBS2 | TBS2 | TBS2 | TBS2 | PTSS1 | PTSS1 | PTSS1 | PTSS1 | PTSS1 | PTSS1 | PTSS1 | PTSS1 | PTSS1 |
| SiO2 | 65.76 | 82.19 | 79.35 | 78.29 | 83.80 | 79.60 | 66.85 | 66.54 | 60.26 | 0.17 | 36.53 | 36.51 | 89.31 | 95.21 | 87.62 | 84.53 | 66.70 | 65.86 | 93.85 | 79.10 | 91.59 | 74.86 | 63.96 |
| TiO2 | 0.02 | 0.04 | 0.01 | 0.00 | 0.02 | 0.00 | 0.01 | 0.00 | 0.00 | 0.00 | 0.03 | 0.05 | 0.00 | 0.02 | 0.18 | 0.00 | 0.00 | 0.01 | 0.01 | 0.01 | 0.00 | 0.01 | 0.00 |
| Al2O3 | 18.65 | 10.34 | 12.13 | 12.52 | 8.83 | 12.02 | 19.86 | 19.86 | 23.54 | 0.05 | 24.01 | 25.07 | 3.70 | 1.07 | 3.28 | 6.59 | 17.72 | 17.87 | 1.50 | 10.17 | 3.53 | 15.15 | 16.59 |
| Cr2O3 | 0.00 | 0.02 | 0.00 | 0.00 | 0.05 | 0.00 | 0.00 | 0.01 | 0.00 | 0.00 | 0.03 | 0.03 | 0.00 | 0.01 | 0.01 | 0.00 | 0.00 | 0.01 | 0.00 | 0.00 | 0.00 | 0.00 | 0.00 |
| FeO | 0.64 | 0.19 | 0.23 | 0.75 | 0.06 | 0.40 | 0.01 | 0.02 | 0.50 | 0.04 | 10.43 | 9.43 | 0.02 | 0.02 | 3.44 | 0.12 | 0.71 | 0.05 | 0.06 | 0.07 | 0.23 | 0.06 | 0.08 | 1.21 |
| MnO | 0.04 | 0.00 | 0.01 | 0.00 | 0.01 | 0.01 | 0.01 | 0.00 | 0.09 | 0.00 | 0.50 | 0.71 | 0.00 | 0.00 | 0.01 | 0.00 | 0.00 | 0.01 | 0.00 | 0.00 | 0.00 | 0.00 | 0.00 | 0.01 |
| MgO | 0.05 | 0.04 | 0.03 | 0.05 | 0.01 | 0.15 | 0.01 | 0.00 | 0.21 | 0.00 | 0.03 | 0.04 | 0.00 | 0.01 | 0.01 | 0.00 | 0.03 | 0.02 | 0.01 | 0.01 | 0.07 | 0.01 | 0.01 | 0.08 |
| ZnO | 0.00 | 0.00 | 0.05 | 0.02 | 0.08 | 0.04 | 0.02 | 0.00 | 0.01 | 0.00 | 0.00 | 0.01 | 0.01 | 0.03 | 0.00 | 0.00 | 0.00 | 0.00 | 0.01 | 0.01 | 0.02 | 0.06 | 0.00 | 0.00 |
| CaO | 0.15 | 0.06 | 0.26 | 0.36 | 0.30 | 0.03 | 0.35 | 0.19 | 0.35 | 81.46 | 22.93 | 22.79 | 0.07 | 0.02 | 0.03 | 0.00 | 0.05 | 0.04 | 0.04 | 0.03 | 0.12 | 0.03 | 0.04 | 0.18 |
| Na2O | 3.14 | 1.03 | 4.02 | 6.41 | 3.64 | 0.25 | 11.93 | 11.61 | 8.36 | 0.03 | 0.00 | 0.00 | 0.86 | 0.11 | 0.49 | 1.33 | 5.32 | 5.70 | 0.94 | 0.29 | 0.78 | 0.66 | 7.69 | 4.01 |
| K2O | 12.48 | 7.66 | 5.35 | 1.65 | 2.36 | 9.14 | 0.03 | 0.09 | 2.64 | 0.03 | 0.00 | 0.00 | 1.66 | 0.42 | 2.04 | 4.08 | 7.87 | 0.11 | 15.12 | 0.66 | 6.29 | 1.95 | 1.70 | 4.49 |
| Cl | 0.02 | 0.09 | 0.00 | 0.00 | 0.02 | 0.01 | 0.00 | 0.08 | 0.03 | 0.00 | 0.00 | 0.00 | 0.00 | 0.00 | 0.00 | 0.00 | 0.00 | 0.00 | 0.01 | 0.01 | 0.00 | 0.00 | 0.02 | 0.03 |
| F | 0.00 | 0.00 | 0.01 | 0.00 | 0.00 | 0.00 | 0.00 | 0.00 | 0.00 | 37.48 | 0.00 | 0.00 | 0.00 | 0.00 | 0.00 | 0.00 | 0.00 | 0.00 | 0.00 | 0.00 | 0.01 | 0.00 | 0.00 | 0.02 |
| Total | 100.94 | 101.66 | 100.63 | 101.44 | 100.05 | 99.17 | 101.63 | 99.15 | 98.35 | 95.97 | 103.47 | 94.51 | 94.66 | 95.64 | 96.93 | 97.11 | 96.67 | 98.40 | 96.54 | 99.95 | 96.42 | 96.79 | 97.89 | 99.55 | 90.56 |
| Si | 2.189 | 2.736 | 2.353 | 2.641 | 2.606 | 2.790 | 2.650 | 2.226 | 2.215 | 2.006 | 0.006 | 1.216 | 1.215 | 2.973 | 3.169 | 2.917 | 2.814 | 2.220 | 2.700 | 2.192 | 3.124 | 2.633 | 3.049 | 2.492 | 2.129 |
| Ti | 0.001 | 0.001 | 0.001 | 0.000 | 0.000 | 0.000 | 0.000 | 0.000 | 0.000 | 0.000 | 0.000 | 0.001 | 0.001 | 0.000 | 0.001 | 0.004 | 0.000 | 0.000 | 0.000 | 0.000 | 0.000 | 0.000 | 0.000 | 0.000 | 0.000 |
| Al | 0.549 | 0.304 | 0.493 | 0.357 | 0.368 | 0.260 | 0.354 | 0.584 | 0.584 | 0.693 | 0.001 | 0.706 | 0.738 | 0.109 | 0.032 | 0.097 | 0.194 | 0.521 | 0.279 | 0.526 | 0.044 | 0.299 | 0.104 | 0.446 | 0.488 |
| Cr | 0.000 | 0.000 | 0.001 | 0.000 | 0.000 | 0.001 | 0.000 | 0.000 | 0.000 | 0.000 | 0.001 | 0.001 | 0.001 | 0.000 | 0.000 | 0.000 | 0.000 | 0.000 | 0.000 | 0.000 | 0.000 | 0.000 | 0.000 | 0.000 | 0.000 |
| Fe2+ | 0.009 | 0.003 | 0.006 | 0.003 | 0.010 | 0.001 | 0.006 | 0.000 | 0.000 | 0.007 | 0.000 | 0.145 | 0.131 | 0.000 | 0.000 | 0.048 | 0.002 | 0.010 | 0.001 | 0.001 | 0.001 | 0.003 | 0.001 | 0.001 | 0.017 |
| Mn2+ | 0.001 | 0.000 | 0.000 | 0.000 | 0.000 | 0.000 | 0.000 | 0.000 | 0.000 | 0.001 | 0.000 | 0.007 | 0.010 | 0.000 | 0.000 | 0.000 | 0.000 | 0.000 | 0.000 | 0.000 | 0.000 | 0.000 | 0.000 | 0.000 | 0.000 |
| Mg | 0.001 | 0.001 | 0.003 | 0.001 | 0.001 | 0.000 | 0.004 | 0.000 | 0.000 | 0.005 | 0.000 | 0.001 | 0.001 | 0.000 | 0.000 | 0.000 | 0.001 | 0.000 | 0.000 | 0.000 | 0.000 | 0.002 | 0.000 | 0.000 | 0.002 |
| Zn | 0.000 | 0.000 | 0.000 | 0.001 | 0.000 | 0.001 | 0.001 | 0.000 | 0.000 | 0.000 | 0.000 | 0.000 | 0.000 | 0.000 | 0.000 | 0.000 | 0.000 | 0.000 | 0.000 | 0.000 | 0.000 | 0.000 | 0.001 | 0.000 | 0.000 |
| Ca | 0.003 | 0.001 | 0.002 | 0.005 | 0.006 | 0.005 | 0.000 | 0.006 | 0.003 | 0.006 | 1.453 | 0.409 | 0.406 | 0.001 | 0.000 | 0.001 | 0.001 | 0.001 | 0.001 | 0.001 | 0.001 | 0.002 | 0.000 | 0.001 | 0.003 |
| Na | 0.051 | 0.017 | 0.062 | 0.065 | 0.103 | 0.059 | 0.004 | 0.192 | 0.187 | 0.135 | 0.000 | 0.000 | 0.014 | 0.002 | 0.008 | 0.021 | 0.086 | 0.092 | 0.015 | 0.005 | 0.013 | 0.011 | 0.124 | 0.065 |
| K | 0.133 | 0.081 | 0.092 | 0.057 | 0.018 | 0.025 | 0.097 | 0.000 | 0.001 | 0.028 | 0.000 | 0.000 | 0.018 | 0.004 | 0.022 | 0.043 | 0.084 | 0.001 | 0.160 | 0.007 | 0.067 | 0.021 | 0.018 | 0.048 |
| Ni | 0.000 | 0.000 | 0.000 | 0.000 | 0.000 | 0.000 | 0.000 | 0.000 | 0.000 | 0.000 | 0.000 | 0.000 | 0.000 | 0.000 | 0.000 | 0.000 | 0.000 | 0.000 | 0.000 | 0.000 | 0.000 | 0.000 | 0.000 | 0.000 | 0.000 |
| Cl | 0.001 | 0.003 | 0.000 | 0.000 | 0.001 | 0.000 | 0.000 | 0.002 | 0.001 | 0.000 | 0.000 | 0.000 | 0.000 | 0.000 | 0.000 | 0.000 | 0.000 | 0.000 | 0.000 | 0.000 | 0.000 | 0.000 | 0.000 | 0.000 | 0.001 |
| F | 0.000 | 0.000 | 0.000 | 0.000 | 0.000 | 0.000 | 0.000 | 0.000 | 0.000 | 1.973 | 0.000 | 0.000 | 0.000 | 0.000 | 0.000 | 0.000 | 0.000 | 0.000 | 0.000 | 0.000 | 0.000 | 0.000 | 0.000 | 0.000 | 0.001 |

| Type | Kspar | Kspar | Kspar | Kspar | Kspar | Kspar | Kspar | Kspar | Kspar | Kspar | Kspar | Kspar | Kspar | Kspar | Kspar | Kspar | Kspar | Kspar | Kspar | Kspar |
|---|---|---|---|---|---|---|---|---|---|---|---|---|---|---|---|---|---|---|---|---|
| Sample ID | WDD | WDD | WDD | WDD | WDD | WDD | WDD | WDD | WDD | WDD | WDD | WDD | WDD | WDD | WDD | WDD | WDD | WDD | WDD | WDD |
| SiO2 | 66.24 | 65.53 | 61.98 | 62.52 | 62.92 | 63.16 | 62.92 | 60.75 | 62.28 | 63.38 | 67.52 | 66.28 | 62.01 | 62.00 | 63.00 | 66.25 | 62.45 | 66.03 | 63.44 | 63.42 | 63.05 | 62.25 | 62.14 | 63.20 | 65.95 |
| TiO2 | 0.00 | 0.00 | 0.00 | 0.00 | 0.01 | 0.01 | 0.00 | 0.00 | 0.01 | 0.00 | 0.00 | 0.00 | 0.00 | 0.00 | 0.00 | 0.02 | 0.00 | 0.00 | 0.00 | 0.00 | 0.00 | 0.00 | 0.00 | 0.00 | 0.02 |
| Al2O3 | 18.60 | 19.18 | 17.30 | 17.85 | 17.56 | 17.87 | 17.24 | 19.59 | 17.57 | 17.55 | 19.23 | 18.93 | 18.53 | 18.94 | 18.31 | 20.19 | 18.57 | 19.24 | 18.31 | 18.24 | 18.35 | 18.52 | 18.61 | 18.28 | 19.97 |
| Cr2O3 | 0.00 | 0.02 | 0.00 | 0.00 | 0.00 | 0.03 | 0.01 | 0.00 | 0.00 | 0.00 | 0.00 | 0.00 | 0.00 | 0.00 | 0.00 | 0.01 | 0.00 | 0.00 | 0.00 | 0.00 | 0.00 | 0.00 | 0.00 | 0.00 | 0.00 |
| FeO | 0.00 | 0.00 | 0.00 | 0.00 | 0.04 | 0.03 | 0.05 | 0.02 | 0.00 | 0.00 | 0.02 | 0.01 | 0.00 | 0.04 | 0.00 | 0.00 | 0.00 | 1.18 | 0.00 | 0.04 | 0.00 | 0.00 | 0.02 | 0.00 | 1.12 |
| MnO | 0.01 | 0.04 | 0.00 | 0.00 | 0.00 | 0.00 | 0.04 | 0.00 | 0.00 | 0.00 | 0.00 | 0.00 | 0.00 | 0.00 | 0.00 | 0.00 | 0.00 | 0.01 | 0.00 | 0.01 | 0.00 | 0.00 | 0.00 | 0.01 | 0.01 |
| MgO | 0.00 | 0.02 | 0.00 | 0.00 | 0.01 | 0.00 | 0.00 | 0.02 | 0.00 | 0.00 | 0.01 | 0.03 | 0.01 | 0.01 | 0.01 | 0.03 | 0.00 | 0.03 | 0.01 | 0.00 | 0.01 | 0.01 | 0.00 | 0.00 | 0.14 |
| ZnO | 0.01 | 0.00 | 0.00 | 0.00 | 0.00 | 0.03 | 0.00 | 0.00 | 0.00 | 0.04 | 0.00 | 0.06 | 0.00 | 0.00 | 0.00 | 0.03 | 0.00 | 0.01 | 0.01 | 0.00 | 0.04 | 0.00 | 0.00 | 0.00 | 0.04 |
| CaO | 0.45 | 0.63 | 0.01 | 0.02 | 0.01 | 0.01 | 0.01 | 0.02 | 0.02 | 0.01 | 0.20 | 0.20 | 0.02 | 0.04 | 0.02 | 0.27 | 0.01 | 0.43 | 0.01 | 0.01 | 0.01 | 0.03 | 0.02 | 0.00 | 0.34 |
| Na2O | 11.41 | 11.23 | 0.19 | 0.21 | 0.15 | 0.21 | 0.19 | 0.16 | 0.12 | 0.26 | 12.07 | 11.59 | 0.16 | 0.13 | 0.18 | 11.92 | 0.24 | 11.66 | 0.22 | 0.31 | 0.23 | 0.09 | 0.20 | 0.32 | 12.05 |
| K2O | 0.07 | 0.28 | 15.54 | 15.69 | 15.95 | 15.94 | 15.91 | 15.52 | 15.55 | 15.86 | 0.07 | 0.32 | 15.84 | 15.81 | 15.98 | 0.07 | 15.93 | 0.19 | 15.99 | 15.98 | 15.81 | 15.84 | 15.84 | 15.51 | 0.23 |
| Total | 96.84 | 96.97 | 95.02 | 96.28 | 96.64 | 97.30 | 96.37 | 96.08 | 95.56 | 97.09 | 99.14 | 97.43 | 96.57 | 96.97 | 97.50 | 98.77 | 97.20 | 98.81 | 97.99 | 98.02 | 97.51 | 96.73 | 96.86 | 97.33 | 99.91 |
| Si | 2.994 | 2.965 | 3.011 | 2.998 | 3.009 | 3.001 | 3.019 | 2.923 | 3.007 | 3.015 | 2.984 | 2.983 | 2.969 | 2.956 | 2.986 | 2.942 | 2.971 | 2.950 | 2.991 | 2.991 | 2.986 | 2.974 | 2.967 | 2.993 | 2.921 |
| Ti | 0.000 | 0.000 | 0.000 | 0.000 | 0.000 | 0.000 | 0.000 | 0.000 | 0.000 | 0.000 | 0.000 | 0.000 | 0.000 | 0.000 | 0.000 | 0.001 | 0.000 | 0.000 | 0.000 | 0.000 | 0.000 | 0.000 | 0.000 | 0.000 | 0.001 |
| Al | 0.991 | 1.023 | 0.991 | 1.009 | 0.990 | 1.001 | 0.975 | 1.111 | 1.000 | 0.984 | 1.001 | 1.004 | 1.045 | 1.064 | 1.023 | 1.056 | 1.041 | 1.013 | 1.017 | 1.014 | 1.024 | 1.043 | 1.047 | 1.020 | 1.042 |
| Cr | 0.000 | 0.001 | 0.000 | 0.000 | 0.000 | 0.001 | 0.002 | 0.000 | 0.000 | 0.000 | 0.000 | 0.000 | 0.000 | 0.000 | 0.000 | 0.000 | 0.000 | 0.000 | 0.000 | 0.000 | 0.000 | 0.000 | 0.000 | 0.000 | 0.000 |
| Fe2+ | 0.000 | 0.000 | 0.000 | 0.000 | 0.002 | 0.001 | 0.002 | 0.001 | 0.000 | 0.000 | 0.001 | 0.000 | 0.000 | 0.001 | 0.000 | 0.000 | 0.000 | 0.044 | 0.000 | 0.002 | 0.000 | 0.000 | 0.001 | 0.000 | 0.041 |
| Mn2+ | 0.001 | 0.002 | 0.000 | 0.000 | 0.000 | 0.000 | 0.002 | 0.000 | 0.000 | 0.000 | 0.000 | 0.000 | 0.000 | 0.000 | 0.000 | 0.000 | 0.000 | 0.000 | 0.000 | 0.000 | 0.000 | 0.000 | 0.000 | 0.000 | 0.000 |
| Mg | 0.000 | 0.001 | 0.000 | 0.000 | 0.000 | 0.000 | 0.000 | 0.001 | 0.000 | 0.000 | 0.001 | 0.002 | 0.001 | 0.001 | 0.001 | 0.001 | 0.000 | 0.002 | 0.000 | 0.000 | 0.001 | 0.000 | 0.000 | 0.000 | 0.009 |
| Zn | 0.000 | 0.000 | 0.000 | 0.000 | 0.000 | 0.001 | 0.000 | 0.000 | 0.000 | 0.001 | 0.000 | 0.002 | 0.000 | 0.000 | 0.000 | 0.001 | 0.000 | 0.000 | 0.000 | 0.000 | 0.001 | 0.000 | 0.000 | 0.000 | 0.001 |
| Ca | 0.022 | 0.031 | 0.001 | 0.001 | 0.001 | 0.001 | 0.000 | 0.001 | 0.001 | 0.000 | 0.009 | 0.010 | 0.001 | 0.002 | 0.001 | 0.013 | 0.001 | 0.021 | 0.001 | 0.000 | 0.000 | 0.002 | 0.001 | 0.000 | 0.016 |
| Na | 1.000 | 0.985 | 0.018 | 0.020 | 0.014 | 0.019 | 0.018 | 0.015 | 0.011 | 0.024 | 1.034 | 1.011 | 0.015 | 0.012 | 0.016 | 1.026 | 0.022 | 1.010 | 0.020 | 0.028 | 0.022 | 0.008 | 0.019 | 0.029 | 1.035 |
| K | 0.004 | 0.016 | 0.963 | 0.960 | 0.973 | 0.966 | 0.974 | 0.952 | 0.957 | 0.962 | 0.004 | 0.018 | 0.967 | 0.962 | 0.966 | 0.004 | 0.967 | 0.011 | 0.961 | 0.962 | 0.955 | 0.965 | 0.965 | 0.937 | 0.013 |
| Ni | 0.000 | 0.000 | 0.000 | 0.000 | 0.000 | 0.000 | 0.000 | 0.000 | 0.000 | 0.000 | 0.000 | 0.000 | 0.000 | 0.000 | 0.000 | 0.000 | 0.000 | 0.000 | 0.000 | 0.000 | 0.000 | 0.000 | 0.000 | 0.000 | 0.000 |
| Cl | 0.003 | 0.002 | 0.000 | 0.000 | 0.000 | 0.000 | 0.000 | 0.001 | 0.001 | 0.000 | 0.001 | 0.001 | 0.000 | 0.000 | 0.000 | 0.001 | 0.000 | 0.003 | 0.000 | 0.001 | 0.000 | 0.000 | 0.000 | 0.000 | 0.003 |
| F | 0.000 | 0.000 | 0.000 | 0.000 | 0.000 | 0.000 | 0.000 | 0.000 | 0.000 | 0.000 | 0.000 | 0.000 | 0.000 | 0.000 | 0.000 | 0.000 | 0.000 | 0.000 | 0.000 | 0.000 | 0.000 | 0.000 | 0.000 | 0.000 | 0.000 |

| Type | Kspar | Kspar | Kspar | Kspar | Kspar | Kspar | Kspar | Kspar | Kspar | Kspar | Kspar | Kspar | Kspar | Kspar | Kspar | Kspar | Kspar | Kspar | Kspar | Kspar | Kspar |
|---|---|---|---|---|---|---|---|---|---|---|---|---|---|---|---|---|---|---|---|---|---|
| Sample ID | MDS2 | MDS2 | MDS2 | MDS2 | MDS2 | MDS2 | MDS2 | MDS2 | MDS2 | PTSS1 | PTSS1 | PTSS1 | PTSS1 | PTSS1 | PTSS1 | WDS2 | WDS2 | WDS2 | WDS2 | WDS2 | WDS2 |
| SiO2 | 62.25 | 62.26 | 61.73 | 57.60 | 65.07 | 60.18 | 62.18 | 60.79 | 66.26 | 98.02 | 60.16 | 59.60 | 60.12 | 60.25 | 64.53 | 63.77 | 63.39 | 63.57 | 65.03 | 66.60 | 64.92 |
| TiO2 | 0.00 | 0.00 | 0.00 | 0.00 | 0.00 | 0.00 | 0.01 | 0.01 | 0.00 | 0.03 | 0.00 | 0.00 | 0.00 | 0.00 | 0.00 | 0.01 | 0.00 | 0.00 | 0.01 | 0.01 | 0.00 |
| Al2O3 | 17.58 | 17.68 | 17.40 | 24.22 | 19.06 | 20.05 | 17.51 | 17.62 | 18.72 | 0.06 | 17.15 | 17.29 | 17.14 | 16.93 | 18.12 | 18.64 | 17.40 | 17.47 | 18.50 | 19.07 | 18.24 |
| Cr2O3 | 0.01 | 0.00 | 0.00 | 0.00 | 0.02 | 0.02 | 0.00 | 0.00 | 0.00 | 0.02 | 0.00 | 0.00 | 0.00 | 0.00 | 0.02 | 0.03 | 0.00 | 0.00 | 0.00 | 0.00 | 0.00 |
| FeO | 0.07 | 0.45 | 0.06 | 0.35 | 0.08 | 0.01 | 0.05 | 0.02 | 0.00 | 0.02 | 0.01 | 0.12 | 0.02 | 0.06 | 0.00 | 0.05 | 0.10 | 0.14 | 0.11 | 0.47 | 0.12 |
| MnO | 0.00 | 0.00 | 0.00 | 0.01 | 0.00 | 0.00 | 0.00 | 0.00 | 0.00 | 0.00 | 0.00 | 0.03 | 0.00 | 0.00 | 0.00 | 0.00 | 0.00 | 0.00 | 0.00 | 0.00 | 0.00 |
| MgO | 0.01 | 0.00 | 0.01 | 0.16 | 0.02 | 0.05 | 0.01 | 0.00 | 0.02 | 0.01 | 0.00 | 0.01 | 0.01 | 0.02 | 0.00 | 0.02 | 0.00 | 0.02 | 0.02 | 0.03 | 0.02 |
| ZnO | 0.00 | 0.00 | 0.00 | 0.05 | 0.00 | 0.01 | 0.04 | 0.00 | 0.00 | 0.00 | 0.01 | 0.01 | 0.01 | 0.00 | 0.00 | 0.00 | 0.00 | 0.00 | 0.05 | 0.00 | 0.00 |
| CaO | 0.02 | 0.03 | 0.02 | 0.24 | 0.21 | 0.05 | 0.02 | 0.02 | 0.14 | 0.00 | 0.01 | 0.05 | 0.03 | 0.06 | 0.04 | 0.12 | 0.03 | 0.03 | 0.05 | 0.13 | 0.05 |
| Na2O | 0.14 | 0.15 | 0.14 | 7.41 | 11.81 | 0.19 | 0.15 | 0.14 | 11.88 | 0.01 | 0.14 | 0.16 | 0.15 | 0.13 | 11.79 | 11.96 | 0.25 | 1.38 | 3.58 | 11.96 | 2.31 |
| K2O | 16.16 | 16.02 | 16.53 | 4.00 | 0.05 | 15.54 | 16.30 | 15.26 | 0.18 | 0.01 | 16.41 | 16.27 | 16.38 | 16.19 | 0.07 | 0.08 | 16.38 | 14.80 | 12.28 | 0.11 | 13.54 |
| Total | 96.27 | 96.60 | 95.90 | 94.06 | 96.33 | 96.12 | 96.30 | 93.87 | 97.21 | 98.18 | 93.91 | 93.55 | 93.90 | 93.67 | 94.58 | 94.66 | 97.55 | 97.42 | 99.64 | 98.40 | 99.22 |
| Si | 2.997 | 2.991 | 2.993 | 2.733 | 2.963 | 2.899 | 2.997 | 2.990 | 2.987 | 3.995 | 2.984 | 2.970 | 2.983 | 2.993 | 2.990 | 2.960 | 3.012 | 3.009 | 2.985 | 2.974 | 2.999 |
| Ti | 0.000 | 0.000 | 0.000 | 0.000 | 0.000 | 0.000 | 0.000 | 0.000 | 0.000 | 0.001 | 0.000 | 0.000 | 0.000 | 0.000 | 0.000 | 0.000 | 0.000 | 0.000 | 0.000 | 0.000 | 0.000 |
| Al | 0.998 | 1.001 | 0.994 | 1.354 | 1.023 | 1.138 | 0.994 | 1.021 | 0.995 | 0.003 | 1.003 | 1.015 | 1.002 | 0.991 | 0.990 | 1.020 | 0.974 | 0.975 | 1.000 | 1.003 | 0.993 |
| Cr | 0.000 | 0.000 | 0.000 | 0.000 | 0.001 | 0.001 | 0.000 | 0.000 | 0.000 | 0.001 | 0.000 | 0.000 | 0.000 | 0.000 | 0.001 | 0.001 | 0.000 | 0.000 | 0.000 | 0.000 | 0.000 |
| Fe2+ | 0.003 | 0.018 | 0.003 | 0.014 | 0.003 | 0.000 | 0.002 | 0.001 | 0.000 | 0.001 | 0.000 | 0.005 | 0.001 | 0.002 | 0.000 | 0.002 | 0.004 | 0.006 | 0.004 | 0.018 | 0.005 |
| Mn2+ | 0.000 | 0.000 | 0.000 | 0.000 | 0.000 | 0.000 | 0.000 | 0.000 | 0.000 | 0.000 | 0.000 | 0.001 | 0.000 | 0.000 | 0.000 | 0.000 | 0.000 | 0.000 | 0.000 | 0.000 | 0.000 |
| Mg | 0.001 | 0.000 | 0.000 | 0.011 | 0.001 | 0.003 | 0.001 | 0.000 | 0.002 | 0.001 | 0.000 | 0.001 | 0.001 | 0.001 | 0.001 | 0.001 | 0.000 | 0.001 | 0.001 | 0.002 | 0.001 |
| Zn | 0.000 | 0.000 | 0.000 | 0.002 | 0.000 | 0.000 | 0.002 | 0.000 | 0.000 | 0.000 | 0.000 | 0.000 | 0.001 | 0.000 | 0.000 | 0.000 | 0.000 | 0.000 | 0.002 | 0.000 | 0.000 |
| Ca | 0.001 | 0.002 | 0.001 | 0.012 | 0.010 | 0.003 | 0.001 | 0.001 | 0.007 | 0.000 | 0.001 | 0.002 | 0.002 | 0.003 | 0.002 | 0.006 | 0.001 | 0.001 | 0.002 | 0.006 | 0.003 |
| Na | 0.013 | 0.014 | 0.013 | 0.681 | 1.043 | 0.017 | 0.014 | 0.014 | 1.038 | 0.001 | 0.014 | 0.015 | 0.014 | 0.013 | 1.059 | 1.076 | 0.023 | 0.126 | 0.319 | 1.035 | 0.207 |
| K | 0.993 | 0.981 | 1.022 | 0.242 | 0.003 | 0.955 | 1.002 | 0.957 | 0.010 | 0.000 | 1.038 | 1.035 | 1.037 | 1.026 | 0.004 | 0.004 | 0.993 | 0.894 | 0.719 | 0.006 | 0.798 |
| Ni | 0.000 | 0.000 | 0.000 | 0.000 | 0.000 | 0.000 | 0.000 | 0.000 | 0.000 | 0.000 | 0.000 | 0.000 | 0.000 | 0.000 | 0.000 | 0.000 | 0.000 | 0.000 | 0.000 | 0.000 | 0.000 |
| Cl | 0.002 | 0.000 | 0.002 | 0.001 | 0.000 | 0.003 | 0.003 | 0.003 | 0.000 | 0.000 | 0.001 | 0.002 | 0.004 | 0.004 | 0.001 | 0.000 | 0.001 | 0.000 | 0.002 | 0.000 | 0.001 |
| F | 0.000 | 0.000 | 0.000 | 0.000 | 0.000 | 0.000 | 0.000 | 0.000 | 0.000 | 0.000 | 0.000 | 0.000 | 0.000 | 0.000 | 0.000 | 0.000 | 0.000 | 0.000 | 0.000 | 0.000 | 0.000 |

| Type | Pl | Pl | Pl | Pl | Pl | Pl | Pl | Pl | Pl | Pl | Pl | Pl | Pl | Pl | Pl | Pl | Pl | Pl | Pl | Pl | Pl | Pl | Pl | Pl | Pl |
|---|---|---|---|---|---|---|---|---|---|---|---|---|---|---|---|---|---|---|---|---|---|---|---|---|---|
| Sample ID | WDD | WDD | WDD | WDD | WDD | WDD | WDD | WDD | WDD | WDD | WDD | WDD | WDD | WDD | WDD | MDS2 | MDS2 | MDS2 | MDS2 | MDS2 | MDS2 | MDS2 | MDS2 | MDS2 | TBS2 |
| SiO2 | 64.79 | 64.48 | 65.28 | 65.56 | 66.05 | 66.06 | 63.75 | 65.93 | 66.26 | 66.19 | 67.01 | 63.87 | 66.58 | 64.75 | 66.17 | 67.45 | 66.99 | 67.69 | 68.14 | 68.39 | 66.98 | 66.46 | 66.60 | 66.85 | 66.54 |
| TiO2 | 0.03 | 0.01 | 0.00 | 0.01 | 0.01 | 0.02 | 0.00 | 0.01 | 0.00 | 0.00 | 0.01 | 0.01 | 0.01 | 0.01 | 0.00 | 0.00 | 0.00 | 0.00 | 0.00 | 0.00 | 0.00 | 0.01 | 0.00 | 0.01 | 0.00 |
| Al2O3 | 20.16 | 20.50 | 19.85 | 20.46 | 19.74 | 20.18 | 18.19 | 20.68 | 20.14 | 19.15 | 19.17 | 19.45 | 19.22 | 18.73 | 19.20 | 19.03 | 19.01 | 18.71 | 18.75 | 19.00 | 19.40 | 18.97 | 19.15 | 19.26 | 19.86 |
| Cr2O3 | 0.02 | 0.00 | 0.00 | 0.00 | 0.00 | 0.03 | 0.00 | 0.00 | 0.03 | 0.00 | 0.00 | 0.00 | 0.00 | 0.00 | 0.00 | 0.00 | 0.00 | 0.01 | 0.00 | 0.00 | 0.00 | 0.00 | 0.00 | 0.00 | 0.01 |
| FeO | 0.21 | 0.07 | 0.08 | 0.00 | 0.04 | 0.14 | 0.01 | 0.00 | 0.00 | 0.01 | 0.00 | 0.00 | 0.00 | 0.03 | 0.00 | 0.03 | 0.03 | 0.02 | 0.00 | 0.06 | 0.18 | 0.33 | 0.06 | 0.01 | 0.02 |
| MnO | 0.00 | 0.00 | 0.01 | 0.01 | 0.00 | 0.00 | 0.01 | 0.00 | 0.00 | 0.01 | 0.00 | 0.01 | 0.00 | 0.00 | 0.03 | 0.00 | 0.00 | 0.00 | 0.00 | 0.00 | 0.02 | 0.02 | 0.00 | 0.01 | 0.00 |
| MgO | 0.06 | 0.05 | 0.04 | 0.07 | 0.01 | 0.02 | 0.02 | 0.02 | 0.01 | 0.02 | 0.02 | 0.01 | 0.01 | 0.00 | 0.02 | 0.01 | 0.02 | 0.02 | 0.01 | 0.01 | 0.01 | 0.04 | 0.02 | 0.01 | 0.00 |
| ZnO | 0.04 | 0.00 | 0.00 | 0.01 | 0.09 | 0.01 | 0.00 | 0.00 | 0.07 | 0.01 | 0.00 | 0.03 | 0.02 | 0.04 | 0.01 | 0.00 | 0.01 | 0.09 | 0.03 | 0.01 | 0.02 | 0.00 | 0.00 | 0.02 | 0.00 |
| CaO | 0.67 | 0.74 | 0.62 | 0.36 | 0.63 | 0.78 | 0.41 | 0.44 | 0.47 | 0.56 | 0.71 | 3.03 | 0.63 | 0.33 | 0.45 | 0.24 | 0.32 | 0.08 | 0.27 | 0.14 | 0.30 | 0.22 | 0.28 | 0.33 | 0.35 | 0.19 |
| Na2O | 10.87 | 11.19 | 10.84 | 11.15 | 11.22 | 11.16 | 11.69 | 11.28 | 11.45 | 11.61 | 11.85 | 11.14 | 11.64 | 11.11 | 11.45 | 11.66 | 11.54 | 11.79 | 11.59 | 11.82 | 11.80 | 12.01 | 11.68 | 11.80 | 11.93 | 11.61 |
| K2O | 0.40 | 0.37 | 0.41 | 0.41 | 0.31 | 0.15 | 0.06 | 0.07 | 0.13 | 0.11 | 0.08 | 0.18 | 0.13 | 0.06 | 0.09 | 0.16 | 0.12 | 0.23 | 0.18 | 0.15 | 0.06 | 0.07 | 0.19 | 0.16 | 0.03 | 0.09 |
| Total | 97.27 | 97.44 | 97.13 | 98.08 | 98.14 | 98.56 | 94.14 | 98.42 | 98.57 | 97.68 | 98.85 | 97.88 | 98.25 | 95.06 | 97.41 | 98.57 | 98.04 | 98.63 | 98.29 | 99.31 | 100.04 | 98.48 | 98.17 | 98.29 | 99.15 | 98.35 |
| Si | 2.926 | 2.910 | 2.947 | 2.931 | 2.953 | 2.940 | 2.974 | 2.932 | 2.946 | 2.971 | 2.974 | 2.891 | 2.972 | 2.980 | 2.975 | 2.994 | 2.990 | 3.004 | 3.002 | 3.001 | 2.990 | 2.983 | 2.972 | 2.972 | 2.956 | 2.961 |
| Ti | 0.001 | 0.000 | 0.000 | 0.000 | 0.000 | 0.001 | 0.000 | 0.000 | 0.000 | 0.000 | 0.000 | 0.000 | 0.001 | 0.000 | 0.000 | 0.000 | 0.000 | 0.000 | 0.000 | 0.000 | 0.000 | 0.000 | 0.000 | 0.000 | 0.000 | 0.000 |
| Al | 1.073 | 1.091 | 1.056 | 1.078 | 1.040 | 1.058 | 1.000 | 1.084 | 1.056 | 1.013 | 1.003 | 1.038 | 1.011 | 1.016 | 1.017 | 0.995 | 1.000 | 0.979 | 0.983 | 0.986 | 1.000 | 0.996 | 1.009 | 1.013 | 1.035 | 1.041 |
| Cr | 0.001 | 0.000 | 0.000 | 0.000 | 0.000 | 0.001 | 0.000 | 0.000 | 0.001 | 0.000 | 0.000 | 0.000 | 0.000 | 0.000 | 0.000 | 0.000 | 0.000 | 0.000 | 0.000 | 0.000 | 0.000 | 0.000 | 0.000 | 0.000 | 0.000 | 0.000 |
| Fe2+ | 0.008 | 0.003 | 0.003 | 0.000 | 0.002 | 0.005 | 0.000 | 0.000 | 0.000 | 0.000 | 0.000 | 0.000 | 0.000 | 0.001 | 0.000 | 0.001 | 0.001 | 0.001 | 0.000 | 0.000 | 0.002 | 0.007 | 0.012 | 0.002 | 0.000 | 0.001 |
| Mn2+ | 0.000 | 0.000 | 0.000 | 0.000 | 0.000 | 0.000 | 0.000 | 0.000 | 0.000 | 0.000 | 0.000 | 0.000 | 0.000 | 0.000 | 0.001 | 0.000 | 0.000 | 0.000 | 0.001 | 0.001 | 0.000 | 0.001 | 0.001 | 0.000 | 0.001 | 0.000 |
| Mg | 0.004 | 0.003 | 0.003 | 0.004 | 0.001 | 0.002 | 0.001 | 0.001 | 0.001 | 0.001 | 0.001 | 0.001 | 0.001 | 0.001 | 0.001 | 0.001 | 0.001 | 0.001 | 0.001 | 0.001 | 0.001 | 0.001 | 0.002 | 0.001 | 0.000 | 0.000 |
| Zn | 0.001 | 0.000 | 0.000 | 0.000 | 0.003 | 0.000 | 0.000 | 0.000 | 0.002 | 0.000 | 0.000 | 0.001 | 0.001 | 0.001 | 0.000 | 0.000 | 0.000 | 0.003 | 0.001 | 0.000 | 0.001 | 0.000 | 0.000 | 0.002 | 0.000 | 0.000 |
| Ca | 0.032 | 0.036 | 0.030 | 0.017 | 0.030 | 0.037 | 0.021 | 0.021 | 0.023 | 0.027 | 0.034 | 0.147 | 0.030 | 0.016 | 0.022 | 0.011 | 0.016 | 0.004 | 0.013 | 0.007 | 0.014 | 0.011 | 0.014 | 0.016 | 0.017 | 0.009 |
| Na | 0.952 | 0.980 | 0.949 | 0.967 | 0.973 | 0.963 | 1.057 | 0.972 | 0.987 | 1.011 | 1.020 | 0.977 | 1.008 | 0.991 | 0.997 | 1.004 | 0.998 | 1.015 | 1.000 | 1.009 | 1.001 | 1.037 | 1.013 | 1.021 | 1.023 | 1.002 |
| K | 0.023 | 0.021 | 0.024 | 0.023 | 0.017 | 0.008 | 0.003 | 0.004 | 0.007 | 0.006 | 0.005 | 0.010 | 0.007 | 0.004 | 0.005 | 0.009 | 0.007 | 0.013 | 0.010 | 0.009 | 0.003 | 0.004 | 0.011 | 0.009 | 0.002 | 0.005 |
| Ni | 0.000 | 0.000 | 0.000 | 0.000 | 0.000 | 0.000 | 0.000 | 0.000 | 0.000 | 0.000 | 0.000 | 0.000 | 0.000 | 0.000 | 0.000 | 0.000 | 0.000 | 0.000 | 0.000 | 0.000 | 0.000 | 0.000 | 0.000 | 0.000 | 0.000 | 0.000 |
| Cl | 0.004 | 0.001 | 0.000 | 0.004 | 0.003 | 0.000 | 0.000 | 0.000 | 0.000 | 0.000 | 0.000 | 0.001 | 0.001 | 0.001 | 0.000 | 0.000 | 0.000 | 0.000 | 0.000 | 0.001 | 0.000 | 0.000 | 0.000 | 0.000 | 0.006 | 0.002 |
| F | 0.000 | 0.000 | 0.000 | 0.000 | 0.000 | 0.000 | 0.000 | 0.000 | 0.000 | 0.000 | 0.000 | 0.036 | 0.000 | 0.000 | 0.000 | 0.000 | 0.000 | 0.000 | 0.000 | 0.000 | 0.000 | 0.000 | 0.000 | 0.000 | 0.000 | 0.000 |
| An | 3.2 | 3.4 | 3.0 | 1.7 | 3.0 | 3.7 | 1.9 | 2.1 | 2.2 | 2.6 | 3.2 | 13.0 | 2.9 | 1.6 | 2.1 | 1.1 | 1.5 | 0.4 | 1.3 | 0.7 | 1.4 | 1.0 | 1.3 | 1.5 | 1.6 | 0.9 |
| Ab | 94.5 | 94.5 | 94.6 | 96.0 | 95.3 | 95.5 | 97.8 | 97.5 | 97.1 | 96.8 | 96.4 | 86.1 | 96.4 | 98.0 | 97.4 | 98.0 | 97.8 | 98.4 | 97.7 | 98.5 | 98.3 | 98.6 | 97.7 | 97.7 | 98.2 | 98.6 |
| Or | 2.3 | 2.1 | 2.4 | 2.3 | 1.7 | 0.8 | 0.3 | 0.4 | 0.7 | 0.6 | 0.5 | 0.9 | 0.7 | 0.4 | 0.5 | 0.9 | 0.7 | 1.2 | 1.0 | 0.8 | 0.3 | 0.4 | 1.0 | 0.9 | 0.2 | 0.5 |

# APPENDIX D: FULL METHODS

## Core logging and taking samples

Drillcores from Menninnie Dam that intersected the GRV were identified using SARIG. These drillholes (MD31, MD32, and MD25) were chosen to be inspected at Glenside Core Library. During the visit, each of the 3 drill cores were logged and described by their textures, mineralogy and contact relationships with the help of Stacey McAvaney. This was done with the aid of a notebook, pencil, hand lens, camera and water spray bottle to make minerals more visible and easier to identify. Photos of each core tray from each drill core were taken whilst the core was wet from water. Whilst logging MD31, three geochemistry samples from A. Fabris were identified (R1948228, R1948227, R1948226) and data was obtained from SARIG. Points of interest (based on unidentifiable clasts/minerals and general drillhole geochemistry) were sampled and taken from the core library under the provision of the Mining Act 1971 and conditions of sample removal set out by the Department of State Development.

## Methods of field work

Six areas where the Bittali Rhyolite and Waganny Dacite have been mapped by A.H Blissett were selected to look at during a 10 day field trip. The areas chosen (from west to east) were Toondulya Bluff, Locailty 2 (a hill north of Mt Centre and west of Eurilla Hill, GPS – 0517658, 6424821), Waganny Dam area, Pt Thurlga Station area, Buckleboo area, Menninnie Dam. Geochemical data and field observations for Wartaka Station was collected and provided by the Geological Survey of South Australia from prior field work.

At each locality, a number of stops were recorded in places where the BR or WD had been previously mapped. At each stop the GPS coordinates were recorded as well as general field observations in a Markrite Field Book 102 using a mechanical pencil. Photos were taken of notable outcrop features which included flow banding, flow folding, xenoliths, depositional contacts, rock samples, and textures. Representative rock samples were collected at each stop for geochemical analysis as well as hand sample use.

To obtain samples, land owners and Gawler Ranges National Park rangers were first contacted to gain approval. At each locality, large boulder sized rocks that showed the least amount of weathering were split open using a sledgehammer, and smaller rock fragments amounting to ≈10 kg were collected and placed into a labelled sample bag (locality and stop number labelled on bag). Some stops were too weathered to obtain samples from, however an even spread of 20 samples was obtained across the extent of BR and WD outcrop with 4 from Toondulya Bluff (2 Waganny, 2 Bittali), 2 from ‘Locality 2’ (both Bittali), 4 from the Waganny Dam area (2 Waganny, 1 Bittali, 1 Unknown Rhyolite), 3 from Pt Thurlga Station (2 Waganny, 1 Bittali), 4 from Buckleboo (1 Waganny, 2 Bittali, 1 Bittali/Ma2), 3 from Menninnie Dam (all Bittali). At localities where flow banding and flow folds could be seen, measurements were taken using a compass to get dip/dip directions and plunge/trends.

## General sample preparation

### ROCK SAW

Due to the hardness of the rock samples, it was easier to break up certain pieces further using a sledgehammer rather than using the rock saw. After rocks were reduced to a manageable size ≈12cm, they were then washed with water using a hose to remove any dirt on the surface. The rock saw was then used to cut off any weathered rinds, which were distinguished by their bleak colour and lack of fresh minerals when juxtaposed with the fresher interior. The procedure for using the rock saw is as follows;

1. Put on the required safety equipment – earplugs, safety glasses, apron and plastic gloves
2. Wash down the stage and saw with the hose to remove any material
3. Clear the drain of any loose material and discard it into the metal bin underneath the rock saw
4. Take sample and place on the stage (Note – the sample must be of suitable size to pass through the saw completely)
5. Switch on rock saw by pressing the green button
6. Turn the tap handle to provide water to the saw
7. Grip the sample with thumbs facing forward and pull the sample back until it reaches the back of the stage
8. Allign the sample to the saw for sections that are to be cut
9. Slowly feed the sample into the saw until it completely passes through
10. Switch off by pressing the large red button
11. Turn off the tap
12. Move rock pieces onto a hotplate with fresh aluminium foil over the top and on the low setting
13. Remove rocks from hotplate after 30mins, then leave to cool for 5mins
14. Transfer rocks to a large zip lock plastic bag, labelled with sample number and name
15. Repeat above steps for each sample

### LARGE JAW CRUSHER

Reducing the rocks to a gravel.

1. Clean the room

1.1 Use compressed air to blow down workspace benches and table
1.2 Wipe benches and table with ethanol
1.3 Blow down again with compressed air to dry

2. Clean the jaw crusher

2.1 Open up hatches on jaw crusher and blow it interior down with compressed air
2.2 Clear any gaps of rock fragments if necessary
2.3 Use wire brush on jaw crusher “teeth”

2.4 Blow down with compressed air
2.5 Wipe down with ethanol and paper towel
2.6 Repeat step 2.4
2.7 Blow off rock particles on the collection tray, wipe with ethanol and paper towel and dry using compressed air
2.8 Insert collection tray beneath jaw crusher and close up doors and hatch
3. Slide open the metal cover tray and drop sample into the hole making sure to immediately close up the hole with the metal cover tray to avoid any rock fragments escaping
4. Do this for each rock piece and press stop when finished
5. Collect crushed sample by opening the turning the metal wheel, then pulling the doors open and removing the metal tray
6. Empty contents onto a piece of butcher's paper
7. Repeat step 2

## VIBRATING MILL (10G TUNGSTEN CARBIDE MILL HEAD)

Milling the gravel to a fine powder.

1. Clean each component of the tungsten 'pot' (Note – If powder is stuck to the bottom of the pot or any of the components, run the mill with pure quartz then proceed with cleaning procedure)
1.1 Blow down each component with compressed air
1.2 Wipe them with ethanol and paper towel
1.3 Blow down with compressed air
1.4 Piece the mill parts back together
2. Divide gravel sample in half and then half again using a ruler to get a representative sample of the original rock
3. Pour one of these divisions into the milling pot, while evenly distributing sample into the outer and inner spaces up to around 40% full
4. Put the lid on and place onto the milling platform
5. Place the cushioning material on top and pull the lever down and over the top
6. Latch the 2$^{nd}$ lever onto the 1$^{st}$ lever by fitting together the 'teeth' at the end and pull down firmly
7. Hook both together using the plastic ring
8. Set the timer to 2mins and press start
9. When finished, remove sample by unhooking levers and taking the pot from the machine
10. Open lid and pour the fine powder onto butchers paper
11. Repeat step 1

Sample was then poured into a labelled plastic bag.

## PRESSED PELLETS

*Cleaning and weighing samples*

1. Clean enough glass vials for pressed pellet use (1 per sample)

1.1 Fill a bucket with warm soapy water and dump all vials and their plastic caps in
1.2 Clean each with a plastic brush
1.3 Clean off any prior labels with ethanol
1.4 Rinse vials and lids with reverse osmosis water 3 times
1.5 Place vials onto a large enough petri dish and put into a glassware drying over for ≈ 1 hour at 130C
1.6 Put plastics caps on the top of the oven on paper towel

2. After 1 hour remove vials and caps from the oven making sure to not cause any contamination
3. Tare the scale and brush down the stage using a paintbrush
4. Weigh out ≈6g of sample using scales and a clean metal spoon
5. Record weighed value in a notebook
6. Clean metal spoon with ethanol and dry it with paper towel
7. Tare the scale again with the vial still on the stage
8. Weigh out ≈1.5g of licowax powder and add to the same vial which has sample in it
9. Record the weighed amount of wax powder in notebook
10. Put cap on vial and label it with a permanent marker
11. Shake the vile to ensure wax and sample have completely mixed
12. Repeat steps 3-11 for each sample

*Using pressing machine*

1. Clean the machine components with ethanol and paper towel
2. Fit the pieces together
3. Remove the solid cylinder its hole and put a labelled aluminium cap inside
4. Push the cap to the bottom with the metal cylinder and carefully pour sample inside from its vial
5. Slowly drop the solid cylinder once more into the hole until it stops
6. Hold the newly pieced together apparatus at the base and top and place it on the stage
7. Use the metal rod to tighten the screw on the left of the machine
8. Now use the metal rod to jack up the stage until the pressure gauge reaches 3
9. Unscrew the screw on the left of the machine
10. Remove apparatus from the stage as well as the metal base
11. Place the remaining apparatus pieces on top of a hollowed metal cylinder and sit it all on top of a piece of paper towel
12. Now place all of this onto the stage
13. Repeat step 7
14. Jack up the stage until the solid cylinder has almost completely gone through the hole
15. Repeat step 9

16. Remove apparatus from the machine whilst holding the paper towel at the base
17. Pressed pellet has been removed and is sitting on the paper towel
18. Repeat steps 1-17 for each sample

## FUSED DISCS

### Preparing samples for fusion

1. Clean vials, caps, and crucibles in warm soapy water (1 x vial with lip and 1 x vial without, 1x cap, 1x crucible)
2. Rinse each 3 times with deionised water
3. Wipe out a glass dish and place all glassware and crucibles facing up in a large enough glass dish
4. Put the glass dish into the glassware drying oven for a minimum of 30-40 minutes at 110˚C
5. Place the plastic vial caps on top of the oven on a sheet of paper towel
6. After the suggested drying time has elapsed, remove glass dish from oven as well as the lids sitting on top
7. Leave them to cool down
8. Weigh out 3-4g of each sample into the vials with lip (without caps), and label them
9. Place these vials onto a glass dish and put them into the sample drying oven at 60˚C for ≈ 3hours
10. Remove samples from oven and leave to cool
11. Transfer dry samples from vials to crucibles by first recording the weight of each crucible, then the weight of sample + crucible, as well as the sample name, crucible number and date in the booklet
12. Place filled crucibles onto silica trays and then load into the furnace

### Operation of furnace (Refer to laboratory manual for complete instructions)

13. Press the reset button
14. Set the cycle to "2" and press enter twice
15. Then press the cycle button repeatedly until the control on light comes on
16. Once cycle is complete (≈8hours), switch furnace off at the power point and carefully remove the silica trays with the aid of tongs ad oven mitts

### Preparation cont.

17. Let samples cool in a desiccator for ≈30mins until cool

18. Re-weigh crucibles and record in the booklet, the loss over ignition (LOI)% can also be calculated
19. Dry x-ray flux in oven at 110˚C for 5 hours
20. Remove from oven and let it cool in desiccator for 1.5 hours
21. Weigh 1g of sample and 4g of flux into each vial (without lip) and cap them
22. Give them a shake to mix

### Fused disc preparation

1. Clean the equipment (Pt/5% Au crucible and Pt/Au mould) by wiping the inside with paper towel and water
2. Submerge them into HCl and then rinse 3 times with deionized water
3. Dry with paper towel
4. Pour contents of vial into crucible
5. Using Norrish-Chapman Prometheus Fusion Apparatus, crucible is heated above an oxy-propane flame (1100˚C) for ≈10mins until fusion is complete
6. Carefully pour melt into the mould and then turn on the air jets to force cool it
7. Leave the mould to cool, then place a sticky label on it (sample number and date) and remove from mould, making sure to only handle it by the edges

## ND-SM AND SR ISOTOPE ANALYSIS

Six samples were analysed for Nd-Sm, and Sr, 3 representative of the Bitalli Rhyolite and 3 of the Waganny Dacite along an even geographic spread.

### Cleaning vials and teflon bombs

1. Clean off any previous sample labels on the outside and on the caps
2. Fill each with ≈2mL of 7M HCl and leave on hotplate for 2 hours
3. Submerge the vials and caps in a large beaker filled with HCl and again leave on the hotplate for 2 hours
4. Remove beaker from the hotplate and drain off the HCl
5. Stack vials and caps onto the large plastic cleaning apparatus
6. Fill with 700mL HCl, turn on hotplate and leave for 3 days
7. Drain off HCl and then add deionized water and leave for 2 days
8. Remove vials and caps from the apparatus and fill each with ≈2mL $HNO_3$ and 0.5mL HF
9. Cap the vials and place on the hotplate
10. Leave overnight
11. Discard contents of viles into appropriate waste container
12. Rinse with deionized water
13. Leave in a contained plastic box

14. Vials are now clean for isotope collection

## Sample Preparation

1. Firstly, check the accuracy of the scale by testing using a 100g weight
2. Use the antistatic gun on the inside of the teflon bomb
3. Weigh out 0.04g for Waganny samples, or 0.05 for Bittali samples to adjust for the estimated Nd ppm
4. Add the Nd-Sm 2M HCl spike, 0.4g for Waganny and 0.6g for Bittali samples
5. Prepare the "blank"
6. Prepare the "standard" by weighing 0.1g of USGS RGM2 1997 and 0.4g of the spike
7. Add 2mL $HNO_3$
8. Record all measurements into a log book
9. Leave them to dry on a hotplate
10. Add 4mL diluted HF to each bomb and cap them
11. Place them into bomb inserts and then into the oven at 150˚C for 3 days
12. Remove from the oven and wipe down bombs with deionized water and soft tissue
13. Carefully open caps and leave to dry on hotplate
14. At the point in which all liquid has evaporated, add 2mL $HNO_3$
15. Leave on hotplate until all $HNO_3$ has evaporated, then add 6mL HCl and cap them once cool
16. Place each into bomb inserts and then into the oven at 150˚C overnight
17. Remove from oven and leave to dry on hotplate
18. Dissolve in 15M nitric acid
19. Transfer bomb contents to labelled teflon vials

## Separating Nd, Sm and Sr

20. Follow the column procedure set out in the booklet
20.1. Start pre-wash by discarding 6mL 6M HCl (AR grade)
20.2. Discard 10mL 6M HCl (AR grade)
20.3. Discard 10mL 6M HCl
20.4. " 5mL deionized water
20.5. Rinse tip with 6M HCl
20.6. Pre-wash is finished, now equilibrate with 6mL 2M HCl
20.7. Load sample in 1mL 2M HCl
20.8. Discard 1mL 2M HCl (2x)
20.9. Discard 8mL 2M HCl
20.10. Discard 2mL 3M HCl
20.11. Remove waste acid beakers from under columns and replace with vials

20.12. Collect the Sr by adding 2mL 3M HCl
20.13. Cap vials and put waste acid beakers back under columns
20.14. Discard 1mL 6M HCl
20.15. Place other clean vials under the columns for collecting Nd-Sm
20.16. Add 5mL 6M HCl
20.17. Cap the vials
20.18. Repeat steps 20.2 to 20.5 for a clean up
21. Evaporate the contents of the vials to dryness on a hotplate
22. Follow the column procedure for Nd-Sm separation set out in the booklet
22.1. Start pre-wash by discarding 10mL 6M HCl (AR grade)
22.2. Discard 10mL 6M HCl
22.3. " 5mL 0.5M HCl
22.4. Pre-wash is finished, now rinse tip with 0.16M HCl
22.5. Equilibrate with 4mL 0.16M HCl
22.6. Load sample in 0.5mL 0.16M HCl
22.7. Discard 1mL 0.16M HCl (2x)
22.8. " 13mL 0.16M HCl
22.9. " 0.5mL 0.27M HCl
22.10. Replace waste acid beakers with clean vials
22.11. Collect Nd by adding 3.5mL 0.27M HCl
22.12. Discard 2mL 0.27 HCl into waste beakers
22.13. Replace with clean vials
22.14. Collect the Sm by adding 3mL 0.5M HCl
22.15. Add 1 drop of H3PO4 and leave vials to evaporate to dryness on hotplate
22.16. Cap the vials, they are now ready to be loaded into the mass spectrometer
23. Follow column procedure set out in booklet for collecting Sr

## ELECTRON MICROPROBE

Five thin sections were analysed under the microprobe and chosen based on presence of feldspars, and quartz hosted melt inclusions when they were viewed under plane polarized light.

1. Load samples
1.1. Remove previous samples
1.1.1. "SX FIVE Control" window – "vacuum" tab – "sample exchange" button – "transfer the sample out of the chamber" option - follow instructions in pop up box
1.1.2. Open transfer valve using the lever to the left of the sample-loading door by pushing in and sliding up. The lever will flick to the left at the top.
1.1.3. Flick the latch to the left so that the arrow on the top points out
1.1.4. Release handle and slide slowly forward (spring loaded so needs to be held the whole time), slide back – watch through window to ensure sample plate comes back with it

1.1.5. Close the valve by twisting the lever on the left to the right, then sliding it down
1.1.6. Click “ok” on pop up window
1.1.7. Wait for air lock to vent
1.1.8. Push screw on left side of access door in and pull door back to open (swings right)
1.1.9. Push sample plate to release, slide out and place on bench
1.1.10. Close door
1.2. Put carbon coated thin sections on sample plate
1.2.1. Put latex gloves on
1.2.2. Have sample plate with hole in one end facing you
1.2.3. Slide previous thin sections out by pushing down gently and sliding up/down
1.2.4. Slide new thin sections in with carbon coating facing up
1.2.5. Record sample numbers and order of thin sections on the plate (with first furthest away)
1.2.6. Stick carbon tape where two thin sections meet, ensuring that some tape also covers the edge of the sample plate to ensure thin sections do not move. Remove white backing of tape with tweezers
1.2.7. Overlay plastic grid on samples and record rough coordinates of where the marked circles are (x,y)
1.2.8. Remove grid before loading samples
1.3. Load new samples
1.3.1. Open access door and slide sample tray into place, hole end first, push until it clicks on (but don’t push so far that it releases)
1.3.2. Close door
1.3.3. “SX FIVE Control” window – “vacuum” tab – “sample exchange” button – “transfer the sample into the chamber” option – if door is properly closed, click “ok” to pump airlock – follow instructions in pop up box
1.3.4. Open transfer valve with lever as above
1.3.5. Flick latch back up so that the arrow is pointing inwards
1.3.6. Slide handle forward and then back, watching through window to make sur sample plate does not come back out
1.3.7. Close transfer valve as above
1.3.8. Click “ok”
2. Turning the electron beam on
2.1. “Beam and SEM setup” window – click “File” – select “load” from drop down menu – choose appropriate settings (in this case the first settings in the list were selected “hv15nA20”
2.2. Wait for beam to load
2.3. Go to “SX FIVE Control” window, select “Beam” tab. The diagram will show a red beam when the beam is finished loading. Can also check kV setting here.
3. Navigating to circles
3.1. Go to “SX FIVE Control – Roller” window
3.2. Enter x- and y-coordinates obtained from the grid laid over the samples before loading into boxes labelled “X” and “Y”
3.2.1 Type the number, then press “Enter” on keyboard and wait for the stage to move before adding the next coordinate.

3.3. In the same window, beam and light options are shown in the top right. Check Beam "Cut" and Scanning "Off", then Light "On"
3.4. Press the button on the top right of the joystick control to auto focus.
3.5. Return to same window and select Light "Off", Beam "On" and Scanning "On". A back-scatter image will now be visible in the top right screen.
3.6. Use the joystick to navigate the back-scatter image to find the circle and desired area of analysis
4. Quick analysis to help identify minerals of interest
4.1. To obtain a quick look at what elements are present in a particular area, turn Scatter "Off" and go to the "Esprit" window and click "Acquire" button
4.2. Wait while data is acquired.
4.3. A graph will be shown with peaks where a response has been recorded.
4.4. Elements can be assigned to these peaks by clicking approximately in the centre of each peak and selecting the most likely element from the selection in the box in the top right corner of the graph.
4.5. To return to navigating around the sample via back-scatter image, switch Scanning "On" and Beam "On" (Beam will automatically switch to "Cut" when finished)
5. Saving a back-scatter image (Light "Off", Beam "On", Scanning "On")
5.1. Set the position of the image using the joystick navigation
5.2. Adjust focus and magnification as necessary using the knobs labelled "MAG." And "FOCUS".
5.3. Go to the "Acquire" window (left screen) – "Imaging" button – new window will open up – "Start Image" button
5.4. Wait for image to develop in the new window
5.5. Click "Save As" button – name the file identifying the image by samples number and circle number.
5.6. Close the new window (click "No" when the pop-up asks to save to probe database)
6. Choosing points for analysis and recording them.
6.1. Navigate to desired area using joystick (Beam "On", Scanning "On", Light "Off")
6.2. Go to the "Automate window – "Digitize" button – new window will pop up "Digitize Samples" – name the position in the "Unknown position name" box (name the same as the image i.e. sample number circle number) – "Add new unknown to position list" button
6.3. New position will appear in the "Position List" in "Automate" window
7. Choosing single points for analysis.
7.1. Navigate to specific mineral/point – in "Digitize samples" window, select "Single Point(s)" button to record the location of the desired point of analysis (x- and y- coordinates will now appear in the "Automate" window.
7.2. Repeat step (a) until desired number of points for the circle have been recorded
8. Choosing a grid of points for analysis
8.1. Instead of clicking "Single Point(s)" button, select "Rectangular Grid" button – new window will open.
8.2. Set top left corner coordinates by navigating to a particular area and selecting the "Update Start" button

8.3. Set the bottom right corner coordinates by navigating to a point down and right of the starting point and click “Update Stop” button
8.4. Set grid step sizes in microns using the “X-step” and “Y-step” boxes
8.5 Click the “ok” button
8.6. List of points will appear in the “Automate” window under the same unknown position name
9. Choosing points along a linear traverse
9.1. Instead of “Single Point(s)” button, select “Linear Traverse” button
9.2. As with selecting a grid of points, a new window will pop up and ‘Start’ and ‘Stop’ positions will need to be selected by navigating to them and clicking the appropriate “Update Start” or “Update Stop” button
9.3. Input he desired number of steps in the traverse into the “Traverse Steps” box
9.4. Click “OK”
9.5. A list of points will appear in the “Automate” window under the same unknown position name
10. To begin adding points to the next circle, navigate to it using the joystick and/or enter new x- and y- coordinates as appropriate. Repeat steps 3-6, followed by steps 7,8, and/or 9 as desired
11. To record points onto the back-scatter image
11.1. Have the current circle selected in the “Position List”
11.2. In “Digitize” window, select “Picture Snap” button. A new window will pop up
11.3. Open “File” drop down menu – “Load BMP Image” – select image file that corresponds to the open circle number – “Open”
11.4. In “Display” drop down menu, select “Digitized unknown position samples” and “Digitized position sample long labels” (a tick will appear to the left of each option to indicate they are activated)
11.5. Red circles and corresponding number labels will appear at approximately the same location on the open back-scatter image as they were on the actual back-scatter image
11.6. To save the back-scatter image with the points, open “File” drop down menu-select “Save as BMP (with graphics data)” – name file wth the same sample number and circle number information, add ‘spots’ to the end to identify the image as one with the points information on it.
12. To run full analysis of selected points.
12.1. “Automate” window – select samples to analyse from the “Position List” by clicking and dragging up/down to the end of the currently loaded sample set – “Sample Setups” button, new window pops up – click “OK” – click “Yes” – returns to “Automate” window – select “Run selected samples” button – pop up gives estimated time to completion and asks for confirmation – click “Ok”

# APPENDIX E: GEOCHEMICAL AND ISOTOPIC DATA

GPS Coordinates can be found in Appendix A.

| Sample id. | | TBS2 | TBS3 | TBS5 | TBS7 | L2S2 | L2S3 | WDR | WDRD | WDD | WDS2 | PTSS1 | PTSS5 | PTSS6 | BBS1 | BBS3 | BBS4 | BBS6 | MDS2 | MDS4 |
|---|---|---|---|---|---|---|---|---|---|---|---|---|---|---|---|---|---|---|---|---|
| | | | | | | | | | | | | | | | | | | | | |
| SiO2 | (%) | 66.91 | 72.05 | 76.10 | 65.16 | 72.16 | 72.98 | 75.63 | 75.86 | 69.04 | 77.11 | 78.89 | 70.05 | 71.68 | 74.78 | 76.50 | 59.72 | 68.79 | 74.63 | 71.20 |
| TiO2 | (%) | 0.69 | 0.44 | 0.26 | 0.74 | 0.47 | 0.33 | 0.16 | 0.18 | 0.58 | 0.18 | 0.17 | 0.56 | 0.33 | 0.06 | 0.18 | 0.86 | 0.49 | 0.20 | 0.19 |
| Al2O3 | (%) | 14.45 | 13.20 | 12.65 | 19.80 | 13.30 | 12.62 | 11.42 | 12.34 | 14.43 | 11.37 | 11.95 | 14.58 | 13.47 | 12.63 | 12.98 | 16.50 | 14.67 | 13.37 | 13.09 |
| Fe2O3 | (%) | 4.21 | 3.20 | 2.14 | 4.68 | 3.31 | 2.74 | 0.89 | 1.22 | 2.54 | 0.92 | 1.37 | 2.53 | 1.39 | 1.50 | 0.30 | 9.42 | 3.00 | 1.44 | 1.40 |
| MnO | (%) | 0.12 | 0.06 | 0.04 | 0.05 | 0.09 | 0.09 | 0.01 | 0.04 | 0.09 | 0.02 | 0.02 | 0.10 | 0.09 | 0.03 | 0.00 | 0.13 | 0.06 | 0.05 | 0.05 |
| MgO | (%) | 1.43 | 0.44 | 0.49 | 0.44 | 0.33 | 0.23 | 0.18 | 0.28 | 0.62 | 0.13 | 0.16 | 0.62 | 0.95 | 0.08 | 0.17 | 1.88 | 0.69 | 0.33 | 0.40 |
| CaO | (%) | 2.34 | 0.23 | 0.25 | 0.47 | 0.86 | 0.67 | 0.14 | 0.28 | 1.27 | 0.24 | 0.17 | 1.44 | 1.18 | 0.70 | 0.18 | 4.18 | 1.65 | 1.19 | 1.48 |
| Na2O | (%) | 3.96 | 3.10 | 3.01 | 1.02 | 3.28 | 1.34 | 2.26 | 2.54 | 4.01 | 2.25 | 2.87 | 3.15 | 3.90 | 4.02 | 2.89 | 2.27 | 3.52 | 3.49 | 3.19 |
| K2O | (%) | 4.22 | 5.72 | 5.71 | 5.59 | 4.95 | 6.42 | 5.06 | 5.71 | 5.39 | 5.58 | 4.96 | 5.84 | 5.20 | 4.54 | 5.52 | 3.74 | 5.49 | 5.41 | 5.20 |
| P2O5 | (%) | 0.30 | 0.09 | 0.04 | 0.04 | 0.09 | 0.05 | 0.02 | 0.02 | 0.11 | 0.02 | 0.02 | 0.13 | 0.03 | 0.02 | 0.03 | 0.28 | 0.14 | 0.06 | 0.07 |
| SO3 | (%) | <0.001 | <0.001 | 0.00 | <0.001 | <0.001 | <0.001 | 0.00 | <0.001 | <0.001 | <0.001 | <0.001 | 0.02 | 0.02 | <0.001 | <0.001 | <0.001 | <0.001 | 0.02 | 0.01 |
| | | | | | | | | | | | | | | | | | | | | |
| Total | (%) | 98.62 | 98.54 | 100.69 | 97.99 | 98.85 | 97.47 | 95.78 | 98.47 | 98.07 | 97.82 | 100.60 | 99.00 | 98.24 | 98.36 | 98.75 | 99.10 | 98.50 | 100.32 | 96.27 |
| | | | | | | | | | | | | | | | | | | | | |
| Cl | (ppm) | 37 | 33 | <10 | <10 | 35 | <10 | <10 | <10 | 17 | 28 | <10 | <10 | 39 | <10 | <10 | 1255 | 69 | 1411 | 50 |
| Ag | (ppm) | <5 | <5 | <5 | <5 | <5 | <5 | <5 | <5 | <5 | <5 | <5 | <5 | <5 | <5 | <5 | <5 | <5 | <5 | <5 |
| As | (ppm) | <3 | <3 | <3 | 6 | <3 | 5 | 23 | 7 | <3 | <3 | <3 | 4 | <3 | 4 | <3 | <3 | <3 | <3 | <3 |
| Ba | (ppm) | 825 | 941 | 535 | 1046 | 985 | 790 | 254 | 184 | 1614 | 117 | 106 | 1323 | 697 | <20 | 440 | 1160 | 1566 | 517 | 533 |
| Bi | (ppm) | <5 | <5 | <5 | <5 | <5 | <5 | <5 | <5 | <5 | 9 | <5 | <5 | <5 | <5 | <5 | <5 | <5 | <5 | <5 |
| Br | (ppm) | <3 | <3 | <3 | <3 | <3 | <3 | <3 | <3 | <3 | <3 | <3 | <3 | <3 | <3 | <3 | <3 | <3 | <3 | <3 |
| Cd | (ppm) | <5 | <5 | <5 | <5 | <5 | <5 | <5 | <5 | <5 | <5 | <5 | <5 | <5 | <5 | <5 | <5 | <5 | <5 | <5 |
| Ce | (ppm) | 106 | 138 | 156 | 138 | 152 | 167 | 191 | 142 | 145 | 127 | 77 | 141 | 129 | 95 | 368 | 122 | 165 | 124 | 107 |
| Co | (ppm) | 27 | 33 | 22 | 11 | 26 | 27 | 28 | 28 | 18 | 29 | 25 | 13 | 18 | 45 | 30 | 45 | 31 | 29 | 33 |
| Cr | (ppm) | 7 | <5 | <5 | <5 | <5 | <5 | <5 | <5 | <5 | <5 | <5 | <5 | <5 | <5 | <5 | 402 | 9 | <5 | <5 |
| Cs | (ppm) | <10 | <10 | <10 | 24 | 15 | 15 | <10 | 11 | <10 | <10 | 11 | 11 | <10 | <10 | <10 | 42 | <10 | <10 | <10 |
| Cu | (ppm) | 3 | <3 | <3 | 4 | <3 | <3 | 5 | <3 | <3 | <3 | <3 | <3 | <3 | <3 | 4 | 3 | <3 | <3 | <3 |
| Ga | (ppm) | 17 | 18 | 16 | 26 | 19 | 19 | 16 | 17 | 17 | 16 | 15 | 17 | 9 | 24 | 18 | 20 | 17 | 14 | 14 |
| Ge | (ppm) | 3 | <3 | <3 | 3 | <3 | 3 | <3 | <3 | <3 | <3 | <3 | <3 | <3 | <3 | <3 | <3 | <3 | <3 | <3 |
| Hf | (ppm) | <10 | <10 | <10 | 13 | <10 | <10 | <10 | <10 | 12 | <10 | <10 | 10 | <10 | <10 | <10 | <10 | <10 | <10 | <10 |
| I | (ppm) | <10 | <10 | <10 | <10 | <10 | <10 | <10 | <10 | <10 | <10 | <10 | <10 | <10 | <10 | <10 | <10 | <10 | <10 | <10 |
| La | (ppm) | 58 | 68 | 76 | 44 | 73 | 80 | 96 | 67 | 77 | 33 | 22 | 72 | 67 | 25 | 201 | 52 | 80 | 68 | 59 |
| Mo | (ppm) | <3 | <3 | <3 | <3 | <3 | <3 | <3 | <3 | <3 | <3 | <3 | <3 | 26 | <3 | <3 | <3 | <3 | <3 | <3 |
| Nb | (ppm) | 14 | 20 | 20 | 22 | 20 | 20 | 20 | 23 | 18 | 21 | 22 | 17 | 18 | 42 | 17 | 11 | 14 | 10 | 10 |
| Nd | (ppm) | 48 | 60 | 63 | 39 | 64 | 66 | 70 | 60 | 62 | 41 | 30 | 58 | 55 | 53 | 149 | 48 | 59 | 45 | 43 |
| Ni | (ppm) | <3 | <3 | <3 | <3 | <3 | <3 | <3 | <3 | <3 | <3 | <3 | <3 | <3 | <3 | <3 | 36 | <3 | <3 | <3 |
| Pb | (ppm) | 15 | 12 | 13 | 28 | 18 | 57 | 299 | 84 | 12 | 29 | 9 | 38 | 9 | 41 | 24 | 7 | 21 | 28 | 16 |
| Rb | (ppm) | 128 | 218 | 228 | 299 | 223 | 265 | 272 | 330 | 171 | 273 | 240 | 193 | 149 | 376 | 198 | 228 | 135 | 133 | 139 |
| Sb | (ppm) | <10 | <10 | <10 | <10 | <10 | <10 | <10 | <10 | <10 | <10 | <10 | <10 | <10 | <10 | <10 | <10 | <10 | <10 | <10 |
| Sc | (ppm) | 10 | 7 | <5 | 14 | 7 | 9 | <5 | <5 | 7 | <5 | 6 | 8 | <5 | <5 | <5 | 20 | 6 | 5 | <5 |
| Se | (ppm) | <3 | <3 | <3 | <3 | <3 | <3 | <3 | <3 | <3 | <3 | <3 | <3 | <3 | <3 | <3 | <3 | <3 | <3 | <3 |
| Sm | (ppm) | <15 | <15 | <15 | <15 | <15 | <15 | <15 | <15 | <15 | 18 | <15 | <15 | <15 | 23 | 30 | <15 | <15 | <15 | <15 |
| Sn | (ppm) | <5 | <5 | <5 | <5 | <5 | <5 | <5 | <5 | <5 | <5 | <5 | <5 | <5 | <5 | <5 | <5 | <5 | <5 | <5 |
| Sr | (ppm) | 208 | 55 | 33 | 45 | 90 | 68 | 32 | 53 | 162 | 16 | 15 | 153 | 73 | 6 | 69 | 420 | 195 | 154 | 153 |
| Ta | (ppm) | <10 | <10 | <10 | <10 | <10 | <10 | <10 | <10 | <10 | <10 | <10 | <10 | <10 | <10 | <10 | <10 | <10 | <10 | <10 |
| Te | (ppm) | <10 | <10 | <10 | <10 | <10 | <10 | <10 | <10 | <10 | <10 | <10 | <10 | <10 | <10 | <10 | <10 | <10 | <10 | <10 |
| Th | (ppm) | 24 | 40 | 39 | 48 | 40 | 42 | 42 | 45 | 26 | 40 | 42 | 26 | 29 | 71 | 40 | 26 | 31 | 33 | 34 |
| Tl | (ppm) | 8 | 10 | 8 | 6 | 7 | 7 | 10 | 9 | 6 | 7 | 7 | 7 | 6 | 8 | 7 | 7 | 6 | 6 | 8 |
| U | (ppm) | 7 | 8 | 9 | 11 | 11 | 14 | 11 | 13 | 9 | 9 | 10 | 9 | 8 | 21 | 8 | 11 | 8 | 8 | 7 |
| V | (ppm) | 44 | <10 | <10 | <10 | <10 | <10 | <10 | <10 | 17 | <10 | <10 | 16 | <10 | <10 | <10 | 163 | 17 | 11 | 17 |
| Y | (ppm) | 39 | 50 | 54 | 33 | 51 | 55 | 55 | 59 | 45 | 45 | 54 | 42 | 43 | 95 | 53 | 31 | 30 | 20 | 19 |
| Yb | (ppm) | <15 | <15 | <15 | <15 | <15 | <15 | <15 | <15 | <15 | <15 | <15 | <15 | <15 | <15 | <15 | <15 | <15 | <15 | <15 |
| Zn | (ppm) | 73 | 66 | 49 | 65 | 81 | 108 | 12 | 38 | 62 | 24 | 31 | 60 | 31 | 25 | 7 | 85 | 43 | 46 | 63 |
| Zr | (ppm) | 235 | 363 | 290 | 528 | 392 | 327 | 199 | 210 | 505 | 196 | 194 | 414 | 239 | 152 | 227 | 198 | 455 | 152 | 152 |

| Sample # | Input age of rock T (Ma) | Unmixed143/144Nd | Nd ugg-1 | Sm ugg-1 | 147Sm/144Nd | eNd (T=0) | 143Nd/144Nd (T) | eNd (T) | TDM (Ma) | TCHUR (Ma) | DM at age of rock (T) | CHUR at age of rock (T) |
|---|---|---|---|---|---|---|---|---|---|---|---|---|
| PTSS5 | 1592 | 0.51 | 66.74 | 11.36 | 0.10 | -19.92 | 0.51 | -0.79 | 2086.35 | 1657.35 | 0.51 | 0.51 |
| WDD | 1592 | 0.51 | 68.03 | 12.53 | 0.11 | -19.32 | 0.51 | -1.92 | 2210.78 | 1765.93 | 0.51 | 0.51 |
| BBS4 | 1592 | 0.51 | 45.37 | 8.88 | 0.12 | -19.49 | 0.51 | -3.53 | 2384.29 | 1939.94 | 0.51 | 0.51 |
| WDS2 | 1592 | 0.51 | 44.47 | 8.53 | 0.12 | -19.30 | 0.51 | -2.87 | 2314.29 | 1866.81 | 0.51 | 0.51 |
| PTSS1 | 1592 | 0.51 | 32.06 | 6.92 | 0.13 | -19.06 | 0.51 | -5.60 | 2689.17 | 2246.22 | 0.51 | 0.51 |